Effect of biomass burning emissions on the carbon cycle of the Amazon for 2010-2015

Author:
Santiago Botía B

Supervisors:
dr. Ingrid van der Laan-Luijkx
Prof. dr. Maarten Krol

Department of Meteorology and Air Quality

Wageningen University

April 24, 2017

Acknowledgements

Image: Fire Season-2014 in the Bolivian-Brazilian border. Retrieved from the NASA EOSDIS Worldview tool at: https://worldview.earthdata.nasa.gov.

Abstract

Fire emissions represent one of the main pathways by which carbon is transported from the land to the atmosphere, and thereby represents a fundamental component of the carbon cycle. Tropical forests are known to contribute extensively to fire emissions. The Amazon, in particular, contributes a significant amount of fire emissions as it has fire seasons driven by dry periods, which are further enhanced by seas surface temperature anomalies in the Pacific and Atlantic oceans. Previous studies have shown that the effect of drought on fire emissions of the Amazon could significantly affect the carbon uptake, by turning the forest from a net sink to a net source of carbon for a particular year. In this study the work of van der Laan-Luijkx (2015) is extended to the period 2010-2015 including a new set of fire emissions and a new biosphere flux source. Fire inventories based on burned area (Global Fire Emissions Database version 4), radiative power (Global Fire Assimilation System versions 1 and 1.2) and fire hotspots (Fire Inventory from NCAR) will be used as biomass burning fluxes for the TM5 global transport model. The fire inventory comparison showed that burned area based estimates can differ due to different fire scheme approaches within the carbon stocks framework (SiBCASA and CASA biosphere models) and land cover distribution. Mortality and combustion completeness need to be revised within SIBCASA's fire scheme to get better regional estimates. The TM5 simulations showed better agreement for CO_2 than for CO with the observations, although the model had a good match aloft, above 3000 m for both tracers. The simulations tend to overestimate concentrations during the wet season and underestimate during the fire season at lower heights, below 1000m. In conclusion, it was difficult to find a better fire inventory to reproduce the observed the CO_2 and CO vertical profiles due to spatial and temporal factors.

Keywords: Biomass burning, fire inventory, net biome exchange, vertical transport, carbon dioxide, carbon monoxide, Amazon

Contents

Chapter 1

1 General Introduction

The atmosphere, together with the terrestrial biosphere, the soils and the ocean are the reservoirs in which the carbon biogeochemical cycle acts at timescales that range from hours to millenia. Geologic reservoirs play an important role but at much longer timescales [Le Queré et al., 2016]. The oceanic and terrestrial reservoirs act as sinks of carbon, capturing it from the atmosphere. Atmospheric carbon dioxide concentrations (CO_2) have risen from 277 parts per million (ppm) to 400 ppm in less than 300 years, from 1750 to 2015 [Le Queré et al., 2016]. The rise in the last century has been more steep due to anthropogenic activities such as fossil fuel combustion and land use change [Stocker et al., 2013]. During the last decades there has been great interest in the response of oceanic and terrestrial sinks to the input of CO_2 to the atmosphere and also on the radiative balance of the atmosphere itself [Ciais et al., 2013, Stocker et al., 2013, Le Queré et al., 2016]. The sinks of carbon together with the radiative properties of the atmosphere are highly dependent on the concentrations of CO_2 in the lower part of the atmosphere: the troposphere [Ciais et al., 2013, Stocker et al., 2013]. High CO_2 concentrations lead to disturbances in the energy balance of the Earth system, and rising atmospheric temperature which results in global warming [Stocker et al., 2013, Schimel et al., 2014].

Tropical forests act as a large carbon reservoir, they store 471 ± 93 PgC representing 55% of the global total carbon stock and from which 56% is stored biomass [Pan et al., 2011]. The Amazon forest represents 50% of the total tropical forest area [Malhi et al., 2006] and its carbon stock was estimated between 77-95 PgC [Saatchi et al., 2007] as aboveground biomass, but another estimate reports a range of 90-120 PgC [Andreae et al., 2015]. The global terrestrial carbon sink, of which the Amazon is an important contributor, has been estimated in 2.6 ± 1.2 PgC/yr by Ciais et al. [2013] and more recently in 3.1 ± 0.9 PgC/yr by Le Queré et al. [2016], which represents approximately 30% of the annual fossil fuel and land use change emissions. The latter has been estimated as the difference between the terms of the global carbon balance: on one side land use change emissions and fossil fuel emissions, on the other oceanic sink and the growth rate in atmospheric CO_2 concentration. Therefore there is high uncertainty associated to this estimate [Le Queré et al., 2016]. It has been reported that world's forests have been a sustain carbon sink in the last decades [Pan et al., 2011]. On that study it was concluded that tropical deforestation was mostly compensated by carbon uptake of both, tropical regrowth and tropical intact forests, thus boreal forests were responsible for driving the net terrestrial carbon sink. However, a recent study by Brienen et al. [2015] showed a long term decreasing trend on biomass accumulation in the Amazon. They concluded that this was due to an increased biomass mortality which in turn affects carbon residence times. Brienen et al. [2015] were based on an established network of plots that are well distributed in the Amazon forest, representing one of the largest bottom-up studies in this field. The authors acknowledged the fact that this decline has not been yet observed in the atmosphere mainly because not all dying biomass is immediately converted into CO_2, it is subjected to a decomposition process in which a fraction is converted into soil carbon. Thus the Amazon's necromass pool has increased considerably. Hence, the continuity of the terrestrial carbon sink represents one of the main issues that triggers research on land use change emissions (i.e. fire) and carbon cycle dynamics [Pan et al., 2011, Ciais et al., 2013, Schimel et al., 2014, Brienen et al., 2015]. It is unknown how this sink will develop in the future under changing climate, affected by biomass burning and biospheric CO_2 exchange. [Pan et al., 2011, Stocker et al., 2013, Brienen et al., 2015].

The Amazon carbon sink is strongly affected by land use change emissions, which are driven by human activities such as deforestation, logging, shifting cultivation, and non anthropogenic activities such as forest regrowth after disturbances or abandonment of agricultural activities [Le Queré et al., 2016]. Deforestation is directly linked to biomass burning [Van Der Werf et al., 2010], which in tropical regions is the most changing and largest contributor to land use change emissions [Van Der Werf et al., 2010, Le Queré et al., 2016]. This human induced disturbance has been recently associated to rainfall patterns upwind and downwind of deforested areas, mainly during the dry season in the Amazon [Khanna et al., 2017]. Thus, deforestation together with natural phenomena, such as enhanced droughts by sea surface temperature (SST) anomalies, have a huge impact on the carbon cycle of the Amazon [Lewis et al., 2011, Espinoza et al., 2011, Feldpausch et al., 2016]. Biomass burning in the Amazon represents one of the main mechanisms by which carbon is transported from the land to the atmosphere and is highly influenced by the aforementioned forcings [Baldocchi, 2008, Wiedinmyer et al., 2010].

Fire and biomass burning effects on the carbon cycle and climate materialize at different spatial and temporal scales; fire events occur on timescale of minutes to days and on a spatial scale of individual stands to hectares [Loehman et al., 2014]. In the tropics and the subtropics most of the fires are ignited by humans [Kaiser et al., 2012], which represents a threat added to the fact that the frequency of fires in the Amazon is likely to increase in the future [Gloor et al., 2012, Liu et al., 2014]. The net carbon uptake by the biosphere is influenced by fires as well as the variability of the atmospheric CO_2 growth rate. Fires also contribute to the atmospheric burden of CH_4, CO, N_2O, and other combustion products such as aerosols and ozone precursors [Hantson et al., 2016]. Greenhouse gases lead to global warming with a positive radiative forcing [Bowman et al., 2009, Stocker et al., 2013, Le Queré et al., 2016]. Aerosols have a direct and an indirect effect. The first one is related to the aerosol optical properties which can result in scattering or absorption of radiation, resulting in negative or positive radiative forcing, respectively. The second one, is due to the cloud-aerosol interaction, in which two opposing effects are found: 1. increasing amount of cloud condensation nuclei can decrease cloud droplet size resulting in a larger cloud lifetime and increased albedo and 2. black carbon can inhibit cloud formation in the lower atmosphere by increasing the susceptibility to evaporation and resulting in less cloud cover [Bowman et al., 2009, Stocker et al., 2013, Liu et al., 2014]. Furthermore, diffuse radiation due to aerosols during the fire season of the Amazon has been related to an increase net primary productivity (NPP) [Rap et al., 2015], representing another indirect effect of aerosols in the carbon cycle. Ozone resulting from fires has a direct effect on plants reducing photosynthesis and indirectly affecting the lifetime of GHG such as methane by changing the abundance of the OH radical [Hantson et al., 2016]. These interactions are a source of large uncertainty in current climate models [Stocker et al., 2013].

Each year an area larger than the Indian subcontinent is burned by biomass burning and wildfires [Giglio et al., 2013, Hantson et al., 2016], representing almost 4% of the global vegetated area [Randerson et al., 2012, Giglio et al., 2013]. Thus, fire represents one of the main disturbances that affects vegetation dynamics, it impacts ecosystem functioning, biodiversity, plant community structure and carbon storage [Hantson et al., 2016]. All these interactions and effects depend on the seasonality, fire intensity and the frequency that fire affects a particular region [Hantson et al., 2016]. For the Amazon region, it has been shown that during dry years fires are intensified [Gatti et al., 2014, Van Der Laan-Luijkx et al., 2015, Marengo and Espinoza, 2016].

During 1997, 1998, 2005 and 2010 anomalously low river levels and deficient rainfall were recorded, suggesting that during the last two decades extreme hydrological events have been more frequent [Gloor et al., 2015, Marengo and Espinoza, 2016]. Droughts are associated to El Niño Southern Oscillation in the Pacific Ocean, but it is important to note that droughts are not always occurring during El Niño years [Marengo and Espinoza, 2016]. The tropical Atlantic ocean plays also an important role in the Amazon hydrology due to moisture inflow and its changes during the dry and the wet season [Gloor et al., 2015, Marengo and Espinoza, 2016]. The 2005 drought was associated to a positive sea surface temperature anomaly of the tropical Atlantic during a non El Niño year [Marengo and Espinoza, 2016]. The fire season is dependent on these hydro-meteorological patterns which are found to be intensified in the last years [Gloor et al., 2015].

Furthermore, fires can also have important social impacts. [Hantson et al., 2016] report that more than 5 million people globally were affected by 300 major fire events in the past 30 years, and that the effects on air quality result in 260,000 to 600,000 premature deaths globally each year. Interestingly, human activities can influence fire regime and enhance feedback mechanisms involving vegetation, climate and human health. Land use change in the tropics enhance fire activity while fire can be suppressed by altering the fuel load of some regions [Hantson et al., 2016]. Therefore understanding the interaction between human disturbances such as deforestation via biomass burning is crucial to cope with forthcoming changes in the Amazon region and in the global carbon balance.

1.1 Problem Statement

Previous studies [Gatti et al., 2014, Van Der Laan-Luijkx et al., 2015, Alden et al., 2016], have shown that drought is affecting the annual carbon balance of the Amazon by turning the terrestrial sink into a source of carbon. Gatti et al. [2014] present the carbon budget for the Amazon with an observation based analysis that is used to calculate fluxes for the years 2010 and 2011. Their fire emissions are derived from $CO:CO_2$ ratios. It is shown that the carbon balance for 2010 was of 0.48 $\pm$ 0.18 PgC yr^{-1}and for 2011 a value of 0.06 $\pm$ 0.1 PgC yr^{-1}was reported. These results are revisited by Van Der Laan-Luijkx et al. [2015] using a South American version of the CarbonTracker Data Assimilation System (CT-SAM), which uses inverse modeling to study the carbon cycle. CT-SAM uses the TM5 model to transport a set of carbon fluxes from which CO_2 mole fractions are estimated. In CT-SAM the difference between the simulated and the observed mole fractions is minimized using an ensemble Kalman filter. Their results showed that for the dry year 2010 the carbon budget of the Amazon represented a net source ranging from 0.07 $\pm$ 0.42 to 0.31 $\pm$ 0.42 PgC yr^{-1}whereas the 2011 represented net sink ranging from -0.15 $\pm$ 0.42 to -0.27 $\pm$ 0.42 PgC yr^{-1}. These results are slightly different from those of Gatti et al. [2014] as the 2010 (in Van Der Laan-Luijkx et al. [2015]) represents a smaller source and the 2011 a stronger sink. Van Der Laan-Luijkx et al. [2015] work represents the first effort to integrate CO_2 and CO observations from the Amazon forest with the regional biospheric CO_2 exchange and the spatio-temporal information of fires. A more recent study [Alden et al., 2016], presents a sub-regional approach in which NBE is calculated for a three year period (2010-2012) in 5 subregions in the Amazon. A Bayesian atmospheric transport inversion was used for the flux estimates. Their results are focused more into the NBE annual and interannual variability. However, their results are statistically consistent with the results of Gatti et al. [2014] and Van Der Laan-Luijkx et al. [2015] for the 2010-2011 NBE difference (i.e. 2011-2010). The value reported by Alden et al. [2016] was 0.28 $\pm$ 0.45 PgC, that for Gatti et al. [2014] was 0.22 $\pm$ 0.26 PgC and the range reported by Van Der Laan-Luijkx et al. [2015] was of 0.08-0.26 PgC yr^{-1}.

Given these facts, it is clear that dry years in the Amazon are affecting fire emissions and carbon uptake. In this regard, it is worth noting that the last ENSO event (2015-2016) had a large impact on the Amazon forest with unprecedented warming and larger extent of extreme drought [Jiménez-Muñoz et al., 2016]. Hence understanding the behavior of fires under these stresses by monitoring their emissions is fundamental to estimate carbon sinks and sources. Several efforts have been made on this line of research, fire emissions and burned area have been monitored and reported by different initiatives producing several fire inventories, such as: The Global Fire Emission Database (currently the fourth version, GFED4), which provides burned area, the Global Fire Assimilation System (GFAS) and the Fire Inventory (FINN) from the National Center for Atmospheric Research (NCAR), both reporting fire emissions estimates. Burned area, which is given by a fraction of the grid cell area that burns, is currently coupled to biosphere models in order to obtained biomass burning emissions [Van Der Werf et al., 2010, Van Der Velde et al., 2014]. GFED4 coupled to a biosphere model, GFAS and FINN were used by Van Der Laan-Luijkx et al. [2015]. There it was shown that these fire inventories have considerable differences in the Amazon, that need to be further analyzed for an extended period of time to obtain a better idea of their variability.

The present study aims to compare these fire inventories with a regional approach in the Amazon. It also focuses on the biosphere CO_2 exchange as well as the atmospheric transport of CO_2 and CO emitted by fires. Therefore, in this study the following challenges will be addressed: 1. assessing the variability between current fire inventories to estimate fire emissions in the Amazon and 2. a comparison of the simulated transport of fire emissions with observations in the Amazon for an extended period of time (2010-2015) relative to Van Der Laan-Luijkx et al. [2015]. The research questions derived from the aforementioned:

Research Question 1: *What are the differences (in terms of yearly values, spatial distribution and biome attribution) between the fire inventories used to calculate fire emissions in the Amazon for years 2010-2015?*

Research Question 2: *What is the carbon balance in the Amazon for the years 2010-2015, based on fire and NBE fluxes?*

Research Question 3: *What are the main drivers causing different emission estimates between SiBCASA-GFED4 and CASA-GFED4, considering they have the same burned area input?*

Research Question 4: *How well do transported atmospheric CO mole fractions match CO observations made in four aircraft sites in the Amazon for the period of 2010-2015?*

Research Question 5: *How well do transported atmospheric CO_2 mole fractions match CO_2 observations made in four aircraft sites in the Amazon for the period of 2010-2015?*

1.2   Conceptual Background

The present section gives an overview of the general processes and tools that are treated or used in this thesis. First a description of the combustion process, focused on biomass combustion is given. Secondly, the generic approach to calculate fire emissions is described followed by the fundamental concepts of biosphere models. Finally a definition of the data assimilation cycle is provided to contextualize the reader with the main framework that embraces the present research.

1.2.1   Combustion Process

Radiative forcing, as defined by the IPCC, is a measure of the net change in the energy balance of the Earth system in response to some external perturbation (expressed in W m^{-2}) [Stocker et al., 2013]. In Figure 1 the impacts of the combustion products on the radiative forcing terms are shown. Vegetation fires affect 8 out of the 14 radiative forcing terms that disturb the energy balance of the Earth system. Therefore the products from combustion are abundant and they vary according physical and chemical factors.
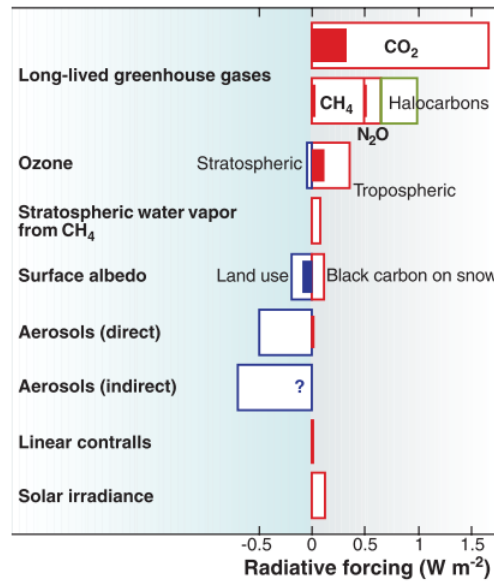
Figure 1: Estimated contribution of fire associated with deforestation to changes in radiative forcing compared to 1750 A.D. The shaded inner bar (blue indicates cooling; red, warming) is the estimated fire contribution to the total radiative forcing of individual agents identified by the IPCC (unshaded, outlined bar). From Bowman et al. [2009]

The combustion process consists in four stages, each contributing with different products to the bulk fire emissions: CO_2, CO, CH_4, aerosols and ozone precursors, among others. These stages depend highly on meteorological factors and vegetation characteristics. These stages are described below based on Van Leeuwen and Van Der Werf [2011]:

1. Ignition: The ignition phase is driven by environmental and fuel factors. Environmental factors such as temperature, wind speed and relative humidity and fuel characteristics such as size, density and water content. When the fuel meets the correct conditions, mainly low water content, the flaming stage can begin.

2. Flaming: During this stage a thermal degradation of fuel enhanced by air releases several compounds, mainly CO_2, volatiles and water. When almost all volatiles are released the flaming slows down and the smoldering stage comes into play.

3. Smoldering: In this stage the combustion proceeds at lower temperatures, resulting in the emission of incomplete oxidized compounds, like CO. This stage can last for several days even under relatively high fuel water content. Slower rate of heat production in this stage leads to the extinction stage.

4. Extinction: The principal causes of fire extinction are rainfall, fire spread to moist fuel sources, and physical gaps of fuel that prevent fire from spreading farther.

As Van Leeuwen and Van Der Werf [2011] show, the stages of combustion can occur at the same time, thus these stages are simplified in this description. Additional factors like topography and aboveground biomass need also to be taken into account in open fires. The ratio between stage 2 and 3 determine the proportion of emitted substances in a particular fire and it is also associated to the combustion efficiency, which is the fraction of carbon converted to CO_2 [Van Leeuwen and Van Der Werf, 2011].

1.2.2   Fire emission methods

Fire emissions are currently estimated using mainly two methods. The first, used in the GFAS inventory, uses satellite measurements that obtain fire radiative power (FRP), integrated to fire radiative energy (FRE), which correlates with total fire emissions, in particular to dry matter combusted [Kaiser et al., 2012]. Other methods use surface reflectance to obtain burned area and burn day estimates [Giglio et al., 2013]. The latter is used by GFED4 and FINN. These fire inventories based on burned area follow the traditional approach, in which carbon (C) emissions are calculated within a grid cell for a given time interval is based on Seiler and Crutzen [1980] following equation 1:

$$F_{carbon} \, or \, (E_i) = A_{x,t} * B_x * FB * (EF_i) \tag{1}$$

Where F_{carbon} (E_i) is the carbon emission (or emission of a given specie i), $A_{x,t}$ the area burned at time t and location x, B_x is the biomass loading at location x (on dry weight basis), and FB_i the fraction of the biomass burned. This approach together with emission factors (EF_i) can also be used to estimate emissions from other species. Emission factors (EFs) correspond to grams of trace gas emitted per kg of dry matter consumed during combustion [Van Leeuwen, 2014]. In this thesis, the focus is not directly in emissions emission, as the fire inventories used already incorporate them to calculate biomass burning emissions, thus here the focus is on CO and CO_2 emissions. In chapter 2 an overview of the fire inventories used and their main characteristics are described.

1.2.3   Carbon balance

The traditional approach to calculate a global carbon balance follows equation 2 and is based on Le Queré et al. [2016]. On the left side of the equation the sources of carbon and on the right side the sinks of carbon. These fluxes are in balance, thus an unknown term of the equation can be calculated as the residual of the others, as is currently the case for $C_{biosphere}$. The sources are mainly fossil fuel combustion emissions (ff) and land use change emissions (LUC). The sinks are the carbon that remains in the atmosphere (C_{atm}), the carbon that is captured by the ocean (C_{ocean}) and that taken up by the biosphere ($C_{biosphere}$). All the fluxes are in PgC/yr, although C_{atm} is commonly reported in parts per million (ppm, 1ppm corresponds to 2.12 PgC [Le Queré et al., 2016]).

$$E_{ff} + E_{LUC} = C_{atm} + C_{ocean} + C_{biosphere} \tag{2}$$

E_{ff} and C_{atm} are relatively well known. Fossil fuel emissions rely mainly on national energy consumption data and the atmospheric CO_2 concentration has been directly measured at remote locations. Land use change emissions are constrained mainly by book keeping methods [Le Queré et al., 2016], fire based inter-annual variability [Van Der Werf et al., 2010] and dynamic vegetation models [Le Queré et al., 2016], all having some differences between them. The oceanic uptake is based on both, direct observations and also ocean biogeochemical models [Le Queré et al., 2016]. The uncertainty of each one of these methods is given in detail in Le Queré et al. [2016]. Therefore, the biospheric sink is calculated as the residual of the other terms. However, dynamic vegetation models also provide the Net Biome Exchange (NBE), which represents the net flux from the biosphere to the atmosphere, or viceversa. NBE is equivalent to $C_{biosphere}$ and is calculated as:

$$NBE = NPP - Resp_{het} \tag{3}$$

All terms also in PgC/yr. NPP is the net primary productivity by plants, which is the difference between the gross primary productivity, the amount of carbon allocated to plant tissues, and the autotrophic respiration, the fraction that is respired back to the atmosphere. $Resp_{het}$ is the heterotrophic respiration at a biome scale, mainly in CO_2 form that is due to microbial respiration in decomposition processes. These terms can be calculated by biogeochemical models and in this study the focus is mainly on NBE. NBE can be also defined as the non fire fluxes between the vegetation-soils and the atmosphere [Alden et al., 2016].

NBE and the seasonal biomass burning are the main components driving the regional carbon balance in the Amazon. Fossil fuel emissions and oceanic uptake from equation 2 play a minor role [Van Der Laan-Luijkx et al., 2015, Alden et al., 2016]. Thus, a carbon balance can be calculated by adding NBE and the bulk fire emission estimates for each each fire inventory used (equation 4). These fire estimate is given by each of the fire inventories described in Chapter 2. From an atmospheric perspective positive values of NBE and $C_{balance}$ mean a flux from the biosphere to the atmosphere (source of carbon) whereas negative values mean a flux from the atmosphere to the biosphere (sink of carbon). The rapid vertical mixing of CO_2 in the Amazon allow this climatological net carbon balance, in which the NBE and Fires are more important that other fluxes. [Van Der Laan-Luijkx et al., 2015].

$$C_{balance} = NBE + Fire \tag{4}$$

1.2.4   General ecosystem carbon model

In this study a comparison of two biosphere models is done, specifically their fire scheme. Their implementation to calculate fire emissions. The SiBCASA [Schaefer et al., 2008] and CASA [Potter et al., 1993] biosphere models share the biogeochemical part (CASA) and they are similar in their approach to obtain carbon stocks. They are described in Chapter 2 as fire inventories based on burned area coupled to carbon stocks and in chapter 3 I touch upon their fire scheme. Here I describe the general approach by which carbon models circulate carbon between the different components of the terrestrial ecosystems. Following the approach of Luo and Weng [2011] this model follows:

$$\frac{dx(t)}{dt} = U(t) \cdot \mathbf{b} + \xi(t) \cdot \mathbf{A} \cdot \mathbf{X} \cdot x(t) \tag{5}$$

Where $x(t)$ describes a carbon pool size vector, depending on the pools each model has. $U(t)$, is the carbon gained and fixed by photosynthesis, b is a vector containing the partitioning coefficients of the fixed carbon to the plant pools (leaves, roots, wood) and finally A and C are the matrices containing coefficients to estimate carbon transfer between pools and the release of carbon via respiration. $\xi(t)$ describe the environmental effects that affect cycling and respiration rates. Equation 5 is illustrated in Figure 2. Fixed carbon ($U(t)$) is commonly modeled using a big leaf approach, in which photosynthesis is scaled up to ecosystem levels by using the leaf area index (LAI) or the absorbed fraction of photosynthetically active radiation (F_{par}). Carbon allocation (b) mainly follows the availability of nutrients, light and water. Cycling rates (C) on biosphere models depend on type of vegetation and latitude for vegetation, and for soils is function of the organic matter. These rates describe the residence time or turnover times of carbon in each pool. The transfer rates (A) dictate how carbon moves or transformed from one pool to another [Sierra, 2015].

This general description aims to contextualize the reader with biosphere models and how they calculate the carbon stocks that will be burned when coupled to a burned area inventory. Chapter 3 describes which of the carbon pools are subject to fire for each of the models studied. It is worth mentioning that this description is by no means exhaustive as these processes were not changed in this study. The SiBCASA and the CASA models' output was used to create experiments that are described in chapter 3. The reader is referred to Potter et al. [1993] and Schaefer et al. [2008] to get a complete description of all the equations and assumptions that are within these models.
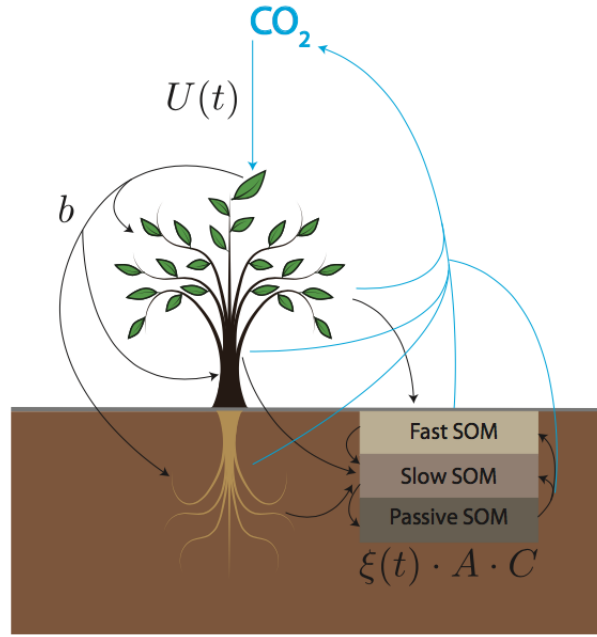
Figure 2: Graphical representation of the components of equation 5. CO_2 fixation by plants is included in the term $U(t)$ and allocation of fixed carbon to plant pools is represented by b. Cycling rates and transfers among different ecosystem compartments are represented by the product $A \cdot C$, which can be modified by the environmental scalar $\xi(t)$. SOM stands for soil organic matter. Figure taken from Sierra [2015].

1.2.5 Carbon Tracker Assimilation System

The general framework in which this thesis takes place is the Carbon Tracker Data Assimilation System [Peters et al., 2007], hereafter CarbonTracker. CarbonTracker is an inverse method to estimate surface CO_2 fluxes using atmospheric observations and prior knowledge of the fluxes from modeling frameworks. Despite the CarbonTracker system was used only in a forward mode, it is considered relevant to describe with which components of this process this research deals with. The CarbonTracker system is described in Figure 3. This system consists on using CO_2 net fluxes from the biosphere, fires, the ocean and fossil fuel combustion to simulated their transport in the atmosphere. A first transport simulation is done to predict CO_2 concentrations at certain locations. This first transport is called here "forward simulations" and they are performed with the TM5 global transport model. Once predicted values are sampled from the TM5 at the locations of interest a comparison to observed or measured concentrations at those same locations is done. So far these are the processes done in this study. The CarbonTracker continues by optimizing the differences between simulation and observed values to obtain optimized fluxes [Peters et al., 2005, Van Der Laan-Luijkx et al., 2015]. With these, a new cycle is performed again to get better estimates. The optimization process is not done here. In this thesis, a detailed comparison of the fire fluxes for the Amazon is presented and together with the biosphere fluxes from SiBCASA and CASA a carbon balance for the Amazon is estimated. An analysis of optimized fires is given in the appendix, this is considered to be a follow up of this thesis.
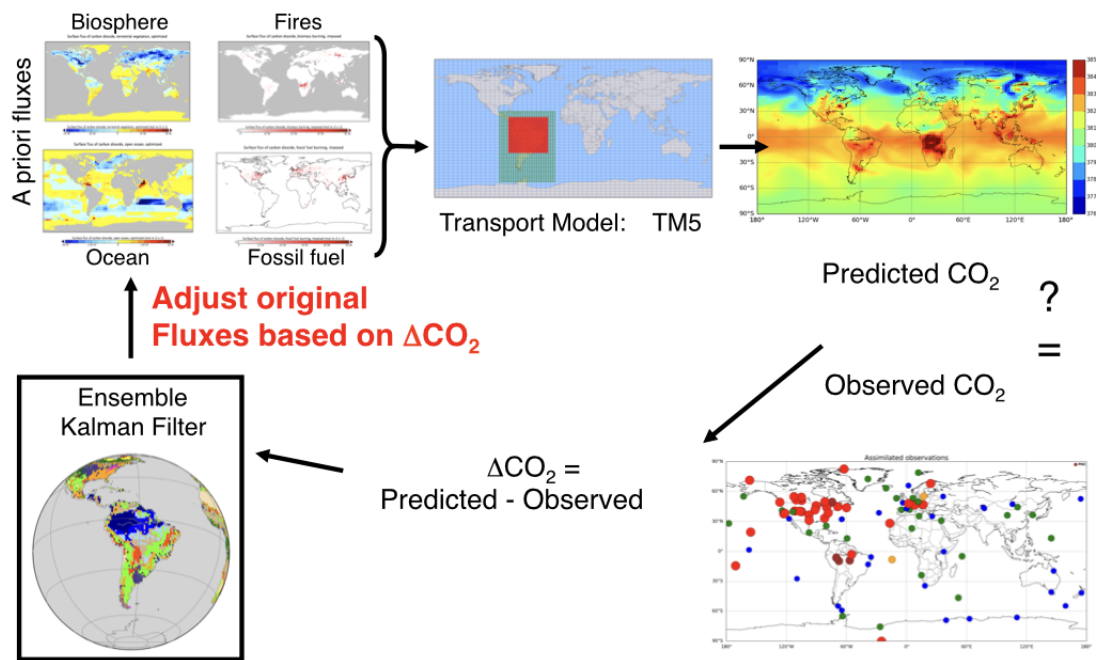
Figure 3: Data assimilation cycle. The ensemble Kalman filter is a data assimilation technique by which differences between simulated and observed concentrations are optimized. Based on [Peters et al., 2005, Van Der Laan-Luijkx et al., 2015]

1.3   Thesis Outline

The following chapters are organized following a step by step approach. Each chapter contains a brief introduction, methods, results, discussion and conclusion sections. It is worth mentioning that although the chapters focus on specific topics they can not be read individually and the structure of the thesis follows a main line of research. The first chapter deals with the first and the second research questions:

> **Research Question 1:** *What are the differences (in terms of yearly values, spatial distribution and biome attribution) between the fire inventories used to calculate fire emissions in the Amazon for years 2010-2015?*
>
> **Research Question 2:** *What is the carbon balance in the Amazon for years 2010-2015?*

In Chapter 2 a comparison of the fire inventories used is presented. In this chapter I also touch upon the net biome exchange obtained from two different biosphere models that are used to estimate a total carbon balance for the Amazon for each year of the study period. Chapter 3, answer the second research question and builds up on the main findings of Chapter 2, by investigating the main drivers of differences between two of the fire inventories, both based on the same burned area input.

> **Research Question 3:** *What are the main drivers causing different emission estimates between SiBCASA-GFED4 and CASA-GFED4, considering they have the same burned area input?*

In Chapter 3, I describe the fire scheme of two biosphere models and illustrate how these models obtain fire emissions from burned area. Chapter 4, answers research questions four and five. It presents the simulated profiles of CO_2 and CO concentrations in four sites of the Amazon. These emissions are provided by the fire inventories described in chapter 2 and their simulated profiles are compared to observations. The simulations are done with the TM5 global transport model, the main settings and drivers of the model are described in the methods section of this chapter. Finally, Chapter 5 summarizes the main conclusions of the previous chapters and provides guidelines for follow up studies. An appendix section follows the last chapter with additional information related to each one of the chapters mentioned. It is worth mentioning that in the appendix a chapter 6 is presented providing a preliminar analysis of an optimized version of the fire inventories. This is part of the follow up recommended in the conclusions and by no means is exhaustive.

> **Research Question 4:** *How well do transported atmospheric CO mole fractions match with CO observations made in four aircraft sites in the Amazon for the period of 2010-2014?*
>
> **Research Question 5:** *How well do transported atmospheric CO_2 mole fractions match with CO_2 observations made in four aircraft sites in the Amazon for the period of 2010-2014?*

Disclaimer: In the present document when the plural "we" is used it means that in that particular context more people were involved. This happens specifically in Chapter 3 and Chapter 4. But in other chapters may also be the case when referring to other chapter's results.

Chapter 2

2 Fire Inventories Comparison and Net Biome Exchange (NBE)

In this chapter the main characteristics of the fire inventories used are mentioned (methods section). The results focus on a regional comparison of these fire inventories for the Amazon. Fire emissions are analyzed form a spatio-temporal perspective, showing the main points of differences. The results are followed by a discussion section, which focuses on the main sources of differences seen in the results and finally the conclusions are presented in the last section.

2.1 Methods and datasets description

2.1.1 Fire inventories description

An overview of each fire inventory is presented based on the articles in which each one was thoroughly described. Here, only main features such as spatial and temporal resolution are mentioned. It is important to note that the following description corresponds to the features of the original datasets. For the forward simulations they were modified to the same spatial and temporal resolution to meet the requirements of further analyses done later on the next chapter using the TM5 global transport model (see chapter 5). The fire inventories listed below, except CASA-GFED4, were also used by Van Der Laan-Luijkx et al. [2015]. A summary of the main features of each fire inventory is shown in table 1.

1. Global Fire Emissions Dataset (GFED4): Provides a global burned area at 0.25 degrees spatial resolution from mid 1995 through the present and daily burned area for a subset of the time series extending back until 2000. The daily dataset is constrained to the Moderate Resolution Imaging Spectro-radiometer (MODIS) era, from 1999 onwards, because neither Visible and Infrared Scanner (VIRS) nor Along Track Scanning Radiometer (ATSR) fire counts provide the capability to predict burned area at a time scale shorter than 1 month [Giglio et al., 2013]. To obtain biomass burning emissions from burned area, biosphere models are used to provide the fuel for combustion according to an imposed land cover. In this project two options were used, one in which GFED4 burned area was coupled to the biosphere model SiBCASA to obtain carbon emissions. And the second, is given by the original GFED4 data available in http://www.globalfiredata.org, which is coupled to the CASA biosphere model; this inventory is called here CASA-GFED4. These models calculate the carbon pools which are then subjected to fire. SiBCASA-GFED4 and CASA-GFED4 have different fire schemes. On one hand CASA-GFED4 has dynamic combustion completeness and mortality whereas SiBCASA-GFED4 has prescribed fire parameters. Moreover, their biome distribution is different, thus these two models with the same burned area are represent two distinct fire inventories in this study. GFED4 burned area includes small fires, an addition to previous versions described in Randerson et al. [2012]. An overview of SiBCASA and CASA models is given below.

A. SiBCASA-GFED4 [Schaefer et al., 2008]: SiBCASA is a combination of the Simple Biosphere model (SiB) version 3 and the Carnegie Ames Stanford Approach (CASA) model. The former (SiB) provides the biophysical part and the latter the biogeochemistry (CASA). The model calculates the exchange of carbon, energy, and water at 10 minute time steps and at a spatial resolution of 1ºx1º degree. The fire scheme in SiBCASA was implemented by Van Der Velde et al. [2014], and the GFED4 spatial resolution of 0.25º was aggregated to a 1ºx1º degree. The burned area is used to calculate fire emissions by using prescribed tree mortality, combustion completeness, fraction of biomass available for combustion and carbon pools in each pixel. This is further described in Van Der Velde et al. [2014]. To obtain emissions from a specific specie, emissions factors can be also used, but in this framework emissions are reported as micro-moles of carbon per unit of area per second (μmolC m^{-2} s^{-1}).

B. CASA-GFED4 [Van Der Werf et al., 2010]: This biosphere prior results from coupling the GFED4 database with the global biogeochemical Carnegie-Ames-Stanford-Approach: CASA Potter et al. [1993]. CASA runs on a monthly time interval and simulates the carbon exchange between the atmosphere and the biosphere. The model estimates carbon stocks which are then burned according to the burned area input from GFED4. CASA has a higher spatial resolution than SiBCASA providing information for 0.5ºx0.5º pixels. The combustion completeness is calculated within the model based on meteorological conditions. In the study Van Der Werf et al. [2010] the modifications to the original modeling framework of CASA are well described. Van Der Werf et al. [2010] provide a partitioning between deforestation fires and non deforestation fires. A key difference from SiBCASA is the dynamic approach of tree mortality which depends on the fraction of tree cover in each pixel. Finally, trace gas emissions are derived using emission factors from Akagi et al. [2011] and Andreae [2001]. Furthermore, CASA-GFED4 provides a diurnal cycle of fire emissions. A percentage of the daily value is assigned to every 3 hourly time step in each day. The percentage for each time step is constant for every month.

2. GFAS [Kaiser et al., 2012]: The Global Fire Assimilation System calculates biomass burning emissions by fire radiative power (FRP). The MODIS instruments aboard the Terra and Aqua satellites provide the observations of FRP, which is the rate of electromagnetic energy emitted by a fire [Randerson et al., 2012]. Using biome specific conversion factors from the GFED database version 3.1 dry matter burned is estimated from FRP [Andela et al., 2013]. The GFAS mechanism has the capability of detecting fires in real time at high spatial (0.5ºx0.5º) and temporal resolution (daily). These data is available online at almost near real time. Biomass combustion rate is calculated from specific land-cover emission factors from Andreae [2001]. Regarding the geographical distribution, the detection of small fires is limited by the pixel resolution: when a fire burns over an area less than 500 x 500 m it is not detected. In this study GFAS version 1 and 1.2 were used. Version 1.2 was used from 22-09-2014 onwards until 2016.

3. FINN [Wiedinmyer et al., 2010]: This product is based on satellite observations of active fires and land cover, together with emission factors and estimated fuel loadings. Active fires are detected with information provided from the MODIS instruments onboard the NASA Terra and Aqua satellites. The dataset provides daily fires with a horizontal resolution of 1km^2. Observations of active fires are used to estimate burned area, instead of FRP as in GFAS. MODIS land cover and vegetation continuous fields products are used to obtain the fraction of woody and non woody vegetation. Each fire count was assumed to be 1 km^2 of burned area for all land cover classes, with the exception of savannas and grasslands which was assumed to be 0.75 km^2 [Andela et al., 2013]. The emission factors used are those reported in the study of Akagi et al. [2011].

Table 1: Summary the main feature for the fire inventories used in this study.

	SiBCASA-GFED4 Van Der Velde et al. [2014] Van Der Werf et al. [2010]	CASA-GFED4 Van Der Werf et al. [2010]
Source of data (MODIS)	Burned Area	Burned Area
Spatial Resolution	1°x1°	0.25°x0.25°
Temporal Resolution	Daily	Daily and 3h
Emission factors	Andreae [2001] [Akagi et al., 2011]	Andreae [2001] [Akagi et al., 2011]
	GFAS Kaiser et al. [2012]	FINN Wiedinmyer et al. [2010]
Source of data (MODIS)	FRP	Active Fires and land cover
Spatial Resolution	0.5°x0.5° degrees	1km
Temporal Resolution	Daily	Daily
Emission factors	Andreae [2001]	Akagi et al. [2011]

2.1.2 Biome Attribution

In this chapter a distribution of the total fire emissions is done according to an underlying land cover map. This is done to have an idea of which of the biomes are contributing to the total fire emission estimates in the defined regions of study and if this contribution changes between fire inventories. The study region is given in Figure 4 and 5. The biome attribution was based on the land cover map used in SiBCASA, which was further subdivided to get a better spatial resolution in the rainforest biome, "Tall broadleaf-Evergreen trees", the most dominant biome in the Amazon. For this the Koppen climate classification was used [Kottek et al., 2006]. Figure 4 shows the biomes of SiBCASA and Figure 5 shows the modified SiBCASA-Koppen land cover. Note that the biome "Tall broadleaf-Evergreen trees" from Figure 4 is further splitted in 3 climate regions in Figure 5 in the region of the Amazon. The fire emissions of each product were associated to the original SiBCASA landcover map (Figure 5). This approach was previously used by Van Der Laan-Luijkx et al. [2015]; therefore in this study was also applied to maintain consistency and make the results comparable. It is worth mentioning that the SiBCASA calculates the carbon pools globally based on the biomes listed in Figure 4.
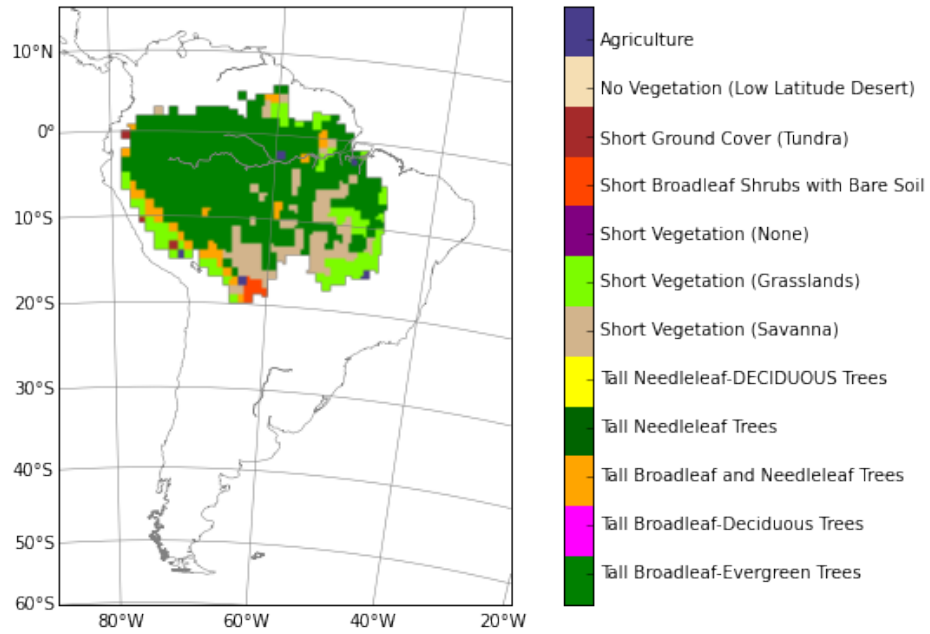
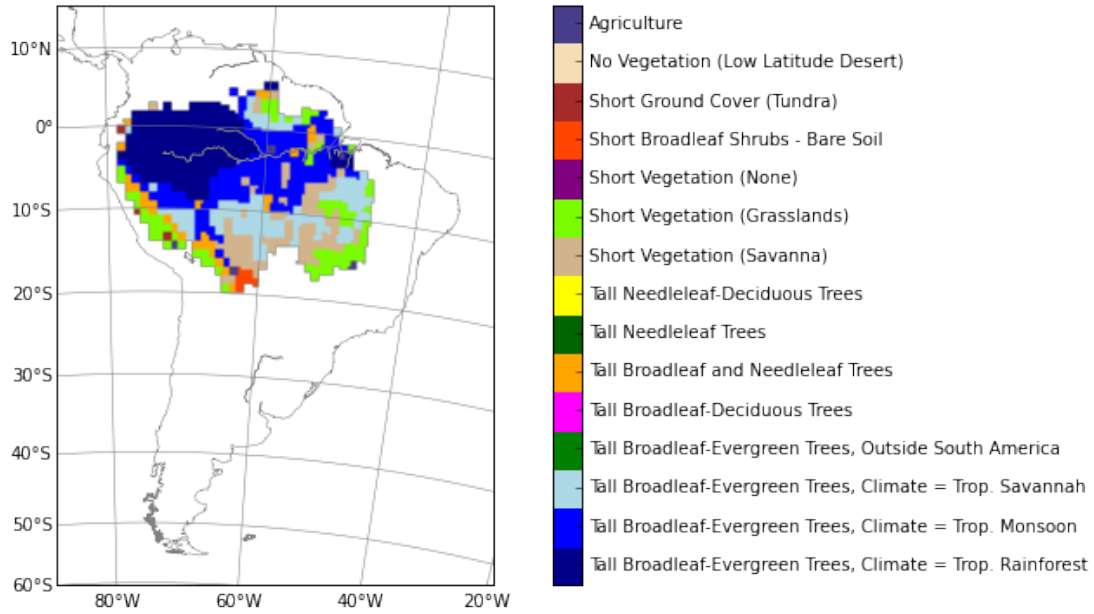Figure 4: Land Cover map used in the SiBCASA model for the Amazon.

Figure 5: Land Cover map used in SiBCASA for the Amazon, with further split into Koppen climate regions in the Amazon.

2.2   Results

2.2.1   Yearly Values and daily time series

Figure 6 shows an annual average biomass burning carbon emissions. All fire products show that 2010 had the highest emissions in the 2010-2015 period. However, there is a large difference between products, ranging between: 0.54 PgC/yr (SiBCASA-GFED4) and 0.24 PgC/yr (GFAS). Note that for 2011 the emissions decreased and the variability between products is much lower; remarkably three of the products report similar values 0.10, 0.08, 0.09 PgC/yr for SiBCASA-GFED4, GFAS, CASA-GFED4, respectively, whereas for FINN I obtained 0.17 Pg/yr. For 2012 the fire emissions increase again along with the variation between fire inventories. The next year (2013) in general has lower emission for all fire products. Note that FINN estimate decreases again in 2014, reaching a value of 0.05 PgC/yr. The other three fire products show increasing values from 2013 until 2015. In Table 2 a detailed summary of the yearly values for each fire product is presented. Biomass burning emissions scale with drought conditions and emissions are therefore larger in 2010 [Lewis et al., 2011, Gatti et al., 2014, Van Der Laan-Luijkx et al., 2015]. The effect of 2015 El Niño event, might be more evident during 2016 fire emissions. It is interesting to note that on average, SiBCASA-GFED4 has higher estimates, GFAS lies on the low side compared to the other fire inventories and CASA-GFED4 and FINN are between the first two mentioned.
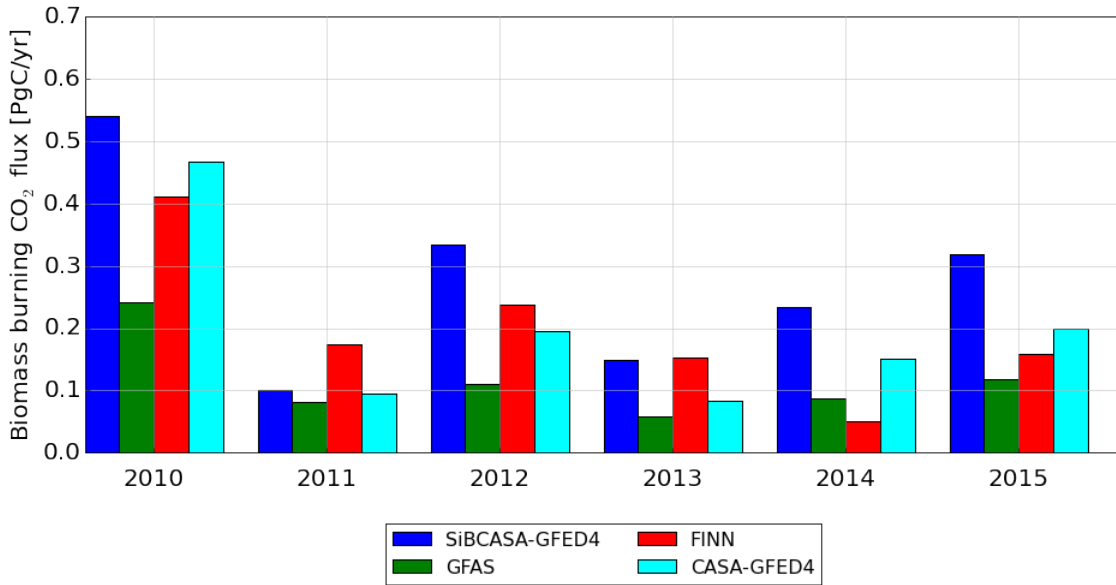

Figure 6: Annual mean carbon emissions from biomass burning according to different fire products: SiBCASA-GFED4, GFAS, FINN, and CASA-GFED4.

Table 2: Annual mean carbon emissions from biomass burning for the years 2010-2015 [PgC/yr]

	Fire					
	2010	2011	2012	2013	2014	2015
SiBCASA-GFED4	0.54	0.10	0.33	0.14	0.23	0.31
GFAS	0.24	0.08	0.10	0.05	0.08	0.11
FINN	0.41	0.17	0.23	0.15	0.05	0.15
CASA-GFED4	0.46	0.09	0.19	0.08	0.15	0.19

In Figure 7 the time series of the daily fire emissions is shown. Note that the y axis range is larger than that for the yearly values. Each value of this graph represent the yearly sum if that value would happen for all days of the year, representing a yearly daily average. The fire season in the Amazon, which occurs generally during the months of August until October, is well captured by all fire products. The maximum daily emissions in the year 2010 clearly exceed those of the following years in each fire product. However the variation between fire inventories is again considerable, mainly in 2010. In addition, notice that the fire season for FINN is stretched towards the months after October for all the years except 2014. Moreover, it is interesting to see the timing of the fire season for each fire inventory. For SiBCASA-GFED4 generally the fire season starts earlier than for the others, the difference is larger compared to GFAS and FINN and compared to CASA-GFED4 is more perceptible in 2010 than for other years.
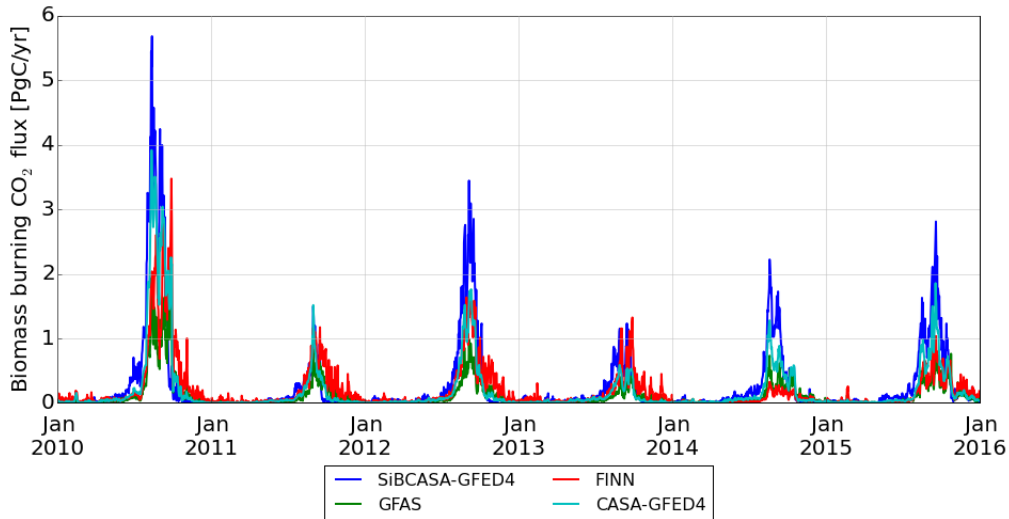

Figure 7: Daily time series of biomass burning carbon emissions in the Amazon for different fire products: SiBCASA-GFED4, GFAS, FINN, and CASA-GFED4. Note that the units PgC year[-1] indicate a yearly average (which represent the value for that particular year if that same estimate would have been present all days of the year).

2.2.2   Spatial Distribution biomass burning carbon emissions in 2010-2015

The spatial distribution for fire emissions was mapped for South America, for each fire product and for 2010-2015. An average for the period of study is also shown (see appendix). For these maps, the original information of each fire product was used in which the units mol C m $^{-2}$ s^{-1} were converted to gC m^{-2} day^{-1}. The spatial distribution of the biomass burning emissions for each fire product are shown for South America in Figure 8. For FINN and CASA-GFED4 the emissions were mostly constrained to the Amazon whereas SiBCASA-GFED4 and GFAS report some emissions more to the south of the Amazon, towards the north of Argentina (GFAS) and east Paraguay (SiBCASA-GFED4). All products show emissions in the east of Bolivia. During 2012, SiBCASA-GFED4 has again the highest emissions spread from east to west, along the 10°S parallel. The other three products follow slightly the same spatial distribution but not with the same magnitude. During 2013 and 2014, GFAS and FINN show low emissions in general, around 0.2 gC m^{-2} day^{-1} while SiBCASA-GFED4 and CASA-GFED4 have several regions with more than 0.6 gC m^{-2} day^{-1}. Finally in 2015, while all fire products have approximately the same spatial pattern their magnitudes differ. However, note that for FINN the emissions are located above the 10°S parallel, for the other products they are along this latitude. SiBCASA-GFED4 has regions with higher magnitudes, whereas the other products with lower. Figure 9 shows the spatial differences between the four fire inventories, where SiBCASA-GFED4 is chosen as a reference. This gives an idea of where are the major differences located. Average fire emissions over 2010-2015 are used to calculate their relative difference and to calculate the ratio between inventories (Figure 9).

The spatial differences shown in the top panel of Figure 9 indicate that SiBCASA-GFED4 has higher emissions relative to the other inventories, mostly in the region northeast of Brazil and north of Bolivia. This could be due to SiBCASA's fire scheme and differences in land cover. In regions like southern Paraguay, where yellow areas are shown, higher values are not consistent for all years. Above zero values are the result of a particular year (i.e 2010). The latter is associated to both SiBCASA's fuel load in those areas and also the burned area reported for that particular location and year in the GFED4 dataset.

In the bottom panel of Figure 9 the ratio of SiBCASA-GFED4 and the added value of SiBCASA-GFED4 and the compared fire inventory (GFAS or FINN, or CASA-GFED4) is shown. A 1 indicates that SiBCASA-GFED4 reports emissions while the other inventory does not; a value of 0.5 indicates that both inventories have the same average fire emissions in that region for the study period; and a value of 0 indicates that SiBCASA-GFED4 does not report emissions in those regions whereas the other inventory does. For the dark blue areas at high latitudes a value of 0 is more likely to indicate that both inventories have no fire emissions detected. It is interesting to see that SiBCASA-GFED4 has higher mean biomass burning carbon emissions in more regions than GFAS, suggesting a lower mean reported by GFAS for the study period. When compared to FINN one can see that there are more pixels along the 10°S parallel that are close to SiBCASA-GFED4's mean, which suggest a better agreement for the 6 multi-year mean between FINN and SiBCASA-GFED4. The ratio between SiBCASA-GFED4 and CASA-GFED4 has more green areas, which is expected because they have the same burned area. However locations with values close to 1 again highlight the fundamental differences between each biosphere model fire scheme.
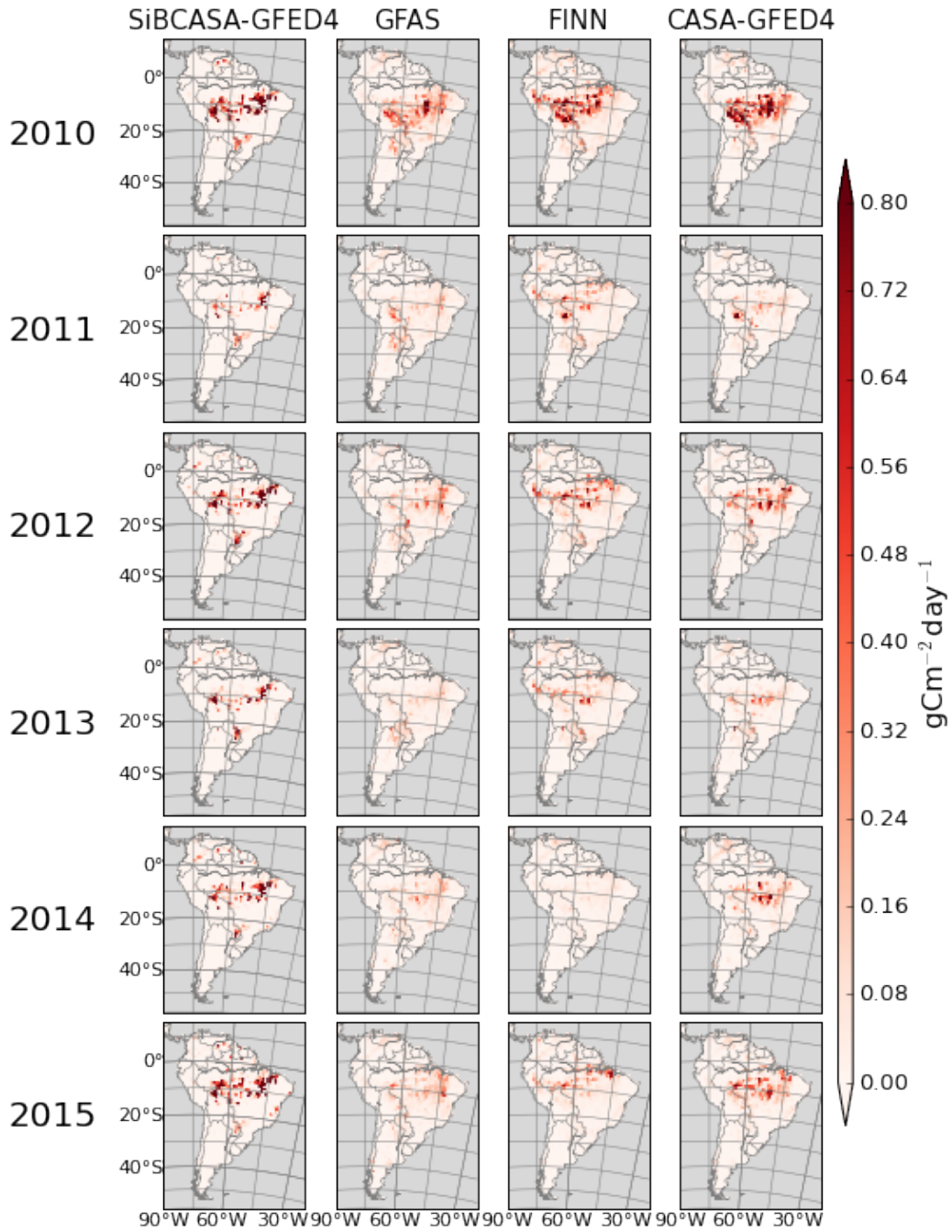
Figure 8: Spatial Distribution of biomass burning carbon emissions (gC m^{-2} day $^{-1}$) for each fire product in South America (2010-2015). Zero indicates that in those areas both inventories have the same average for the study period.
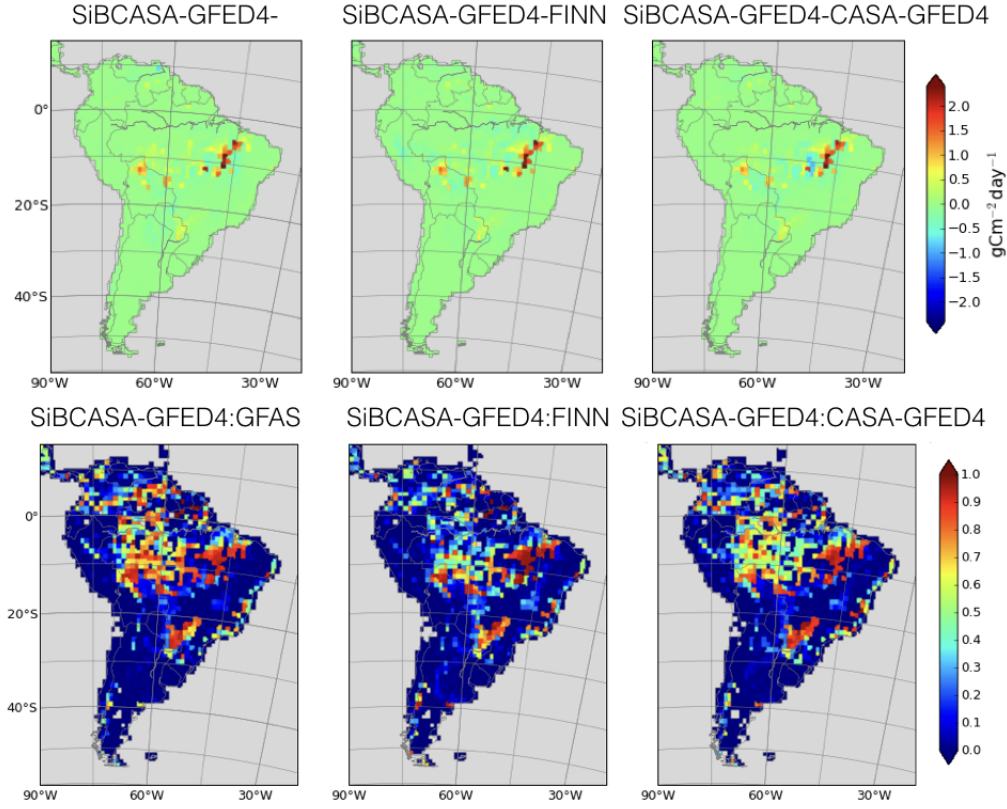
Figure 9: Difference in mean (2010-2015) fire emissions for each fire inventory and SiBCASA-GFED4 (top panel) and ratio of SiBCASA-GFED4 / (SiBCASA-GFED4 + (GFAS or FINN or CASA-GFED4)) (bottom). Note that the bottom panel is unitless as it is a ratio between inventories.

2.2.3 Biome Attribution

The previous spatial differences are now associated to the different biomes present in the Amazon in the SiBCASA model. This is important to see what type of vegetation is being combusted according to each fire inventory. The biome distribution used is based on the SiBCASA land cover map and on the Koppen climate regions [Kottek et al., 2006]. A detailed explanation about the selection of these biomes is provided in the methods section and more general in Van Der Laan-Luijkx et al. [2015]. The latter yields an improved resolution of the biomass burning emissions in the Amazon forest, which in SiBCASA is mainly all defined as Tall Broadleaf-Evergreen Trees (TropFor). This improved biome resolution map was done initially for an atmospheric inversion study [Van Der Laan-Luijkx et al., 2015]. From now on when referring to biomes, these climatic regions are also being considered. The first results in this section refer to a merged year analysis (2010-2015), while in the second part a selected biome analysis is shown. In Figure 10 the percentage of the emissions per biome estimated with each fire product for the 2010-2015 period are shown.

It is important to mention that this biome distribution is all based on SiBCASA's land cover and might not be the same within the other fire inventories' original definitions. Surprisingly, SiBCASA-GFED4 has almost all emissions in TropFor and mainly TropFor: Tropical Savanna, as opposed to the other fire products, which have up to half in Savanna and Grasslands. For GFAS and CASA-GFED4 the TropFor contribution is very similar whereas in FINN amounts to more than half of the total emissions. Furthermore, the emissions associated to Grasslands are not reported in SiBCASA-GFED4, whereas on the other three products they are obviously relevant. The biome Savannah has a minor contribution to the fire emissions of the SiBCASA-GFED4 product, while for the other three products this biome represents at least 25% for FINN and slightly less than 50% for GFAS and CASA-GFED4. Annual differences in the biome distribution are shown in the appendix.
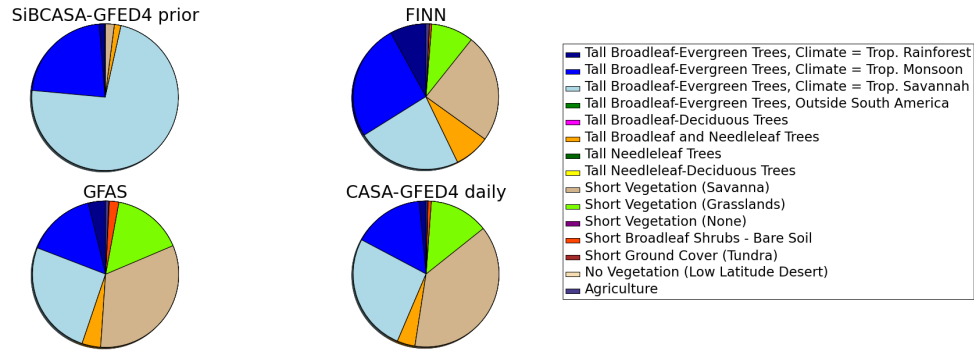
Figure 10: Percent distribution of biomass burning carbon emissions in each biome for the period 2010-2015 for each fire product. The total represents the total sum of emitted carbon for the 2010-2015 period.

In the following results a detailed analysis per biome is presented. The selected biomes were those that had a higher percentage of biomass burning emissions in the previous analysis. The selected biomes and climate regions are: TropFor:Tropical Rainforest, TropFor: Tropical Monsoon, TropFor:Tropical Savannah, Savannah and Grasslands. In Figure 11 the percentual contribution to the total fire emissions in each year is shown for each biome. For the TropFor:Tropical Rainforest all fire products report a rather low contribution to the total, less than 10%, except for FINN in 2013 which reaches slightly more than 10%. In the TropFor: Tropical Monsoon is where the fire products show relatively little variability between them. For each year the difference between the minimum and the maximum percentage is within 8-16%. For the TropFor:Tropical Savannah SiBCASA-GFED4 has the highest percentage, more than 70% for all the years, while the other three fire products are within 20 and 35% for all years. In contrast, the Savannah and the Grasslands biomes are where SiBCASA-GFED4 has the lower percentage compared to the other fire products in all years, which might be explained by the coarser resolution of SiBCASA that could have caused a mismatch between the burned area and the biomes, when aggregating the burned area from 0.25ºx0.25º to 1ºx1º.

Figure 12 shows the absolute fire emissions per biome per year. The TropFor:Tropical Rainforest has indeed low emissions during the 5 year period, following from the low percentage reported earlier. The T-BET:Tropical Monsoon has varying emission magnitudes throughout the 5 years with SiBCASA and FINN having the highest emissions compared to GFAS and CASA-GFED4, except for 2014. Even though there are differences in emission magnitudes, even with similar percentages. In the TropFor:Tropical Savannah biome fire emissions of SiBCASA-GFED4 have rather a high variability, ranging from 0.39 PgC/yr in 2010 to 0.07 PgC/yr in 2011. In the Grasslands, SiBCASA-GFED4 has zero emissions for all years, while the other three fire products have estimated emissions of less than 0.05 PgC/yr, except for CASA-GFED4 in 2010. Even though CASA and SiBCASA had the same burned area input, there are remarkable differences in the biome attribution of the emissions. The latter suggests that there might be discrepancies with the fuel load associated to the land cover map used in the different biosphere models. This will be further considered in the discussion section and in Chapter 3.
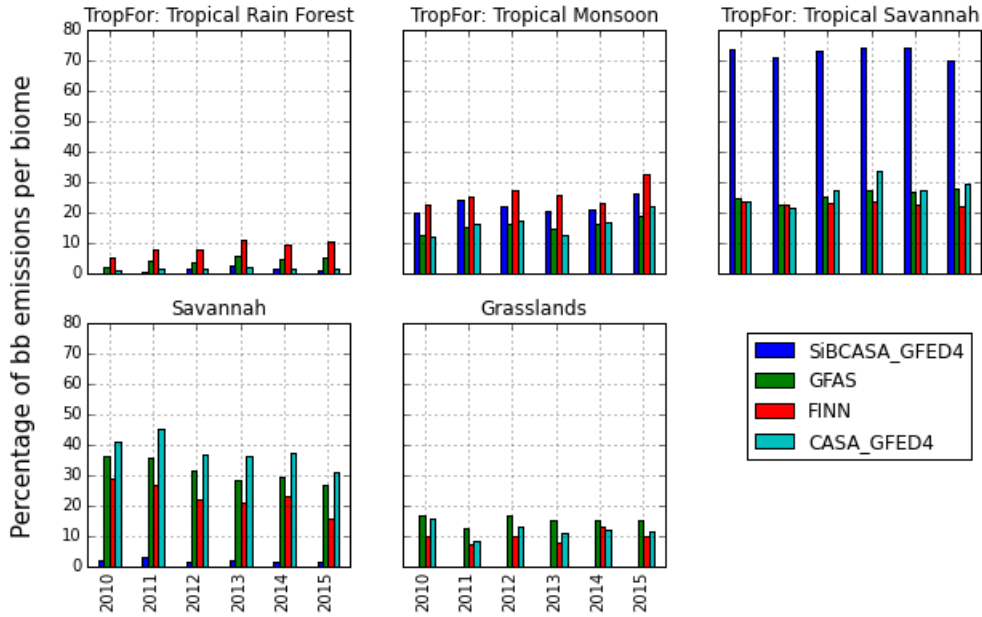

Figure 11: Percentage of biomass burning carbon emissions for each selected biome for the period of 2010-2015 for each fire inventory.
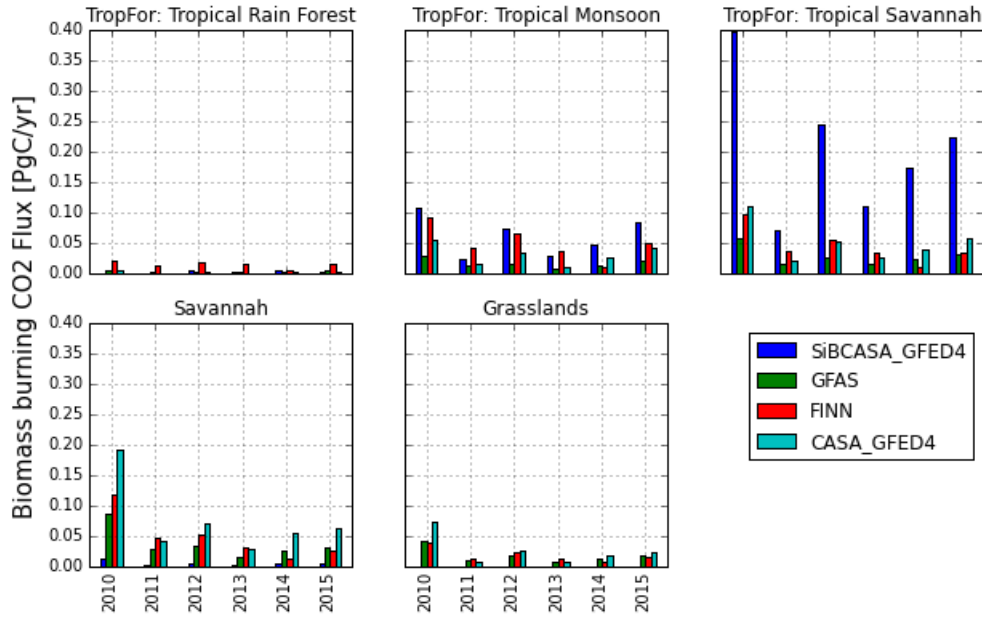
Figure 12: Biomass burning carbon emissions for each selected biome for the period of 2010-2015, according to the fire products used.

2.2.4   Diurnal Cycle for CASA-GFED4

The diurnal cycle is given with the CASA-GFED4 products and as it was mentioned before is the same for each time step in each month. Figure 13 shows averaged fire emissions for each time step in each month and year in the Amazon (region presented in Figures 4 and 5). Note that the time is given in UTC, thus local time is -4 hours considering the time zone of Manaus, Brazil. Therefore the local peak hour of fire emissions would be at 11:00 local time, which corresponds to 15 UTC shown in the graphs. The fire season, according to the diurnal cycle of the CASA-GFED4 product is constrained to the months of August until October, the same as what was seen in the daily time series.

Besides the substantial differences in magnitude when comparing 2010 to other years, note that the fire emission peak alternates between August and September over the study period. For years 2010 and 2014 August was the month in which fire emissions were the highest, reaching 8 PgC/yr and 2 PgC/yr, respectively. Meaning that 8 PgC/yr or 2 PgC/yr would have been the value for all the entire year if that emission would have been reported for all time steps and all days of the year. For years 2011, 2012, 2013 and 2015, September was the peak month, with less than 4 PgC/yr for all years and suggesting a later start of the fire season. In particular 2015 had a rather high late onset of the fire season, which could be already associated to the El Niño event [Jiménez-Muñoz et al., 2016]. It is worth noting that even though the peak emissions changes between August and September, the average fire emissions in each time step are very similar for both. In contrast, in October the magnitude decreases significantly with respect to the previous months (August and September), with relatively high emissions in 2010, 2012, 2014 and 2015. For 2010 it is remarkable that July has a perceptible signal, slightly higher that October, suggesting that the onset in 2010 started before August.
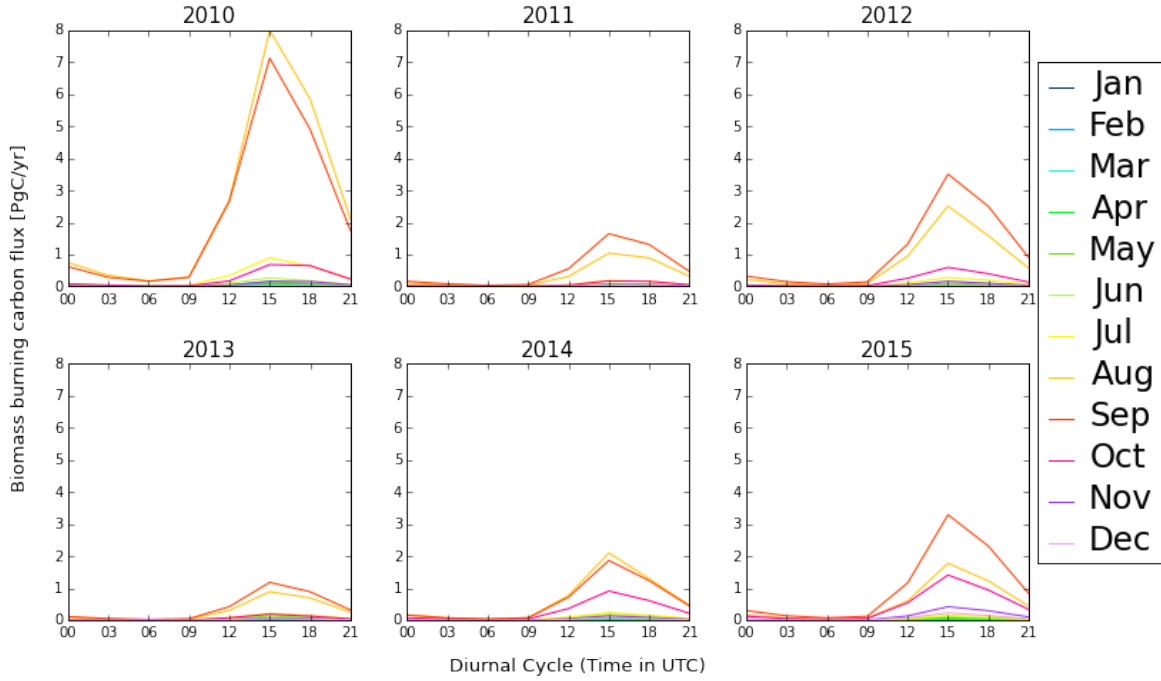
Figure 13: Average fire emissions for each 3 hourly time step in each month and year for CASA-GFED4.

2.2.5 Spatial Distribution of Net Biome Exchange (NBE)

It is worth mentioning that SiBCASA provides a 3 hourly resolution for the NBE whereas CASA has a monthly resolution. For CASA, a further conversion to 3 hourly was done based on its monthly mean and 3 hourly information of temperature and radiation. The spatial distribution of the NBE is shown in Figure 14. The NBE differs notably between the biosphere models. SiBCASA-GFED4 simulates a consistent uptake of carbon throughout the Amazon for all years, without a clear drought response (i.e. 2010). There is a region in the northeast of Brazil where there is a release of carbon, which is present from 2012 until 2015. For CASA-GFED4 the uptake is lower than in SiBCASA-GFED4 and the Amazon even turns into a source of carbon to the atmosphere, particularly in 2010. In 2012 the positive fluxes are present in the northeast of Brazil for CASA-GFED4 as well, but in the following years they weaken considerably. In 2014, there was a release of carbon limited to the central part of the Amazon, which is not visible for the next year, 2015. From this spatial distribution one can argue that CASA has a higher sensitivity for dry periods than SiBCASA, in particular for the 2010 drought in the Amazon.

Figure 14: Spatial Distribution of the NBE simulated for each biosphere model and for the 2010-2015 period in South America.

2.2.6   Carbon Balance

An annual carbon balance for the Amazon was estimated using the annual average fire emissions of each fire product and the Net Biome Exchange (NBE). The total balance was calculated by adding the NBE and Fires as listed in Tables 3 and 4. Note that positive values denote a flux from the biosphere to the atmosphere (release of carbon) and negative values a flux from the atmosphere to the biosphere (uptake of carbon). No NBE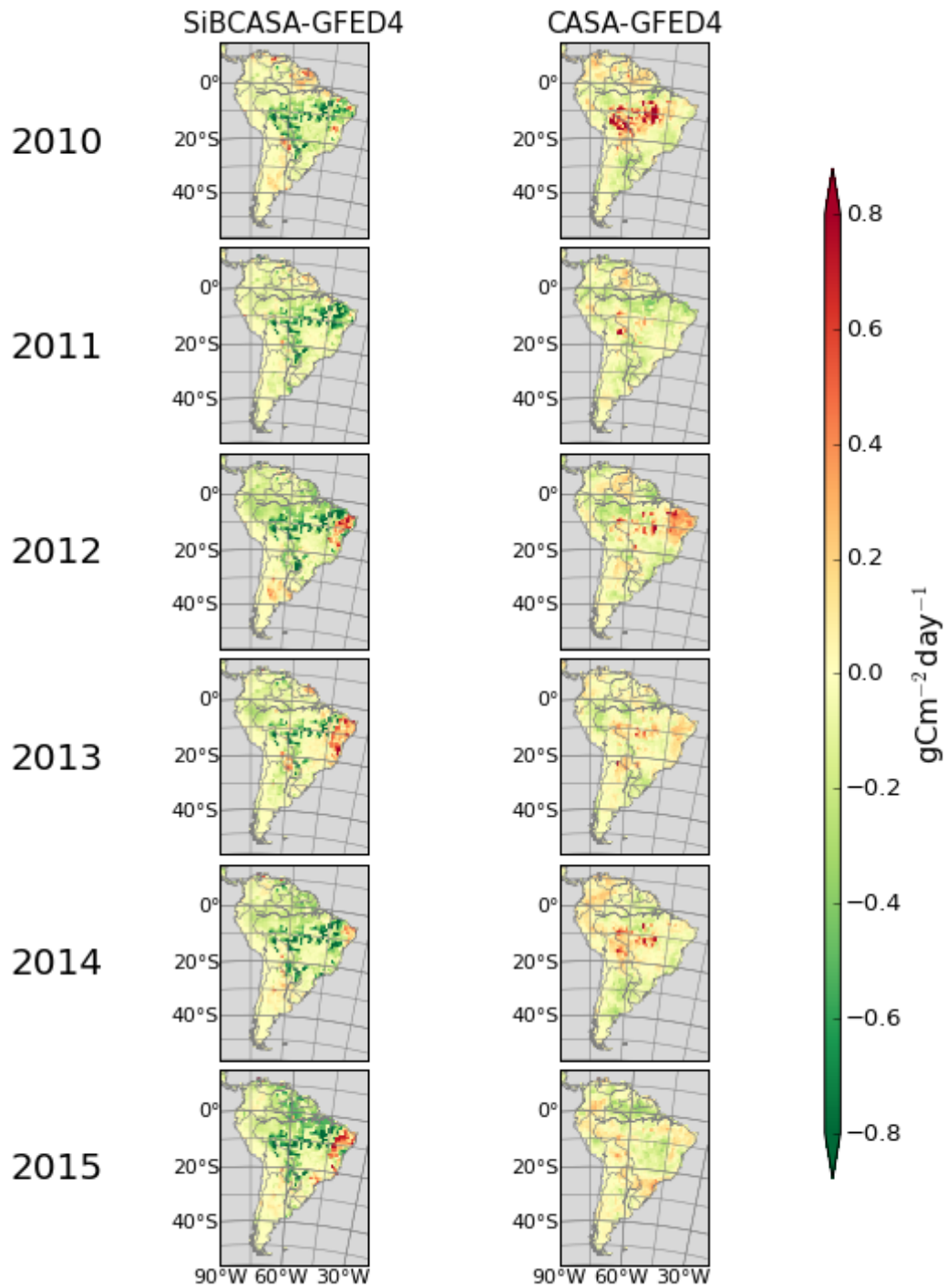 values are attributed to neither GFAS nor FINN, because those products provide direct fire emissions, thus the carbon balance for this two inventories is calculated with SiBCASA-GFED4 NBE values. NBE is different between the two biosphere models. The NBE for 2010 was surprisingly high for CASA-GFED4, which showed a flux to the atmosphere of 0.33 PgC/yr, compared to SiBCASA-GFED4, which estimated a flux to the biosphere of -0.39 PgC/yr. Thus, the former suggests a release, while the latter suggests an uptake of carbon by the biosphere. This happens again in 2014 with -0.52 and 0.11 PgC/yr for SiBCASA-GFED4 and CASA-GFED4, respectively. Years 2011, 2012, 2013 and 2015 are similar in terms of the sign but not in terms of the magnitude, while SiBCASA-GFED4 shows a strong uptake, CASA-GFED4 shows a weak uptake, even close to neutral.

The total carbon balance has interesting results. For 2010 all fire products, except GFAS reported a release of carbon from the biosphere. This is linked to the El Niño event that happened that year which enhanced drought and thus fire emissions as it was already mentioned before [Lewis et al., 2011, Gatti et al., 2014, Van Der Laan-Luijkx et al., 2015]). The next year (2011), all products agree on an uptake of carbon with varying magnitudes, note the relatively small uptake of -0.045 PgC/yr reported by CASA-GFED4. For the next years (2012-2015) SiBCASA-GFED4, GFAS and FINN show a consistent uptake, whereas CASA-GFED4 shows a release of carbon to the atmosphere. In the discussion of this chapter a comparison with other reported values is shown.

Table 3: Annual mean carbon emissions from biomass burning for the years 2010-2015 [PgC/yr]. This Table is the same as Table 2, added here for a complete overview.

| | Fire | | | | | |
	2010	2011	2012	2013	2014	2015
SiBCASA-GFED4	0.54	0.10	0.33	0.14	0.23	0.31
GFAS	0.24	0.08	0.10	0.05	0.08	0.11
FINN	0.41	0.17	0.23	0.15	0.05	0.15
CASA-GFED4	0.46	0.09	0.19	0.08	0.15	0.19

Table 4: Net biome exchange (NBE) for the years 2010-2015 [PgC/yr]

| | NBE | | | | | |
	2010	2011	2012	2013	2014	2015
SiBCASA-GFED4	-0.39	-0.40	-0.60	-0.35	-0.52	-0.68
CASA-GFED4	0.33	-0.14	-0.02	-0.04	0.11	-0.09

Table 5: Prior Amazon carbon budget for the years 2010-2015 [PgC/yr]

	Total					
	2010	2011	2012	2013	2014	2015
SiBCASA-GFED4	0.14	-0.30	-0.27	-0.20	-0.29	-0.36
GFAS	-0.15	-0.32	-0.49	-0.29	-0.43	-0.56
FINN	0.01	-0.23	-0.37	-0.20	-0.47	-0.52
CASA-GFED4	0.80	-0.04	0.17	0.04	0.26	0.10

2.3   Discussion

2.3.1   Yearly values, daily time series and CASA-GFED4 diurnal cycle

It is worth noting that there are several sources of uncertainty for each fire inventory. For FINN, as it is remarked by Wiedinmyer et al. [2010], uncertainties are associated to land cover classifications, fire detections (small fires), the assumed burned area, the biomass loading, the amount of fuel burned, and the emission factors. For GFED4 the total uncertainty for daily burned area is calculated as the combination of: 1. pixel miss-classification when downscaling the MODIS product to a 0.25 degree grid cell and 2. the regression uncertainty when estimating burned area in the pre MODIS era Giglio et al. [2013]. Number 2 does not apply in this study, as the data used was constrained to the MODIS era. For GFAS the biome specific conversion factors from FRP to dry matter combusted are the main source of uncertainty as these factors tend to change in time not only between biomes but also within biomes [Kaiser et al., 2012, Andela et al., 2013].

The fire inventories used in this study were already compared previously at a global scale in [Andela et al., 2013]. In the study regional differences are mentioned but focusing more on hemispheric differences and there is not a detailed analysis for the Amazon. Another difference from that study is the use of a different biosphere model as a source of fuel load for the GFED4 burned area product. Thus, the present chapter provides a zoomed in approach for the region of interest highlighting the main differences between fire inventories. As it was shown before (Figure 6), SiBCASA-GFED4 had higher emissions for all years, with a possible overestimation due to higher fuel loads within the model, a fast forest recovery from one year to the next with a prescribed tree mortality in the fire scheme and a coarse resolution biome map [Van Der Velde et al., 2014]. These differences are more relevant when comparing SiBCASA-GFED4 and CASA-GFED4, as they have the same burned area but different vegetation distribution.

Andela et al. [2013] mention that for some regions of the globe GFAS estimates were in between FINN and GFED (version 3.1) because GFAS is based on the same fire satellite observations as FINN but uses conversion factors derived from GFED to convert fire radiative power to dry matter combusted. This trend is not seen in the results presented here and GFAS was all years in the low side, except for 2014 in which FINN was the lowest. These differences might be explained by the fact that a newer version of GFED was used here and the different period analyzed. An additional reason that might explain why SiBCASA-GFED4 and CASA-GFED4 tend to be higher in the Amazon, is cloud cover in this area. As it mentioned in Andela et al. [2013], cloudy areas might affect FINN and GFAS estimates, as they rely on FRP. Wiedinmyer et al. [2010] also support the limitation that cloud cover presents in each satellite overpass for detection of fires, which may lead to underestimations, in this case by FINN and GFAS. However, in Andela et al. [2013] and Kaiser et al. [2012] also mentioned that GFAS corrects cloud covered areas by assuming the cloudy part of the pixel being the same as the non cloudy part and for completely covered pixels it assigns the last clear observation.

An additional factor that could influence FINN estimates relative to GFAS is that a fire count in FINN corresponds to 1km^2 of burned area, which could be an overestimation for small agricultural fires and on the other hand underestimation of the burned area in locations where it tends to be larger such as Savannas and Grasslands [Andela et al., 2013, Wiedinmyer et al., 2010]. Wiedinmyer et al. [2010] state that the latter tends to cancel at a global scale, but for regional studies this effect has to be taken into account. In regards to the timing of emissions the results presented here (Figure 7) coincide with Andela et al. [2013] showing a better timing of the fire season for FINN and GFAS, somewhat after the timing seen for CASA-GFED4 and SiBCASA-GFED4. From the diurnal cycle of CASA-GFED4 is clear that fire emissions throughout the first months of the fire season (August and September) have the same magnitude, which is similar for SiBCASA-GFED4 as the date of their maximum daily fire emissions coincide but differ for FINN and GFAS.

2.3.2 Biome attribution

SiBCASA-GFED4 for the Amazon region adopted in this study does not have emissions in Grasslands and has very low values in Savannah. This is compensated by high emissions in the Tall Broadleaf Evergreen Trees (TropFor) biome, which indicates that the GFED4 burned area in SiBCASA is burning mainly in the TropFor biome whereas in CASA there is a notable contribution to the total emissions by the Savannah and Grasslands biome. This is unexpected as they have the same burned area input: GFED4. This difference is mainly seen in the year 2010, where CASA-GFED4 had higher emissions in Savanna, of around 0.2 PgC/yr representing more than 40% of the total for than year. It is important to note that in Andela et al. [2013] it is reported that GFED has higher estimates for humid savannas and that FINN emissions for this biome are lower than for GFED and GFAS, in which the largest spatial deviation is found.

The Koppen climate adjustment to divide the TropFor biome suggests that fires in the Amazon are concentrated to the boundaries of the tropical forest where the criteria used by Kottek et al. [2006] to define these regions is: the precipitation of the driest month should be lower than certain threshold in which the mean annual precipitation is taken into account. These areas are likely to coincide with the arc of deforestation in the southeastern part of the Amazon, that in the biome distribution used here are represented as TropFor: Tropical Savanna biome and in CASA as Savannah and Grasslands biome; definitions that might not be precise with reality. The clear differences in percentages and magnitude of fire emissions for SiBCASA-GFED4 in the TropFor: Tropical Savanna biome points again to the differences in carbon pools calculated by the SiBCASA model. The fact that the other three inventories are closer to each other suggests that SiBCASA-GFED4 is likely overestimating emissions (relative to other inventories) by a misrepresentation of the actual type of vegetation present in that area and potentially in others.

2.3.3 Spatial Distribution of Fires and NBE - Carbon Balance

For the spatial distribution of fires emissions and NBE in this study the analysis was done for all South America so fire emissions and carbon exchange outside the defined Amazon region can be seen. In line with Van Der Werf et al. [2010] and Andela et al. [2013] the spatial distribution of fire emissions (Figure 8) correspond to deforestation zones. For years (2013, 2014 and 2015) in which SiBCASA-GFED4 and CASA-GFED4 show clearly more emissions than GFAS and FINN, a possible explanation might be that burned area products like GFED4 are sensible to post burning landscape marks from fires that happened in cloud covered areas as long as the cloud cover is not highly persistent [Randerson et al., 2012].

However, this advantage might be undermined by a wrong representation of the vegetation within a biosphere model, in this case SiBCASA or CASA. Therefore, the spatial analysis supports that SiBCASA is overestimating fire emissions due to larger fuel loads, as it was also mentioned by Van Der Velde et al. [2014]. In the region of northeast Brazil along the 10ºS parallel SiBCASA-GFED4 has a persistent high biomass burning area throughout the study period, which is also seen in other inventories but too a much lesser extent and not for all years. This region is captured in the defined Amazon region but a small portion of the areas farther east are not captured: those along the 45ºW meridian and between the equator and the 10ºS parallel. From the spatial difference shown in Figure 9 one can conclude that GFAS, FINN and CASA-GFED4 have very low emissions or zero emissions in these areas, something that has to be taken into account for regional studies using SiBCASA.

In regards to NBE there are remarkable differences between SiBCASA and CASA. SiBCASA has a sustained uptake whereas CASA has a weaker uptake and for some years (i.e 2010) a net release of carbon. The latter is due to a higher soil respiration caused by the drought that was enhanced by the El Niño event that occurred that same year [Lewis et al., 2011, Gatti et al., 2014, Van Der Laan-Luijkx et al., 2015, Alden et al., 2016]. This aspect, which is not captured by SiBCASA, affects the CO_2 uptake which could be boosted in the biosphere models by a strong CO_2 fertilization effect. It is interesting to note that the uptake regions in SiBCASA coincide with the fire emissions pixels suggesting that carbon uptake and fires emissions are happening in basically the same regions within SiBCASA. Moreover, the differences in NBE can also be associated to the different biome distribution in each biosphere model. This will be analyzed in detail in the next chapter.

The carbon balance shown in Table 5 is highly dependent on the NBE estimated by CASA and SiBCASA. CASA-GFED4 estimates of the carbon budget indicate that this model might be underestimating the carbon uptake for some years, but the magnitude of this underestimations is hard to know, as SiBCASA is, in contrast, showing a larger sink of carbon. For instance, for year 2010 CASA-GFED4 estimates 0.8 PgC year^{-1} released to the atmosphere, whereas SiBCASA-GFED4 estimates is of 0.14 PgC year^{-1}. Compared to other studies, the estimates presented here are within the same order of magnitude, but still show a large variation. For 2010 Gatti et al. [2014] reports 0.48 ± 0.18 PgC year^{-1}, Van Der Laan-Luijkx et al. [2015] 0.07 ± 0.42 PgC yr^{-1} and Alden et al. [2016] 0.72 PgC yr^{-1}.

2.4 Conclusions

A fire inventory comparison has been performed focusing on the Amazon for yearly averages and daily time series. The fire inventories are able to capture the fire season in the Amazon but they present differences for the onset of the fire season and average annual values. These differences are due to fuel load differences and fire scheme for SiBCASA and CASA and more general for all inventories, emission factors, land cover maps, assumed burned area (i.e. FINN) and assumptions within each retrieval algorithm (i.e. for GFAS cloud cover correction). The diurnal cycle, obtained from CASA-GFED4, indicates that at 15 UTC (11 local time) the fire emissions in the fire season reaches its maximum value. August and September are the months in which the onset occurs, varying for some of the years studied. The biome attribution and the spatial analysis of biomass burning carbon emissions provide evidence to conclude that:

1. SiBCASA-GFED4 inventory is overestimating fire emissions in the TropFor: Tropical Savannah biome relative to the other inventories and underestimating fire emissions in the Savannah biome.

2. The regions subject to these clear differences are mainly in the northeast of Brazil where SiBCASA has imposed the presence of 'Tall Broadleaf Evergreen trees' and CASA Savannah and

Grasslands.

3. Using a model specific land cover, in this case, SiBCASA's land cover might give misleading estimates for other burned area based fire products, like CASA-GFED4.

4. Even though SiBCASA-GFED4 has a good agreement at a global scale with other fire inventories [Van Der Velde et al., 2014], when zooming in regionally large differences are found.

5. Models using the same burned area but different fire schemes present large difference in annual average biomass burning emissions and spatial distribution.

It was shown that modeled NBE strongly affects the total carbon budget for particular years. For SiBCASA-GFED4, GFAS, FINN, which all have the same modeled NBE, the Amazon was found to be a net sink of carbon for 2011, 2012, 2013, 2014 and 2015. For 2010 all inventories except GFAS, report a net source of carbon from the Amazon to the atmosphere. CASA-GFED4 showed a different estimate for 2011, 2012, 2013, 2014 and 2015 in which the Amazon was found to be a net source of carbon.

Chapter 3

3   SiBCASA-GFED4 and CASA-GFED4 Comparison: From Burned Area to Fire Emissions

The present chapter aims to investigate why SiBCASA and CASA are estimating different fire emissions while using the same burned area input. In the previous chapter these differences suggested that there are several factors within each model that might be driving these different estimates. The underlying land cover in each model is one of these drivers. Moreover, the fire scheme in each model might also contribute to these differences in which parameters such as tree mortality and combustion completeness directly affect the fuel load given by the aboveground biomass in each model. Therefore general description of each fire scheme is presented in the Methods section. In the results an experiment using CASA's land cover within SiBCASA to calculate fire emissions with the GFED4 burned area is shown as well as a burned area analysis together with fuel load dynamics for SiBCASA. The latter will give an indication of the main factors affecting each model estimates which is important for atmospheric transport studies, in which a good set of fire emissions is needed. Note that in this chapter we refer to SiBCASA and CASA without the GFED4 coupling, because we are dealing with the model itself and not to the fire emissions associated to it. When written SiBCASA-GFED4 or CASA-GFED4 we refer to the fire inventory resulting from this coupling.

3.1   Methods

In the present section the fire scheme of each biosphere model is described. The main mechanisms by which emissions are calculated in each model are highlighted noting their fundamental differences. Posteriorly the experimental set up by which CASA's land cover was represented in SiBCASA for the Amazon is described and finally the main assumptions by which fuel load and fuel consumption were calculated are mentioned. The GFED4 fire inventory was described in the previous chapter and in the general introduction the generic method to calculate fire emissions is described.

3.1.1   Biosphere models fire schemes

The detailed fire schemes of these biosphere models are described elsewhere in detail [Van Der Velde et al., 2014, Van Der Werf et al., 2010], however it is worth highlighting the main mechanisms by which these models calculate fire emissions.

3.1.1.1   SiBCASA fire scheme

The fire scheme in SiBCASA was implemented by Van Der Velde et al. [2014] and the following description is based on their paper. The spatial resolution of the model is coarser than the GFED4 burned area, thus GFED4 burned area was aggregated from 0.25ºx0.25º to the 1ºx1º resolution of SiBCASA. Once aggregated, the burned area is converted to a turnover rate as follows:

$$A = \frac{BA}{GA * S} \tag{6}$$

Where A, (s^{-1}) represents the turnover rate, BA, (m^2) the burned area reported in GFED4, GA, (m^2) the area of each grid cell and S the seconds in each month. This turnover rate is then used to obtain the fire emissions as follows:

$$F_{fire} = A * M \sum_{n=1}^{P} C_p \cdot E_p \tag{7}$$

Where F_{fire} is the total fire flux per grid cell summed for all the p number of aboveground and fine litter pools and calculated in each time step ($\mu mole$ C m^{-2} s^{-1}). M represents the tree mortality ratio given for each biome, C is the carbon stocks in each pool, and E is biomass available for combustion in each pool, also called combustion completeness factor. Table 6 shows the combustion completeness factors and mortality ratios for each pool and biome. Van Der Velde et al. [2014] implemented the fire scheme in SiBCASA assuming that aboveground biomass and fine litter on the surface are affected directly by fires. The fraction of the carbon within the aboveground pools that is not burned is considered dead biomass and transferred to the fine litter pools. The fraction of fine litter pools that is not burned is not further transfered. In SiBCASA's fire scheme peat burning and organic soil combustion are not included.

Table 6: Combustion completeness fractions for each biome and carbon pools. Note that tree mortality is not pool dependent. CWD stands for coarse woody debris, surfmet, surfstr and surfmic stand for surface metabolic, surface structural, and surface microbial, respectively. These represent the surface fine litter pools. This table was adjusted from Van Der Velde et al. [2014], limited to the biomes within the Amazon.

Biomes	Storage	Leaf	Wood	CWD	Surfmet	Surfstr	Surfmic	Mortality
Evergreen Broadleaf trees	0.9	0.9	0.5	0.2	0.9	0.9	0.9	0.9
Broadleaf and needleleaf trees	0.8	0.8	0.2	0.4	0.8	0.8	0.8	0.6
Savanna	0.9	0.9	0.3	0.5	0.9	0.9	0.9	0.05
Grasslands	0.9	0.9	0.3	0.9	0.9	0.9	0.9	0.01
Shrubs	0.9	0.9	0.3	0.9	0.9	0.9	0.9	0.01
Tundra	0.8	0.8	0.2	0.4	0.8	0.8	0.8	0.6
Agriculture	0.9	0.9	0.3	0.9	0.9	0.9	0.9	0.01

3.1.1.2   CASA fire scheme

Despite the fact that the CASA model was not run in this study, the output is analyzed and thus is considered relevant to describe briefly its fire scheme. CASA's main framework was modified by Van Der Werf et al. [2010] and compared to SiBCASA's fire scheme is more complex. For each grid cell in each month the carbon emissions from fires are calculated based on burned area, tree mortality and combustion completeness (CC, fraction of each pool combusted). These parameters are the same in SiBCASA, however, for each carbon pool a minimum and maximum CC is assigned (Table 7). The CC used is then calculated, linearly, based on soil moisture conditions with CC closer to the minimum value under relative moist conditions and closer to the maximum under relative dry conditions .[Van Der Werf et al., 2010].

Table 7: Minimum and maximum combustion completeness factor for different fuel types. These fuel types are represented as pools within the modeling framework. [Van Der Werf et al., 2010]

Fuel Types	CC_{min}	CC_{max}
Leaves	0.8	0.9
Stems	0.2	0.8
Fine leaf litter	0.9	0.9
Coarse woody debris	0.4	0.9

Within CASA's fire scheme there is a class, for each grid cell, to distinguish fire driven deforestation emissions. Moreover, sub-grid cell information on the emissions due to different land cover types, depending on fractional tree cover, is given. The latter also gives the possibility to estimate for each 0.5 degree grid cell the fraction of burned area that corresponds to herbaceous and woody burned area. The deforestation rates are estimated empirically by assuming that deforestation fires are more persistent and can burn for longer time periods. Thus, using active fire detections and burned area in tropical regions where fires are observed consecutively, a cleared area can be estimated. This cleared area is assumed to be the product of fire persistence and wooded burned area within each grid box. From this, vegetations fields can be adjusted over time and account for changes due to fires in the next fire season [Van Der Werf et al., 2010]. A further difference from SiBCASA, is that CASA incorporates a fire induced mortality dependent on the fire persistence. For non deforestation areas the tree mortality of the wooded fraction varies according to the fraction of tree cover in each grid box as described in equation 8. As Van Der Werf et al. [2010] describe in their study, this equation is function of tree cover fraction such that and Savanna and Grasslands type biomes had 1% of mortality that increases as soon as tree cover exceeds 30%, to reach a maximum of 60% when tree cover reaches more than 70%. For deforestation areas this equation was modified to have a mortality ranging from 80 to 100%.

$$M_w = (0.01 + 0.59)/(1 + e^{25x(0.5-TCWBA)}) \tag{8}$$

$$TCWBA = \frac{\sum_{i=1}^{i=20} BA_i \cdot TC_i}{\sum_{i=1}^{i=20} BA_i} \tag{9}$$

Where TCWBA is the tree cover weighted burned area computed from 5% tree cover bins in each grid cell. This TCWBA is then used to obtained the mortality (M_w) as a function of the dynamic tree cover. A detailed explanation of this fire scheme is given in Van Der Werf et al. [2010].

3.1.2 Experimental set up in SiBCASA

In order to study differences due to land cover and fire schemes for SiBCASA-GFED4 and CASA-GFED4 we design two experiments within the SiBCASA model. SiBCASA was run globally from 1851 through 2009 in the study of Van Der Velde et al. [2014]. In 2009 the carbon pools reached equilibrium, which is defined as Net Biome Exchange (NBE) = 0, the standard SiBCASA-GFED4 fire inventory is based on this long term spin up run. In the latter there is no variability due to long term climate change effects. The driver data is used only from 1997-2009, which includes NDVI, meteorology and burned area but in the years prior to 1997 it's internal consistency is checked as is described by Van Der Velde et al. [2014]. For our experiments we did short spin up runs from 2007 to

2009 six times until we obtained NBE = 0. This process was done in a layered form, imposing only one biome type to the entire globe and we did this for each one of the biomes in SiBCASA. Therefore we ended with 13 individual runs. For instance, for the first run the whole world was simulated as being Tall Evergreen Broadleaf trees. For the next run Tall Broadleaf Deciduous trees was the biome simulated and so on for all the other land cover classes. SiBCASA runs on a 1x1 degree grid for all the terrestrial areas of the globe, meaning that it has 14,538 grid points. The model solves energy, CO_2 and water transfer between the atmosphere and the biosphere with a time step of 10 minutes. With the output of each run CASA's land cover was built by identifying for the Amazon:

1. The grid cells that were representing the same biomes in both models. For instance, if a grid cell is Evergreen Broadleaf Forest in CASA and in SiBCASA at this same location the biome is Tall Evergreen Broadleaf trees, there was no further modification of this pixel. The same applies for Savannas and Grasslands.

2. The grid cells that are Evergreen Broadleaf Forest in CASA and at the same location in SiBCASA they are either Savanna or Grasslands. These grid cells were then changed to Tall Evergreen Broadleaf trees.

3. The grid cells that in CASA are grouped in Savanna and Grasslands and in SiBCASA are Tall Evergreen Broadleaf trees. These grid cells, were manipulated in two different scenarios. On one hand it was considered that all the area that meet that criteria was all Grasslands in SiBCASA and on the other, All Savanna. Therefore two experiments were defined: 1. All Grasslands and 2. All Savanna.

3.1.3 Fuel load and fuel consumption in SiBCASA

In SiBCASA the pools that are subjected to fire are those listed in Table 6. Wood, leaves and roots are considered living carbon but note that roots do not burn. Coarse woody debris and surface litter are considered dead carbon and they all burn. These concepts will be used to calculate Fuel Load and Fuel Consumption in SiBCASA. Fuel load (FL) is generally considered as the total amount of aboveground biomass available for combustion [Van Leeuwen et al., 2014]. The fraction of FL that is combusted is given by the combustion completeness (CC) factor. Thus, the product of CC and FL yields fuel consumption (FC), which is the fraction of biomass transferred from the biosphere to the atmosphere due to fires. The first two, FL and CC, are generally given by biosphere models and databases providing values for several type of biomes across the world [Van Leeuwen et al., 2014]. In this work the simulated FL of SiBCASA together with the CC within SiBCASA's fire scheme were used to calculate FC. These estimates were compared to reported values, in particular to those of the study of Van Leeuwen et al. [2014], in which a large amount of fieldwork data on FL and FC was compiled.

For the estimates of FL we used SiBCASA's pools: aboveground woody biomass and total litter carbon. We do not use total living carbon because this output includes the carbon in roots, which are not burned in SiBCASA. The output is given in moles of carbon per square meter (mole C m^{-2}), which is then converted to kgC m^{-2}. By averaging the aboveground woody biomass and total litter carbon over 2009-2015 together with the areas for each biome and the entire Amazon we calculate mass of carbon per unit of area. This is then added to estimate Fuel Load (FL). Averaging the CC factors using those corresponding to the wood and surface pools for each biome we can estimate a averaged CC for each of the biomes. For the Amazon estimates we considered the CC of the wood and surface pools of Tall Evergreen Broadleaf trees. These averaged CC factors are then used to obtain FC. Van Leeuwen et al. [2014] estimates of FL and FC are reported in tonne per hectare (t ha^{-1})

on a dry weight basis. These values are converted to carbon using a dry matter to carbon factor of 0.5, which is reported in that same study. The areas that were used for each of the biomes and the Amazon are listed in Table 14 in the appendix.

3.2   Results

Section 3.2.1 is focused on the description of the land cover used in CASA and SiBCASA for the representation of the Amazon. Afterwards the results of the experiments done building CASA's land cover within SiBCASA are shown. The third section of the results focuses on a burned area analysis and the last section gives a description of the fuel dynamics within SiBCASA.

3.2.1   Biome extent and differences in areas

A closer look to the biomes that are representing the Amazon in SiBCASA and CASA is given in Figure 15. The total area of the Amazon in this study is $7.03 \cdot 10^6$ km^{2}and the percentages shown are calculated with respect to this total. SiBCASA has 66% of Evergreen Broadleaf trees, whereas CASA 81%. The Broadleaf and Needleaf trees biome in SiBCASA is equivalent to Deciduous Broadleaf in CASA which represent the vegetation present in the frontier of the Andes mountain range and the Amazon forest in SiBCASA but in CASA is constrained to the corner between the 20ºS parallel and the 60ºW meridian. For SiBCASA this biome represents 4.8% and for CASA 0.99% of the total area within the Amazon. A considerable difference between land covers is the differentiation of Savanna and Grasslands in SiBCASA which amounts to 26% while in CASA this biome is grouped and represents almost 16%. SiBCASA has a larger agricultural area within the study area (0.85%) but still it might be an underestimation of the real agricultural extent within the Amazon. For CASA the agricultural extent amounts to 0.5%. Shrubs and Tundra add up to 1.5% in SiBCASA and similarly CASA has 1.4% of Shrublands but not accounting for Tundra. These biomes are limited to the same regions approximately: the highlands of the Andes mountain range. From these spatial differences, we can expect higher fire emissions in CASA due a larger extent of tropical forest and less extent of Savanna and Grasslands. As it will be shown in the next sections this is not the case. It is important to note that the native spatial resolution of CASA is 0.25ºx0.25º, the areas reported here were aggregated to 1ºx1º therefore CASA originally has differences within these 1ºx1º grid cells.

In the spatial analysis of Chapter 2 was shown that SiBCASA-GFED4 was overestimating fire emissions relative to the other fire inventories, especially in the region around the 10ºS parallel and the 55ºW meridian. Looking at the biome distribution in Figure 15, SiBCASA and CASA have a mix of broadleaf evergreen trees, savanna and grasslands, but CASA groups the last two biomes which can result in an homogeneous treatment of the fire parameters for two different biomes. Moreover, in SiBCASA there seems to be more broadleaf trees in that area which means more aboveground biomass that could be subject to fire. In the next section a representation of the CASA land cover is done within SiBCASA to estimate fire emissions and get more insight about what is driving the differences between these two models.
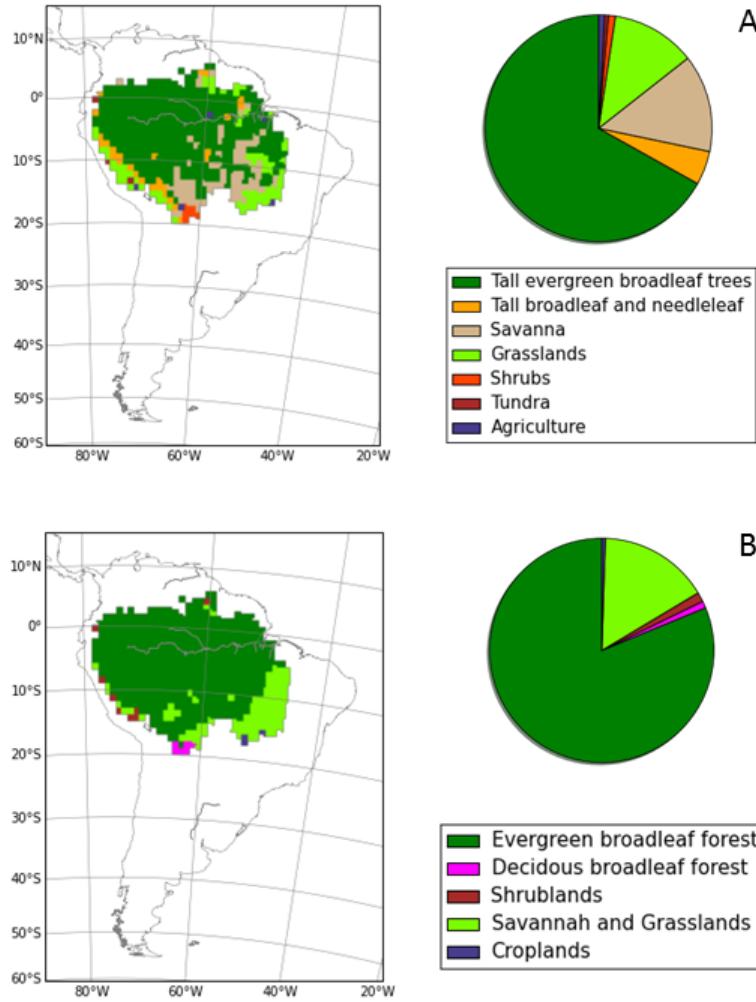
Figure 15: Area distribution (%) for the biomes present in the Amazon for the land cover used by the SiBCASA model (A) and CASA model (B).

3.2.2   SiBCASA-GFED4 experiments with CASA land cover

3.2.2.1   Spatial Mismatch

The CASA land cover was represented in SiBCASA by finding equivalent biomes for each grid cell. For instance, if a grid cell in CASA was found to be Evergreen Broadleaf Forest then the associated emissions of that grid cell would correspond to the Tall Evergreen Broadleaf trees biome in SiBCASA. Figure 16 highlights the regions that were reassigned in SiBCASA to built the CASA land cover. The light green areas correspond to the areas that in CASA represented Savanna or Grasslands while in SiBCASA they represented Tall Evergreen Broadleaf trees. Depending on the experiment these grid cells where either assigned to Savannas or Grasslands in SiBCASA.

The dark green regions are adding emissions to the Tall Evergreen Broadleaf trees biome in SiB-CASA, as they changed from being Grasslands, in the former SiBCASA land cover, to Tall Evergreen Broadleaf trees. The tan regions represent regions that in CASA are Evergreen Broadleaf Forest but in SiBCASA are Savanna, thus they were changed to Tall Evergreen Broadleaf trees. In summary, if a grid cell in CASA had the same biome as in SiBCASA this grid cell did not change. But if the pixel differs with respect to SiBCASA's map, it was assigned to the SiBCASA biome that correspond to that CASA biome. The representation of CASA's land cover in SiBCASA meant that the extent of the Tall Evergreen Broadleaf Forest grew from $4.7 \cdot 10^6$ km^2 to $5.7 \cdot 10^6$ km^2 and that the area subject to the experiments was $0.3 \cdot 10^6$ km^2. In the next section the resulting emissions of the experiments are shown.
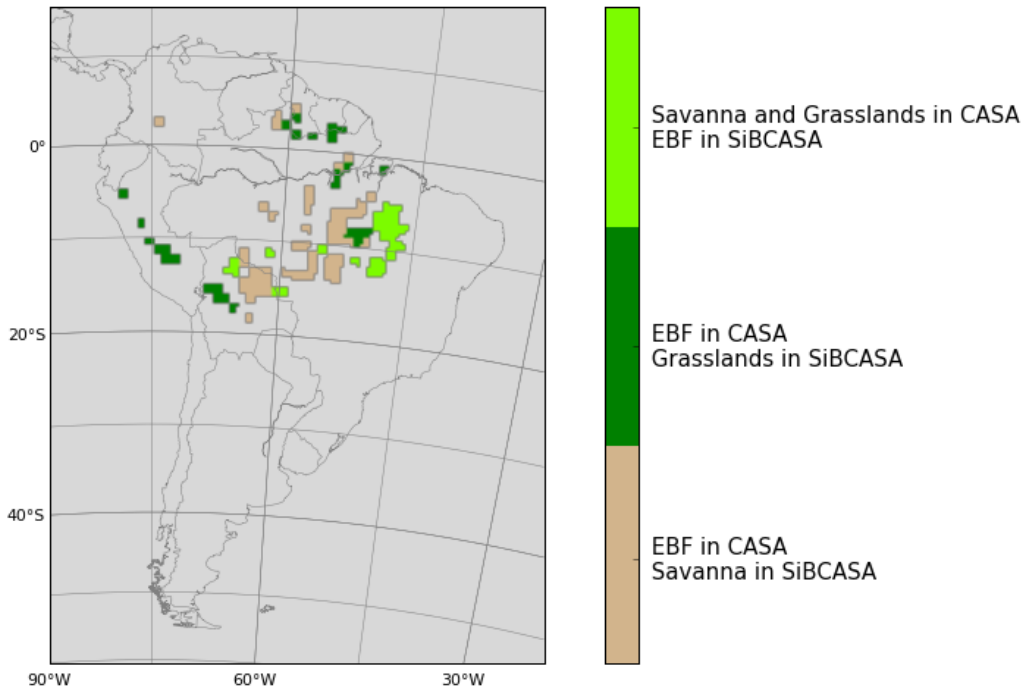

Figure 16: Spatial reassignment of grid cells in SiBCASA to build the CASA land cover. Note that EBF stands for Evergreen Broadleaf Forest.

3.2.2.2 Yearly Emissions

CASA has Savanna and Grasslands grouped together in one biome, whereas SiBCASA has both biomes separated, therefore two experiments were created in SiBCASA: 1. All savanna and 2. All grasslands. In Figure 17 the yearly averages for these two scenarios are compared to the previous fire inventories. Considering that the same burned area is used in both models and that the biome areal extent after the grid cell reassignation resulted in same biome areas in both models, it was expected to have similar estimates as CASA-GFED4. The latter, under the assumption that land cover is the only source of differences. However it is interesting to see that in both cases emissions tend to increase relative to GFAS, FINN and CASA-GFED4, but not always relative to SiBCASA-GFED4. The latter occurs for 2010, 2011 and 2015. This can be explained because CASA has 20% more Evergreen Broadleaf Forest than SiBCASA which means that there is considerably more biomass

available for combustion. However, this does not explain the almost equal estimates for 2012, 2013 and 2014. A possible answer to this might be that SiBCASA treats combustion differently in Savannas and Grasslands than CASA which will be leading to a very low contribution of these two biomes to the total fire emissions. Differences in fuel load can be the cause of the differences between the All Savanna and the All Grasslands scenarios, where the former tends to have slightly higher emissions. A monthly time series for both of the experiments and the other fire inventories can be consulted in the appendix.
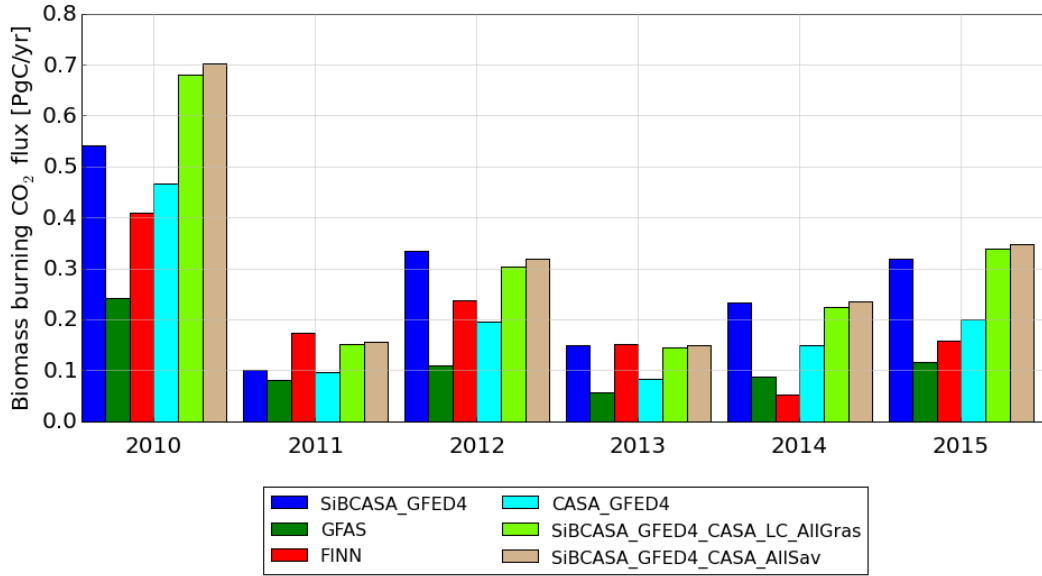

Figure 17: Yearly averages of biomass burning CO_2 emissions according to different fire products: SiBCASA-GFED4, GFAS, FINN, and CASA-GFED4, including the two experiments with CASA land cover within SiBCASA: 1. All Grasslands and 2. All Savanna.

3.2.2.3   Biome Attribution

For these experiments a distribution of the total emissions in the biomes present in the Amazon was done. The total emissions correspond to the accumulated fire emissions in all the simulation period. For this distribution the default land cover in each biosphere model was used. The contribution of the CASA and SiBCASA biomes to the total emissions is shown on Figure 18. Note that the experiments are reported with the CASA biome classes. It is interesting that the experiments have a very similar contribution to the standard SiBCASA-GFED4 even though they have CASA biome distribution. The All Savanna experiment attributes 3% of the total fire emissions in 2010-2015 to the Savanna biome. Tall broadleaf evergreen trees biome has 96.8% of the total emissions for this same period. In this experiment emissions for the other biomes are so low that their contribution is minor on the pie chart. In the All Grasslands experiment Tall Broadleaf Evergreen trees biome has 99.8% of the emissions, whereas the Grasslands biome 0.05%. The latter suggests that the magnitude of total emissions decreased in the All Grasslands experiment and the contribution of Grasslands to the total is less, even though in both experiments the area is the same for the two biomes: Grasslands and Savanna ($1.12 \cdot 10km^2$, 16%, see Figure 15 and Table 15 in the appendix).

In SiBCASA the area of Savanna is less than in CASA, which explains the 1.97% of their contribution in the SiBCASA-GFED4 fire inventory to the total emission magnitude. For the CASA-GFED4 inventory is clear that the contribution of the Savanna and Grasslands biome is much higher compared to both SiBCASA standard and experimental runs; Savanna and Grasslands account for 33% of the total emissions whereas the Evergreen Broadleaf Forest biome to 67%, less relative to the SiBCASA experiments. The latter suggests that Savanna and Grasslands in the CASA model are contributing with more emissions to the total, even if this biome is represented in SiBCASA with the same areal extent. This result is to some extent counter intuitive, as a higher contribution of Savanna and Grasslands was expected in the two experiments. However, in the following sections the main reasons that are triggering this are described.
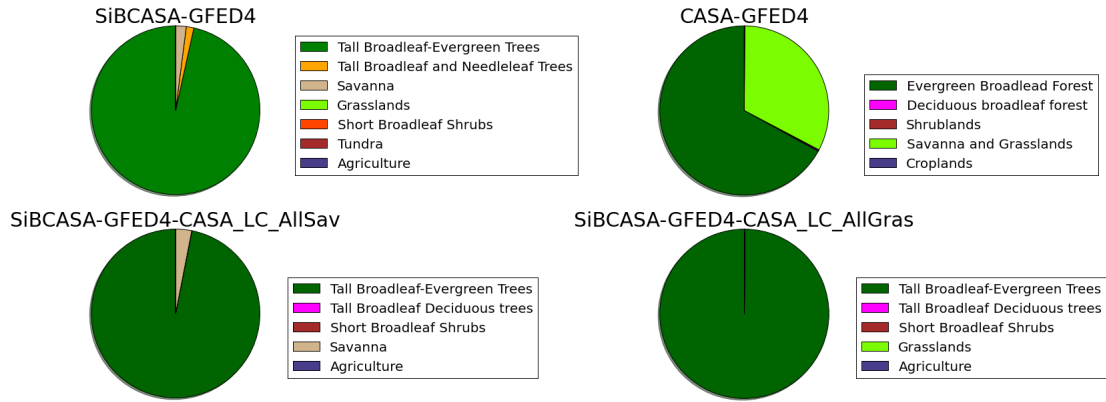

Figure 18: Biome specific contribution to biomass burning CO_2 emissions for each biosphere model and the experiments done in SiBCASA with the CASA land cover. The percentages are calculated with the complete 2010-2015 period as the total. Note that the biomes listed for each of the experiments are those of SiBCASA that are equivalent to the original CASA biome distribution.

3.2.2.4 Burned Area Analysis

As it was mentioned in Chapter 2, the GFED4 burned area was aggregated from 0.25°x0.25 to 1°x1° to meet SiBCASA's spatial resolution. Here this area is used to distribute the amount of burned area in each land cover and thus link the burned area in each biome to the contribution of this biome to the total emissions. The burned area is given as fraction of each 1°x1° grid cell that burns. Despite that the area in each grid cell changes with latitude and considering that this variation in the Amazon is minor, we provide a grid cell area of 12,000 km². With this assumed grid cell area the fraction burned per grid cell can be easily interpreted from Figure 19. In addition, even though the burned area analysis is constrained to 2010-2014, it still provides insight of the areas of consistent fires throughout the years and it enables association to the simulated land cover in each biosphere model. Burned area for each year varies considerably (Figure 19), for the year 2010 more intense fires occurred thus it is possible to see some regions where 20% to 40% of the grid cell was burned. This alternates in the following years after 2010, showing relatively high burned area fractions every other year. Recalling the biome distribution seen in section 3.2.1 it is seen that most of the burned area is concentrated in the Savanna and Grasslands regions of CASA and the Savanna, Grasslands and Broadleaf forest of SiBCASA below the 10°S parallel and between the 60°W and 45°W meridians.
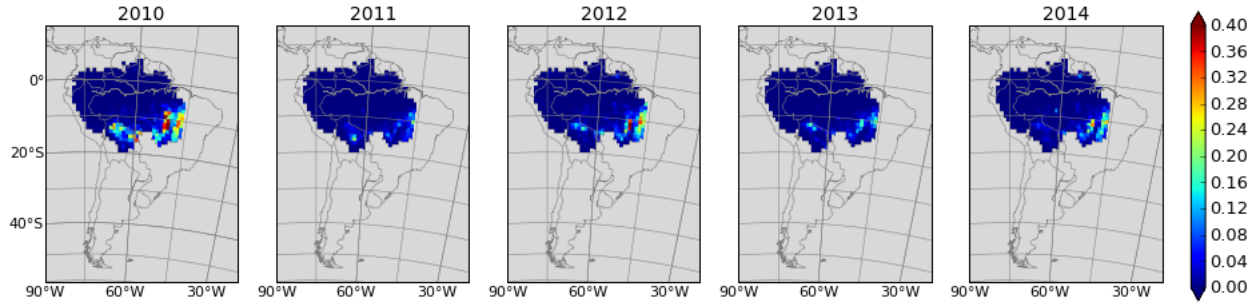
Figure 19: Total fraction of burned area per pixel in the Amazon for 2010-2014. As a reference the 1°x1° grid cell area in the Amazon oscillates around 12,000 km^2. The dark blue areas are places that did not burn during that particular year.

The average burned area in the period 2010-2014 for the Amazon was 107,000 km$^2/yr$ and the following partitioning is based on this average as a total. It is worth noting that for this analysis we used the exact grid cell areas for Amazon region. When associating the average burned area in the Amazon with the biomes in each land cover we estimate that their contribution to the total averaged burned area (107,000 km$^2/yr$) for 2010-2014 is as given on Table 8. In SiBCASA, Savanna had the highest burned area in those years followed by the broadleaf trees and then by Grasslands. For CASA's biomes we estimate Savannas and Grasslands were the main contributor to the total burned area, followed by Evergreen Broadleaf Forest. When adding up the burned area of Savannas and Grasslands in SiBCASA we obtained 68,500 km^2, which is 7,500 km^2 less than for Savannas and Grasslands in CASA, meaning that even though the biosphere models have a different biome distribution the total burned area for these biomes is similar. For the broadleaf forest biome, in contrast, SiBCASA has 3,700 km^2 more of burned area than CASA, regardless of the fact that this biome is larger in CASA than in SIBCASA. This can be explain by looking at the regions where the burned area is concentrated, SiBCASA has more broadleaf forest in these areas than CASA. It is interesting to see that within SiBCASA the difference between fire emissions coming from Tall Evergreen Broadleaf trees, and Savannas and Grasslands biomes is larger than in CASA (see Figure 18), even when the burned area for Savannas and Grasslands in CASA amounts to 65%.

Table 8: Averaged (2010-2014) burned Area for each biome in CASA and SiBCASA land cover. The total averaged burned area for the Amazon is 107,000 km^2. Note that these percentages do not add up to 100% because the contribution of smaller biomes (tundra, agriculture, deciduous forest) was neglected. Grid cell area differences were taken into account.

SiBCASA	km^2	%
Tall Evergreen Broadleaf trees	33,700	32
Savanna	41,500	39
Grasslands	27,000	26
CASA	km^2	%
Evergreen Broadleaf Forest	30,000	28
Savanna and Grasslands	76,000	71

Looking at the spatial distribution of the averaged burned area for the SiBCASA and CASA land covers it is possible to confirm that SiBCASA is burning tropical forest where CASA has a large extent of Savanna and Grasslands (Figures 20 and 21). However, when CASA's land cover is represented with SiBCASA's carbon stocks we do not get the fire emissions expected from these biomes, as it was shown in Figure 18. From Table 19 and Figure 20 we see that in SiBCASA the Tall Broadleaf Evergreen trees are dominating biomass burning emissions with less burned area than Savanna, and Grasslands and with a very low contribution the these last two biomes. In CASA we have the same pattern, less burned area in Evergeen Broadleaf Forest, but the contribution from Savanna and Grasslands is larger.
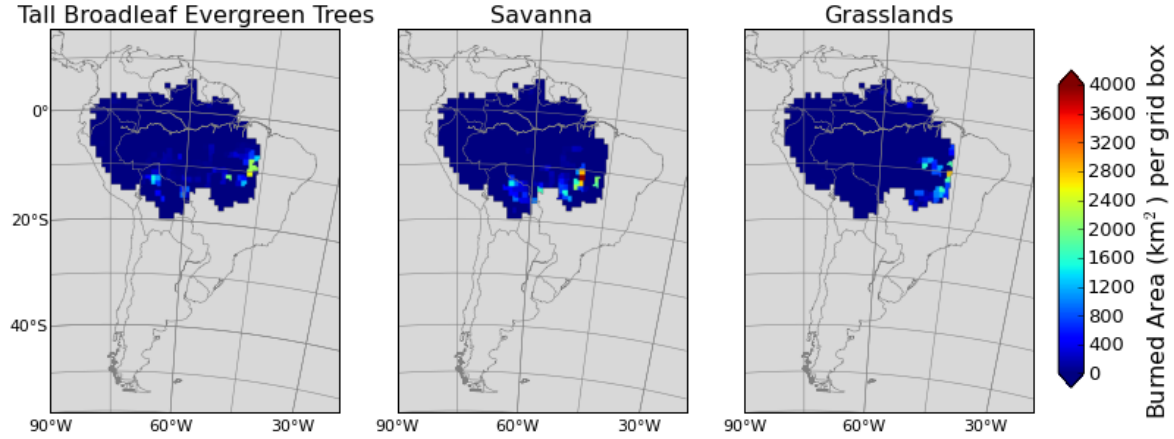

Figure 20: Burned area per grid cell averaged over 2010-2014 for the main biomes in the Amazon simulated by the SiBCASA model
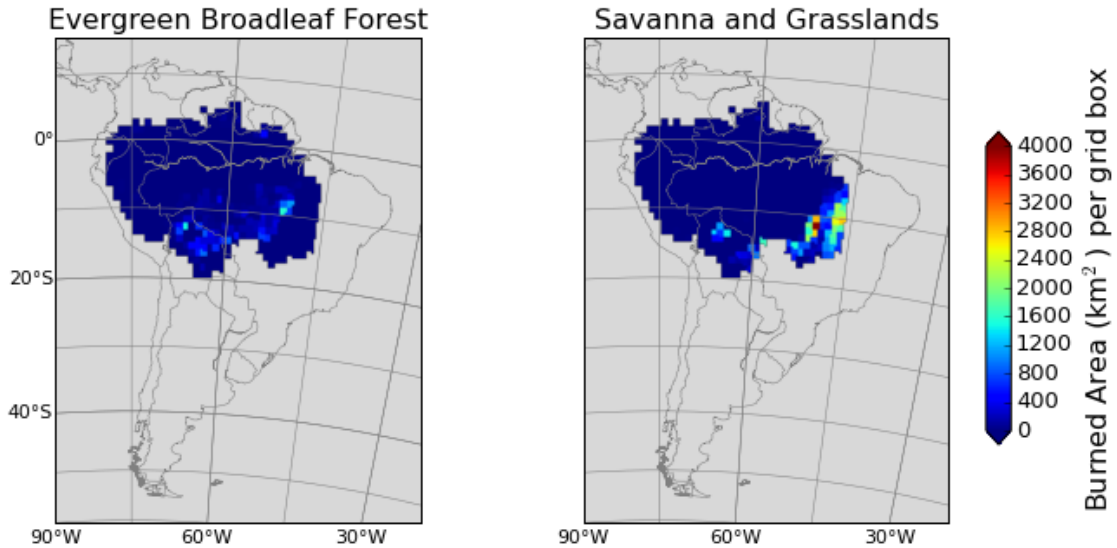

Figure 21: Burned area per grid cell averaged over 2010-2014 for the main biomes in the Amazon simulated by the CASA model

3.2.2.5   Fuel Dynamics in SiBCASA

The amount of carbon prone to fire is one of the main drivers of the estimated emissions in both biosphere models. In this section an analysis of the carbon pools that are subjected to fire in SiBCASA's biomes is presented. We focus mainly on the partitioning of these pools in the Tall Evergreen Broadleaf trees, Savanna and Grasslands biomes, but also on the Amazon as a whole. The total living carbon per unit of area was estimated from Figure 42 and Table 14 in the appendix. For the entire Amazon we obtained 21.7 kgC m^{-2}, for Tall Evergreen Broadleaf Forest 30.52 kgC m^{-2}, for Savanna 5.5 kgC m^{-2}, and for Grasslands 0.3 kgC m^{-2}. The living carbon pool is divided in leaves, roots and wood pools, thus it is important to note that not all of these pools are subject to fire. Roots do not burn and for the wood and leaves pool, SiBCASA determines the available biomass for combustion for each biome and each carbon pool with the combustion completeness factor (see Table 6). Based on the aboveground woody biomass in Figure 22 (which do not include leaves nor roots), and the areas of each biome we estimate on average (2009-2015) the following: for the Amazon 15.8 kgC m^{-2}, for Tall Evergreen Broadleaf trees 22 kgC m^{-2}, for Savanna 3.9 kgC m^{-2}, and for Grasslands 0.06 kgC m^{-2}. These estimates represent a portion of what is burned in SiBCASA in each biome. As it is seen on Figure 22, the evolution of this biomass in each biome presents a fast recovery after each fire season. In some cases, for the next fire season the amount of carbon is back to the initial value relative to the previous year before the fire season. The latter is important from the fuel load perspective, as it seems that in SiBCASA the fuel load is affected by a short time period after each fire event.

To estimate the FL for each of these biomes we considered that the fuel prone to fire and given in SiBCASA's output was the aboveground woody biomass plus the total litter carbon (see Figure 43 in appendix). Here we are neglecting the coarse woody debris, which is also affected by fires according to SiBCASA fire scheme, but is not in SiBCASA's output. The resulting fuel load (FL) is given on Table 9. In order to be able to compare SiBCASA's estimates to what has been published [Van Leeuwen et al., 2014], we calculate fuel consumption (FC), which is obtained from FL and combustion completeness (CC). For these estimates we averaged the combustion completeness of the surface pools and the wood pool for each biome (Table 6) as it was described in the Methods section of this Chapter.

Table 9: Fuel load for the Amazon, and the main biomes analyzed here: Tall Evergreen Broadleaf trees, Savanna and Grasslands. Note that the fuel load is calculated by adding the pools total carbon litter and aboveground wood biomass for each pool.

SiBCASA	FL[kgC m^{-2}]	CC	FC [kgC m^{-2}]
Amazon	19	0.7	13.3
Tall Evergreen Broadleaf trees	27	0.7	18.9
Savanna	4.3	0.6	2.58
Grasslands	0.16	0.6	0.09

The FC is clearly something that triggers differences between CASA and SiBCASA vegetation dynamics and consequently on the fire inventories associated to them. Moreover, the total living carbon and the aboveground woody biomass in the Amazon simulated in SiBCASA is mainly Tall Evergreen Broadleaf trees and it tends to increase over time due to the CO_2 fertilization effect which is quite strong within the model. Therefore, most of the fuel that is combusted in SiBCASA comes from this biome, from which 90% (0.9 Mortality fraction, see Table 6) is dead after a fire event and which is then efficiently turned into emissions, as given in Table 6 for each one of the living carbon pools

excluding roots. The uncombusted fraction of these pools are transferred to the surface litter pools, where they are subjected to fire during the next fire event. The uncombusted fraction of these pools is not further transferred [Van Der Velde et al., 2014]. For Savannas and grasslands there is a lower mortality which means that less of the available fuel dies after a fire event and thus the emissions would be less even if the combustion completeness is high for each living pool. The CO_2 fertilization effect is also strong for the Savanna biome whereas in Grasslands it does not have any effect on the aboveground wood biomass nor living carbon. The former varies without any increasing nor decreasing trend until 2015 when it decreases steeply. It is clear that in SiBCASA the biomes Savanna and Grasslands are affected by the fire season as a decrease of the aboveground carbon biomass is shown between the months of August and November.
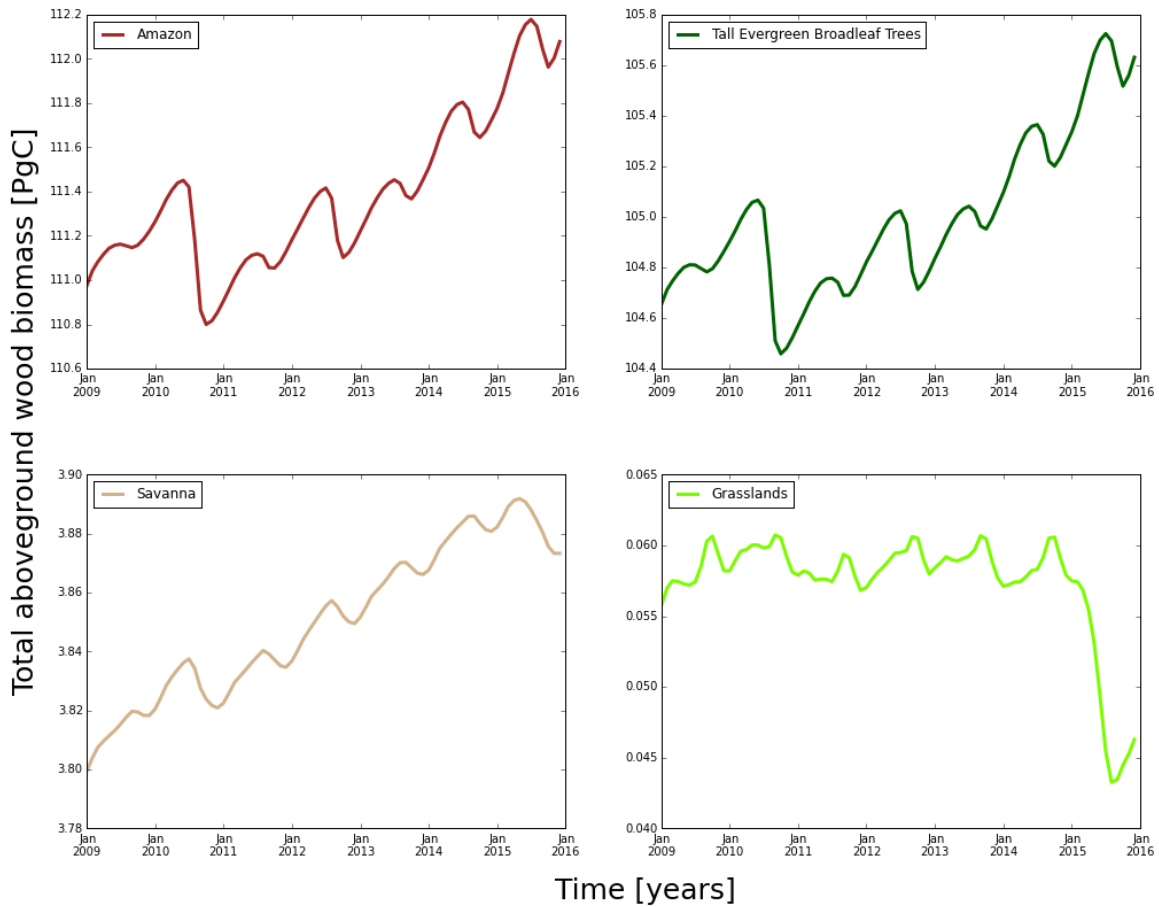

Figure 22: Total aboveground woody biomass evolution (2009-2015) for all the Amazon and the main biomes within the Amazon area: the Tall Evergreen Broadleaf trees, Savanna and Grasslands biomes. Note the different y axis.

3.3 Discussion

In this Chapter CASA's land cover was represented with SiBCASA's carbon stocks to found that regardless of having the same land cover distribution, the experiments resulted in higher fire emissions estimates than in CASA-GFED4 and in some years than SiBCASA-GFED4. When looking at the contribution of each biome to total emissions in 2010-2015 it was found that Savanna and Grasslands in SiBCASA have a minor contribution to the total and, more than 95% of emissions are due to Tall Broadleaf Evergeen Trees. The latter was unexpected as the land cover of CASA has Savanna and Grasslands grouped in one class, which results in a larger areal extent compared to the separate biome classes in SiBCASA. Furthermore, the burned area was shown to be concentrated in the regions where Savanna and Grasslands are present in CASA's biome; supporting the fact that the low emissions of this biome in the experiments are due to, fundamentally, low fuel load and fuel consumption. In contrast, for Tall Evergreen Broadleaf forest fuel load was one to two orders of magnitude higher than Savanna and Grasslands.

Regarding the differences in yearly averages of biomass burning CO_2 emissions between the experiments performed, and SiBCASA-GFED4 and CASA-GFED4, the following can be explained. For 2010 and 2011 both experiments were higher than SiBCASA-GFED4 set up mainly because the burned area for those years using CASA land cover increased in the tropical forest, which has a high mortality (0.9) and high combustion completeness for the leaf (0.9) and wood (0.5) pools. For the next years (2012, 2013 and 2014) the two experiments, even having a larger area of tropical forest (given by the CASA land cover), had very similar fire emissions to the standard SiBCASA-GFED4 inventory. This was driven by two main reasons. The first one is related to a decrease in burned area for these years over the tropical forest. The second one is associated to a very low mortality for the Grasslands (0.01) and Savanna (0.05) biomes. Even though the burned area within these biomes increased for these years with respect to SiBCASA-GFED4, a low mortality affects the overall fire flux, as given in equation 7. The latter explains also the absence of emissions in Grasslands in SiBCASA-GFED4 and is also supported by the Figures 41 and 40 in the appendix. These experiments showed that Tall Evergreen Broadleaf trees in SiBCASA are the main contributor to fire emissions not only because of their high amount of carbon per unit of area, but also due to the differences in mortality relative to the Savanna and Grasslands biomes.

It was already reported that SiBCASA has higher fuel loads compared to CASA [Van Der Velde et al., 2014], but in that study there are no estimates in this study we could not directly confirm that because SiBCASA does not provide direct output for the pools that are subject to fire (i.e. leaves and cwd). CASA's fuel consumption is dependent on tree cover and is reported in Van Der Werf et al. [2010] for Southern Hemisphere South America, as 1.3 kgC m^{-2} of burned area and Northern Hemisphere South America as 1.0 kgC m^{-2} of burned area. These estimates include standing and surface biomass, but they are difficult to compare to our estimates as the focus in this thesis is on the Amazon, where higher fuel loads are found and its extent encompasses part of the northern and southern hemisphere of South America. However, we can compare our estimates to those reported by Van Leeuwen et al. [2014] where a compilation of several field measurements is provided. In this study is reported the averaged fuel consumption for different biomes in t of dry matter per hectare (t ha^{-1}) by using a carbon to dry matter conversion factor of 2. This conversion factor is supported by Andela et al. [2016], where an assumed fuel carbon content of 45% is used to compare dry matter fuel consumption with net primary productivity. This conversion factor is used here to make their estimates comparable to ours in kgC m^{-2}. For tropical forests Van Leeuwen et al. [2014] report 6.3 kgC m^{-2} whereas here we found 18.9 kgC m^{-2} (assuming Tall Evergreen Broadleaf as Tropical Forest), for Savanna they estimate 0.25 kgC m^{-2} while in SiBCASA we obtained 2.58 kgC m^{-2} and finally for Grasslands Van Leeuwen et al. [2014] report 0.21 kgC m^{-2} and SiBCASA 0.09 kgC

m^{-2}. It is interesting to see that for tropical forests and savanna SiBCASA is overestimating the fuel consumption relative to Van Leeuwen et al. [2014] but for grasslands SiBCASA has one order of magnitude less fuel for consumption. However, if we take into account mortality in our estimates, which is affecting the final fire flux (see equation 7), we will still get an overestimation in the tropical forest (17 kgC m^{-2}) but an underestimation in Savanna and Grasslands (0.129 kgC m^{-2} and 0.001 kgC m^{-2}), compared to VanLeeuwen2014 . In SiBCASA mortality within equation 7 is reported to be related to the density of trees in a biome [Van Der Velde et al., 2014], from which it is assumed to be the reason why there is such a low mortality for Savanna and Grasslands. The latter might be reasonable for a global study, but for a regional study this might not be the case.

Furthermore, SiBCASA's aboveground woody biomass was compared to published values of aboveground biomass for the Amazon to assess if the simulated carbon pools where within expected values. For the biome Tall Evergreen Broadleaf trees we estimated 22 kgC m^{-2}. If we consider that this biome is equivalent to old growth trees we can compare to the estimate reported by Saatchi et al. [2007], 25.4 kgC m^{-2}, and not only find a similar value but also lower. However, Malhi et al. [2006] reported 16 kgC m^{-2} for intact forest in the Amazon. For Savanna and Grasslands SiBCASA simulates 3.91 and 0.05 kgC m^{-2}, whereas Saatchi et al. [2007] reports 2.01 and 0.44 kgC m^{-2}. Thus, SiBCASA has a higher amount of aboveground woody biomass in Savanna but one order of magnitude lower in Grasslands which is in line with the aforementioned fuel consumption. It is important to note that these estimates differ on timing as those of Saatchi et al. [2007] and Malhi et al. [2006] were published on 2007 and 2006. For the entire Amazon basin considering an area of approximately $7x10^6$ km^2 we estimate 15 kgC m^{-2} whereas Andreae et al. [2015] with an area slightly smaller, $6.9x10^6$ km^2, estimates 17 kgC m^{-2}. Therefore, SiBCASA's aboveground wood biomass lies within reported values, whereas the fuel consumption is overestimated in the tropical forests suggesting that the combustion completeness and the mortality are both high.

An additional source of overestimation within SiBCASA is the strong recovery of the vegetation after a fire season. The latter was assessed by looking at the aboveground woody biomass and the total living carbon, shown on Figures 22 and 42 (in the appendix). It is known that CO_2 effect in vegetation acts very likely as a negative feedback, canceling out up to 30% of fossil fuel emissions Schimel et al. [2014]. However, it seems that SiBCASA is growing leaves, roots and wood very fast after each fire season, reaching the value of the prior year before the fire season. Although Schimel et al. [2014] report that 60% of the land sinks are due to this feedback at a global scale, there is large variability in the tropics and the inter-annual variability may be increasing. The rapid vegetation recovery induced by a CO_2 fertilization effect added to no water stress (Erik van Schaik, personal communication) in SiBCASA's simulated Amazon might be boosting vegetation growth after each fire season. The latter is related to the simulated net biome exchange by SiBCASA (Chapter 2, Figure 14), which indicates either a very strong uptake of carbon or a weak heterotrophic respiration.

Therefore, further adjustments within SiBCASA such as including a fire induced mortality for the vegetation present in the burned areas might help to differentiate the old growth forests, not affected by fires, and the regrowing vegetation after a fire season. The latter could indirectly account for a non CO_2 fertilization growth and an induced CO_2 induced growth. In addition, a fire induced mortality is needed to represent after fire vegetation growth dynamically taking into account the biomass loss. In this lines the study of Van Der Werf et al. [2010] is a good reference, in which mortality is a function of fire persistance (for deforestation areas) and tree cover (non deforestation areas), both variable in time. It is also worth mentioning that a biome approach to the CO_2 effect is already feasible by implementing within SiBCASA's dynamics the findings of studies recently published, such as that cited in Nowak [2017], where FACE experiments for grasslands over a long time period have shown that this biome has a decreased response to the increasing CO_2 concentrations under extreme conditions: too warm, too dry, or too wet.

3.4   Conclusions

In this chapter SiBCASA's fire scheme and it's response to a different land cover distribution was analyzed, in particular that of CASA's model. Differences in land cover are dependent on where the burned area is concentrated, and by adding more tropical forest to the default SiBCASA set up did not resulted in more fire emissions for all years. This was mainly influenced by the prescribed parameters mortality and combustion completeness, which are driving to a large extent the contribution of Savannas and Grasslands to the total fire emissions in the Amazon. The latter is very likely generating underestimations of these biomes and an overestimation in Tall Evergreen Broadleaf trees, relative to CASA estimates. This was supported by the burned area analysis where it was shown that in SiBCASA there was a considerable amount of burned area in the Savanna and Grasslands biomes, and even though Savanna and Grasslands in SiBCASA amount to a larger areal extent compared to the only class Savannas and Grasslands in CASA, fire emissions were still larger in CASA. The comparison of fuel load and fuel consumption to reported values [Van Leeuwen et al., 2014] supported the fact that SiBCASA has high fuel load and fuel consumption for Evergreen Forest but low for Savannas and Grasslands. Finally, an additional source of overestimation in SiBCASA for Broadleaf Evergreen forests was identified as the rapid growth of vegetation after a fire season. Further adjustments to SiBCASA, such as implementing a fire induced mortality and an adjustment of the CO_2 fertilization effect were recommended to improve fire emission estimates.

Chapter 4

4 Forward simulations in TM5 global transport model

The fire inventories discussed in chapters 2 and 3 were used to simulated the vertical profiles of CO_2 and CO at 4 sites of the Amazon. Observations done between 2010-2014 (2013 and 2014 not shown) at those 4 locations are compared to the TM5 simulations. The overview of the TM5 model is given in the methods and the results show the vertical profiles for each site, focusing on the wet and dry season. To assess how well simulated values, obtain with the different fire inventories, represent observations root mean square differences are calculated for each site and year and for all the simulated period at each site as well. The overall skill of the TM5 to represent the observations depending on the fire inventory used will be approach in the discussion. The conclusions summarize the main findings of this chapter.

4.1 Methods and Observations

4.1.1 Observations

The aircraft sampling program at four sites in the Amazon, described in more detail in Gatti et al. [2014], began in 2010 and it takes bi-weekly flask samples of CO_2, CO, CH_4 and sulphur hexafluoride (SF_6). The aircraft samples at different heights, ranging from the lower boundary layer, around 300 meters until 4500 meters above sea level (a.s.l) [Gatti et al., 2014]. The sites are shown in Figure 23. As is described in Gatti et al. [2014], the sites are located such that the dominant air flow at the lower atmosphere in the Amazon is crossing them from east to west, being Santarem (SAN) and Alta Floresta (ALF) the receivers of the air masses coming from the Atlantic ocean. Tabatinga (TAB) and Rio Branco (RBO) are closer to the Andes mountain range and capture the signal of air masses that predominantly have traveled westward, crossing a large extent of the Amazon forest [Gatti et al., 2014, Andreae et al., 2015]. Santarem and Alta Floresta, besides having a strong signal from the forest and ocean, they are also located close to large portions of agricultural lands and savanna. The aircraft takes the samples, usually between 12:00 and 13:00 local time, time at which the boundary layer present well mixed conditions over the Amazon and its considered to be considerably well developed [Gatti et al., 2014]. The plane descends from 4500 meters to about 300 meters in a spiral trajectory filling 12 flasks for TAB, ALF and RBO and 17 in SAN. The 0.7 litre flasks after each flight are then send to the IPEN Atmospheric Chemistry Laboratory in Sao Paulo, Brazil to be analyzed [Gatti et al., 2014].

Figure 23: Location of aircraft sampling network sites in the Amazon.

4.1.2   TM5 model set up and input fluxes

The TM5 model permits a two way nested zooming which is suitable to perform studies with high resolution regionally but coarser resolution at a global scale. The boundary conditions of the nested regions are provided by the coarser grid and the results within the fine grids are given back to the coarse grid [Krol et al., 2005]. Generally, the set up of the TM5 contains three spatial resolutions, a global coarse grid of 6°x4° and two nested regions of 3°x2° and 1°x1°. The 3°x2° intermediate grid is used, as it is described in Krol et al. [2005], to: 1. study the resolution dependency of various parameterisations 2. generate initial conditions for the underlying 1°x1° region and 3. avoid crude transitions from the 6°x4° to the 1°x1° domains. The vertical levels in each grid are the same but with higher resolution in the troposphere, as in this study there is no interest in the stratosphere [Krol et al., 2005]. Here the same TM5 set up and fluxes as in Van Der Laan-Luijkx et al. [2015] are used. The TM5 global transport model, as it is shown in Figure 24 has a horizontal resolution of 6°x4° (longitude by latitude) and two nested regions, one over South America with 3°x2° and the other over the Amazon with 1°x1°. The injection height of the fire emissions are at the surface. The meteorological information were retrieved from the ERA-Interim reanalysis with 25 vertical levels and a 3 hourly resolution.
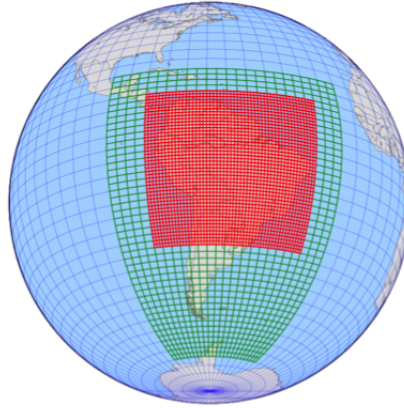
Figure 24: TM5 model grid set up over South America. From the supplementary information of Van Der Laan-Luijkx et al. [2015]

The fluxes needed to run the model are biosphere, fires, ocean and fossil fuel emissions. For the nested regions the biosphere fluxes used here, in particular NBE, are from the SiBCASA and the CASA model. SiBCASA NBE fluxes are used for the simulations with GFAS and FINN, whereas the CASA NBE flux was used only for the CASA-GFED4 simulation. The fire fluxes for the nested regions are given by SiBCASA-GFED4, GFAS, FINN, and CASA-GFED4-daily and 3 hourly. These fire inventories are described in chapter 2 and 3. For the coarser grid outside South America, the background as it is called here, optimized fluxes for the biosphere and the ocean are retrieved from CarbonTracker Europe (http://www.carbontracker.eu). Background fluxes for fires and fossil fuels are also from CarbonTracker Europe, but they are always fixed, meaning that they are not optimized. For the ocean fluxes CarbonTracker uses the oceanic inversions performed by Jacobson et al. [2007] and the fossil fuel dataset is a modified version of the *EDGAR4.2* database from 2011. Table 10 gives a summary of the fluxes used in TM5.

Table 10: Summary of the fluxes used in TM5 for the CO_2. Note that the 3ºx2º grid includes Ocean, thus the fire and biosphere fluxes are used only in the terrestrial regions of South America.

Fluxes	6ºx4º grid	3ºx2º and 1ºx1º grids
Biosphere	CarbonTracker CTE201-FT	SiBCASA or CASA
Fires	SiBCASA-GFED4	Fire Inventories described here
Ocean	Jacobson et al. [2007]	Jacobson et al. [2007]
Fossil Fuel	*EDGAR4.2*	*EDGAR4.2*

It is worth noting that the CO forward simulations were performed by Narcisa Banda at Utrecht University. The TM5 model was also used for these CO forward simulations but with a different set up. For CO the fluxes needed are fossil fuels, fires and oxidation of non methane hydrocarbons. Here the output of these forward simulations is analyzed and compared to the observations at the four sites in the Amazon.

4.2   Results

4.2.1   Simulated CO_2 and CO Profiles

The results are presented per site and per year and each figure shows the wet and the dry or fire seasons. The profiles for 2013 and 2014 are not shown due to data restrictions. For the CO_2 profiles the fire inventory CASA-GFED4 3 hourly is included, whereas for the CO profiles was not included due to time constraints. For Santarem (SAN), Rio Branco (RBO) and Alta Floresta (ALF) observations are available from 2010 until 2014, however for the fire season (August-November) of 2014 there are no observations available. For Tabatinga (TAB) observations are available from 2010-2012. In these results when the fire inventories are mentioned is to refer to the simulations done with each one of them.

The observed CO_2 profiles are generally more variable at lower heights, but during intense fire seasons this variability can be convected aloft. This variability at low heights is due to the mixed signal that the airplane is measuring, the CO_2 coming from the fires, the CO_2 respired by the canopy and the soils and the CO_2 that is removed by the uptake of the biosphere. CO profiles provide a better representation of the fire signal, as the concentrations of CO are strongly dependent on fire activity in the Amazon [Andreae et al., 2015]. In general terms CO profiles show more variability than CO_2 due to a stronger seasonal dependence.

When referred to the height intervals the altitude corresponds to meters above sea level. When the size of the marker in the graphs (in general) is smaller than the minimum size of the legend it means that at this height interval there were less observations than the minimum range shown on the legend, but more than one. For all the observed profiles at each site, the mean concentration every 500 m height interval is plotted. The mean is calculated over the wet or the dry season. The latter is important to keep in mind, as the observed profiles per sampling date might be very different. Therefore, the aim here is to represent with the TM5 model averaged profiles over each one of the seasons and when observations are mentioned I refer to the mean observed values for the season in context. If low amount of observations, less than three or two, resulted in high mean values with respect to the next interval they were removed as they might be sampling errors. This happened in few occasions and mainly at the first altitude interval.

4.2.1.1   Santarem

The simulated and observed CO_2 vertical profiles for Santarem are given in Figure 25. Simulated and observed profiles for the wet and the dry seasons are shown. Note that the variability is plotted with box whiskers showing the 25 and 75 % percentiles. It is interesting to see that for 2010, the simulated CO_2 profile for the dry season are within the 50% of the observations for the lower height intervals. Between 1200m and 3000m SiBCASA-GFED4, GFAS and FINN are on the low side of the observed values. For both CASA-GFED4 inventories, this is not the case as they enter the 50% region after 2200m. After 3200m all simulations fall back to the 50% of the observed values. In 2010 there is more variability aloft that for the other years, note the larger bars for the 25% and 75% percentiles, after 2500m. The dry season for 2011 and 2012 present similar results. The simulations are underestimating at lower heights with respect to the observations and in general they fail to reproduce the observed mean variability. For these 2 years CASA-GFED4-daily falls in the 50% of the observed values until the 2200m (2500) and 2700 (2012). Above 2700m the other fire inventories tend to improve, in particular SiBCASA-GFED4, which captures very well the shape of the observed values in both years. In 2012 CO_2 concentrations were more variable aloft that in 2011 and the range of the

observed CO_2 concentrations for 2012 lies higher as well. The latter might be associated to the fact that in 2012 there were more fire emissions during the dry season than in 2011. However this is not the case when 2010 and 2012 are compared, knowing that 2010 presented the highest annual average fire emission. In 2013 the CASA inventories show again a good match until the fifth height interval, whereas SiBCASA-GFED4, GFAS and FINN only until the third interval (not shown). These three fire inventories improved aloft but in general all fail to reproduce the shape of the mean observed values. However, it is worth noting that these are mean profiles, and the match might be different for individual sampling days. The dry season of 2013 (not shown) has also more observations than 2010 and has a higher concentration range (392-397 ppm) suggesting that lack of sampling in 2010 results in lower concentrations even though it is known it had an intense fire season. The latter is supported spatially as well, as it is seen that Santarem is located in the hot spots presented in Figure 8, in Chapter 2.

Simulated CO_2 concentrations during the wet season in Santarem have in general a better agreement with observed values than simulations during the fire season. Observed values during the wet months (January-August) show a clear pattern, with low variability at high altitudes and high variability at low altitudes; which points to the absence of fire induced CO_2 concentrations. From these profiles I can also argue that the NBE signal is more clear in the absence of fires as there is an evident differentiation of the CASA-GFED4 inventories and SiBCASA-GFED4, GFAS and FINN (FINN and GFAS include the NBE signal calculated by SiBCASA, only here in this thesis). The latter explains why SiBCASA-GFED4, GFAS, and FINN are very similar throughout the years in this season, even overlapping between them. NBE flux in CASA is higher than in SiBCASA thus, vertical CO_2 concentrations tend to be higher as well. Finally, I highlight the good agreement between simulated and observed values for all inventories in 2010 and only for SiBCASA-GFED4, GFAS and FINN in 2012 and 2013 (not shown), following neatly the shape of the observations.

In Figure 26 the CO vertical profiles for Santarem are shown. As it was mentioned before, CO concentrations are more fire dependent, therefore the difference between the seasons is much more clear than for CO_2 . Different from the CO_2 profiles, CO concentrations are not directly linked to vegetation fluxes. During the dry season there are more outliers, which indicate the presence of high CO concentrations due to fire activity. These high concentrations are difficult to reproduce for the TM5 at low altitudes (i.e. in 2010, 2011 and 2012). In 2010, simulated values are considerably out of the variability range and they underestimate the observed values. It is important to note, as with CO_2, that during this year there were less observations done in the fire season. For 2011 and 2012, the match between simulations and observations improves for SiBCASA-GFED4 and FINN. SiBCASA-GFED4 has a distinct shape above 1800m following the variability of the observations, this is particularly seen in 2012. GFAS , FINN and CASA-GFED4-daily fail to match the shape of the observed concentrations at lower heights, however they fall into the 50% range in the last heights intervals, being this the case for 2013 as well (not shown). It is interesting to see that during the fire season CO concentrations at low altitudes are, for all years, almost 100 ppb higher than in the wet season. During the wet season observed CO concentrations are lower at all the sampling heights below 4000m than for the dry season. There is less variability at all heights intervals and for all years the observed values converge to 100 ppb at the last height interval. This is similar for some years in the dry season, which might indicate that CO concentrations above 4000m are not significantly affected by fire emissions. However in 2010 a 50 ppb difference between both seasons is observed at this height, suggesting that during this year there was indeed a fire signal above 4000m. During the wet season the CO signal varies less and the simulations are clearly closer to observed values. SiBCASA-GFED4 tends to have higher CO concentrations when compared to the other simulated fire inventories, which is in line with the higher annual fire emissions averages found for the whole Amazon in chapter 2, when compared to the other inventories.
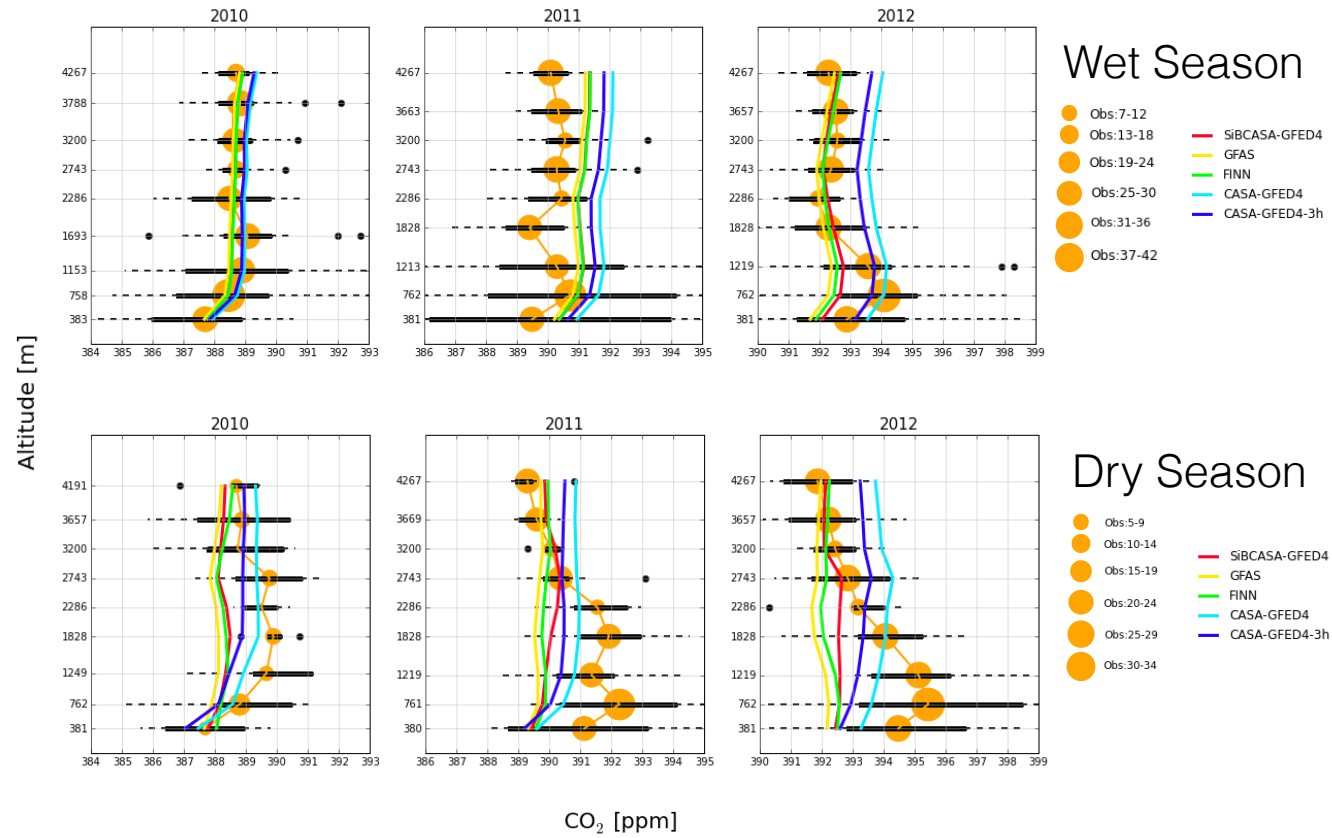
Figure 25: Simulated and observed CO_2 vertical profiles (ppm) for Santarem. The observations (orange) are plotted at the mean sampling height every 500m intervals. The size of the points denote the number of observations done within each 500m interval. The black bars indicate the 25% and 75% percentiles of the observations with dashed lines indicating the minimum and maximum values of the 25% and 75% percentiles. The black dots represent outliers. The red line, which is SiBCASA-GFED4 in some years is behind the green line, which is FINN.
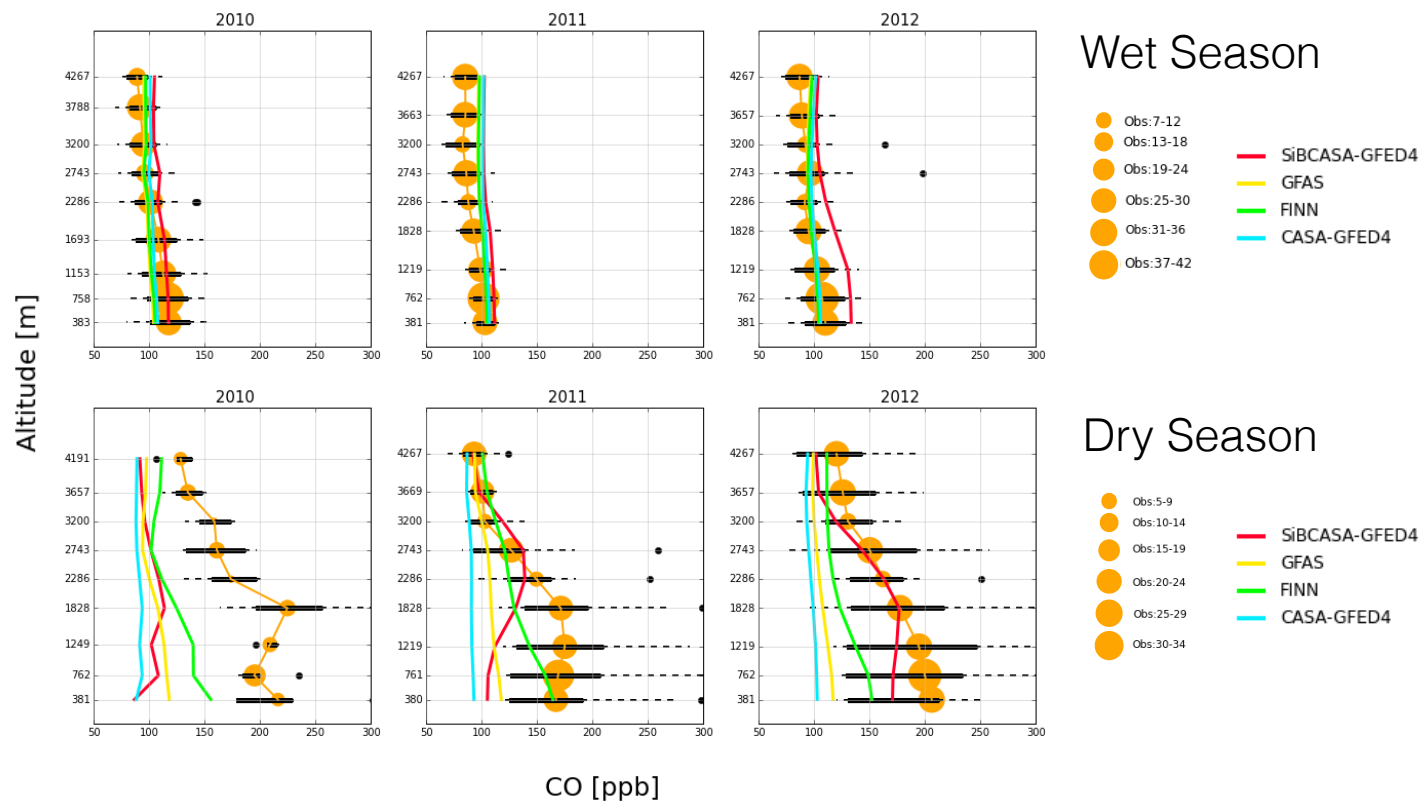
Figure 26: Simulated and observed CO vertical profiles (ppb) for Santarem. The observations (orange) are plotted at the mean sampling height every 500m intervals. The size of the point denotes the number of observations done within each 500m interval. The black bars indicate the 25% and 75% percentiles of the observations with dashed lines indicating the minimum and maximum values of the 25% and 75% percentiles. The black dots represent outliers.

4.2.1.2 Alta Floresta

Figure 27 shows the observed and simulated CO_2 vertical profiles in Alta Floresta for both wet and dry seasons. During the dry season, simulations generally tend to converge to a similar estimate in the free troposphere, above 4000m, but CASA-GFED4-daily and CASA-GFED4-3hourly are consistently having higher values than the other fire inventories. In 2010 CASA-GFED4-daily and CASA-GFED4-3hourly present a good match in the first two height intervals but then they diverge simulating higher concentrations. SiBCASA-GFED4 shows an improvement above 1000m following closely the observed values. FINN and GFAS are on the low side of the observed values, but converging aloft, above 3000m, with the 50% of the observed CO_2 concentrations. During these years, the simulated values at the heights closer to the surface (less than 500m) have the largest difference, 384 ppm for GFAS and 392 ppm for CASA-GFED4-daily . For 2011 there is less spread between the simulations, but they all fall off from the observed values close to the surface. For 2012, the simulations are able to capture the observations, in particular SiBCASA-GFED4 and CASA-GFED4-3hourly fall always within the 50% range. For 2013 (not shown) there was not enough information for the lower height interval, however CASA-GFED4-daily and CASA-GFED4-3hourly are in better agreement with observations between 700m and 1700m whereas the other inventories improved above 2500m.

During the wet season the simulated CO_2 profiles show an considerable improvement with respect to the fire season, in particular for all the years except for 2014 (not shown). For years 2010 and 2011 the simulations are closely following the observations, always within the 25-75% percentiles range. For 2012 and 2013 this is also the case but the differences between the CASA inventories and GFAS, FINN and SiBCASA-GFED4 are more clear. This difference is even more clear in 2014 (not shown), where the CASA inventories are overestimating the observations by almost 2 ppm above 1000m, whereas the SiBCASA-GFED4, GFAS and FINN matched very well the observed values above 500m.

In Figure 28 the CO vertical profiles are shown for Alta Floresta. The dry season profiles has again a strong fire signal, as it was expected for the location, reaching 300 ppb in 2010 below 500m; 80 ppb more than in Santarem at the same height and year. The simulations for this year could reproduce the observations with a defined shape within the 50% of the observed values, note that SiBCASA-GFED4 simulation represents the observed extremes with a remarkable skill. For the next two years the simulated profiles fall within the 50% variability range at almost all heights. For 2013 simulated concentrations at lower altitudes, below 2000m, were underestimated (not shown). However, for this dry season the TM5 simulations are particularly close to the observations. During the wet season, as in Santarem, the CO concentrations do not vary at all showing an almost constant profile along 100 ppb at all heights. Similar as for CO in Santarem, SiBCASA-GFED4 tends to have higher CO concentrations at all heights than the other fire inventories pointing again towards the high values obtained at the Amazon scale in Chapter 2 for this inventory.
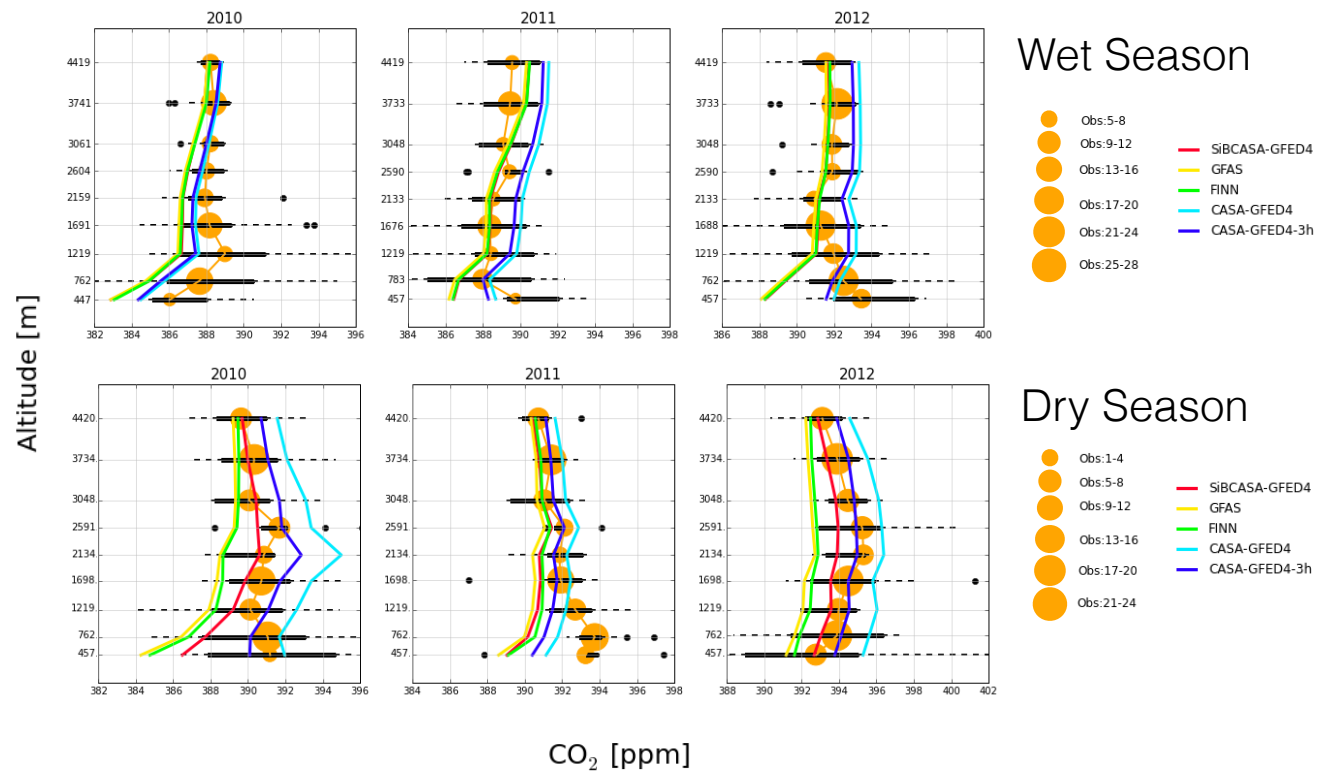
Figure 27: Simulated and observed CO_2 vertical profiles (ppm) for Alta Floresta. The observations (orange) are plotted at the mean sampling height every 500m intervals. The size of the points denote the number of observations done within each 500m interval. The black bars indicate the 25% and 75% percentiles of the observations with dashed lines indicating the minimum and maximum values of the 25% and 75% percentiles. The black dots represent outliers. The red line, which is SiBCASA-GFED4 in some years is behind the green line, which is FINN.

Figure 28: Simulated and observed CO vertical profiles (ppb) for Alta Floresta. The observations (orange) are plotted at the mean sampling height every 500m intervals. The size of the point denotes the number of observations done within each 500m interval. The black bars indicate the 25% and 75% percentiles of the observations with dashed lines indicating the minimum and maximum values of the 25% and 75% percentiles. The black dots represent outliers.

4.2.1.3 Rio Branco

On Figure 29 the dry and wet season CO_2 profiles for Rio Branco are shown. The CASA inventories are again higher than the other fire products for both seasons. Nevertheless, during the fire season for 2011, 2012 and 2013 (not shown) all simulations are lower than observed values presenting large differences below 1300m. As in the previous sites the simulations improved aloft and converge to a similar value. During the 2010 below 2000m GFAS, FINN and SiBCASA-GFED4 underestimate observations whereas CASA-GFED4 daily and 3 hourly overestimate relative to the observations. The spread between simulations is maintained at higher altitudes with a range of almost 4 ppm at the 3500-4000m interval. Note also a large difference for 2013 at the first 500m interval between observed concentrations and simulations. It is also worth noting that in this year for some height intervals the size of the marker is smaller than the minimum size of the legend because at these heights there were less than four observations but more than one. Therefore, the differences at the first interval might be related to a lack of sampling which might bias the mean observation mean to high values.

The wet season for Rio Branco has also some height intervals with less observations than the minimum range shown on the legend. However, the match between observations and simulations for the years 2010, 2011, 2012, and 2013 (not shown) does not seem to be affected by this. There is in general a good representation of the observed values for these years with a slight difference between the CASA inventories and SiBCASA-GFED4, GFAS and FINN. For the year 2014 (not shown) this difference is more clear at all heights and when compared to the observed values CASA-GFED4 daily and 3 hourly are overestimating by 2 ppm above 700m.

The CO vertical profiles for dry and wet seasons in Rio Branco are shown on Figure 30. For the dry season again there is a high CO concentration at lower heights and an intense seasonal influence. The wet season presents the same pattern, as seen for the other sites, with a constant observed and simulated CO concentration (100 ppb) at all heights. For the wet season of 2010 SiBCASA-GFED4 overestimates observed values below 2000m but the simulated profile converges aloft to the observed concentrations.

The dry season in 2010 had again the most variable CO vertical profile which is well captured by CASA-GFED4, GFAS and FINN. SiBCASA-GFED4 for 2010 and 2012 overestimates observed concentrations which is interesting when compared to Santarem, where in these same years this fire inventory underestimates observations. The latter might be related to the high fire emissions seen in Chapter 2 for the SiBCASA-GFED4 inventory in the Rio Branco region (9ºS and 67ºW). Note that the land cover imposed in SiBCASA at this location is mainly broadleaf forest but here there is a strong influence of other biomes and human activity as well as it can be easily seen on satellite images or in google earth. In other words, the vertical profile simulated using SiBCASA-GFED4 might be high due to high fire emissions in that same area due to a misrepresentation of the land cover in SiBCASA. For the dry season in 2011 and 2013 (not shown) the simulated profiles match better with observations.
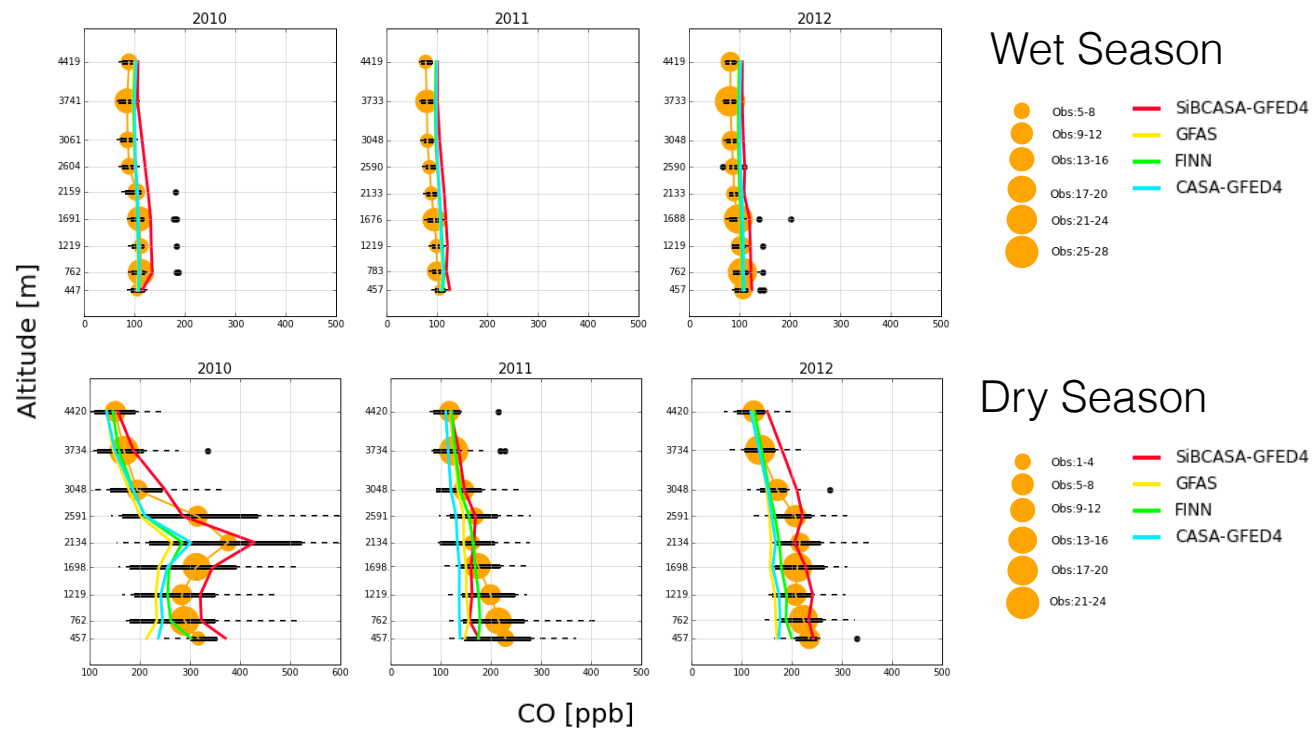
Figure 29: Simulated and observed CO_2 vertical profiles (ppm) for Rio Branco. The observations (orange) are plotted at the mean sampling height every 500m intervals. The size of the points denote the number of observations done within each 500m interval. The black bars indicate the 25% and 75% percentiles of the observations with dashed lines indicating the minimum and maximum values of the 25% and 75% percentiles. The black dots represent outliers.
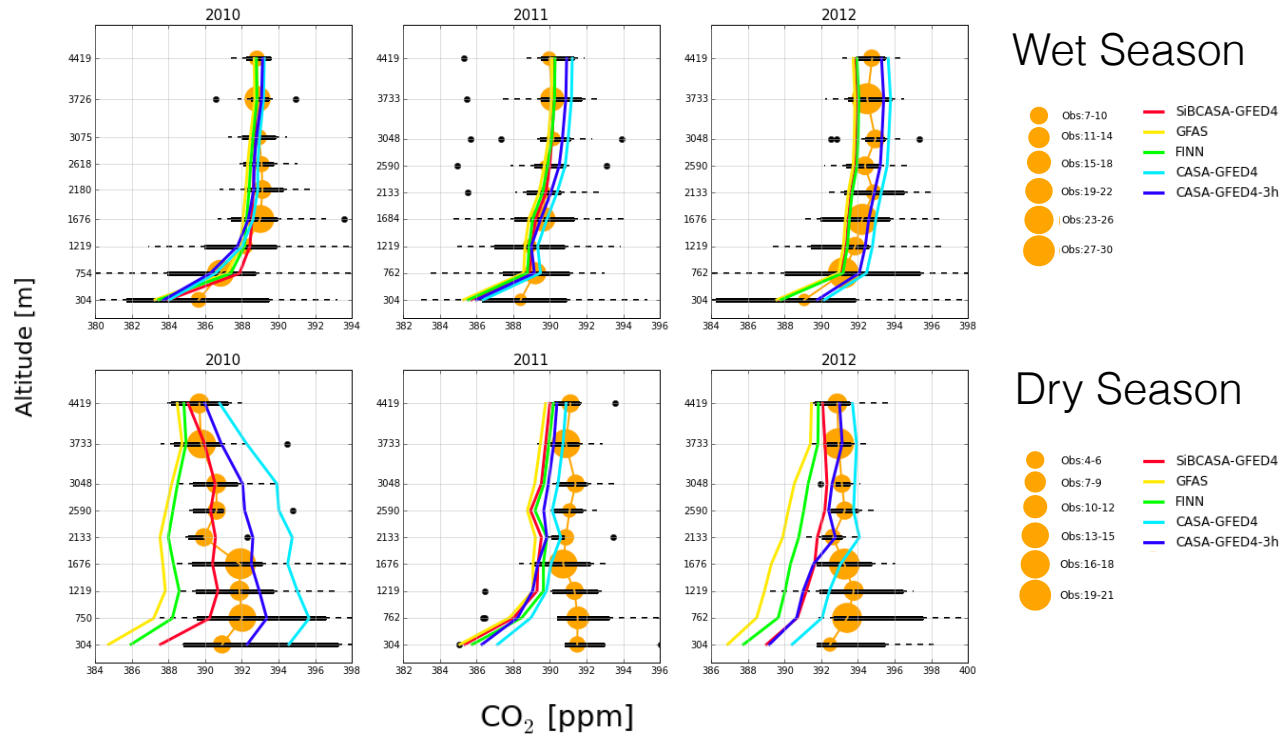
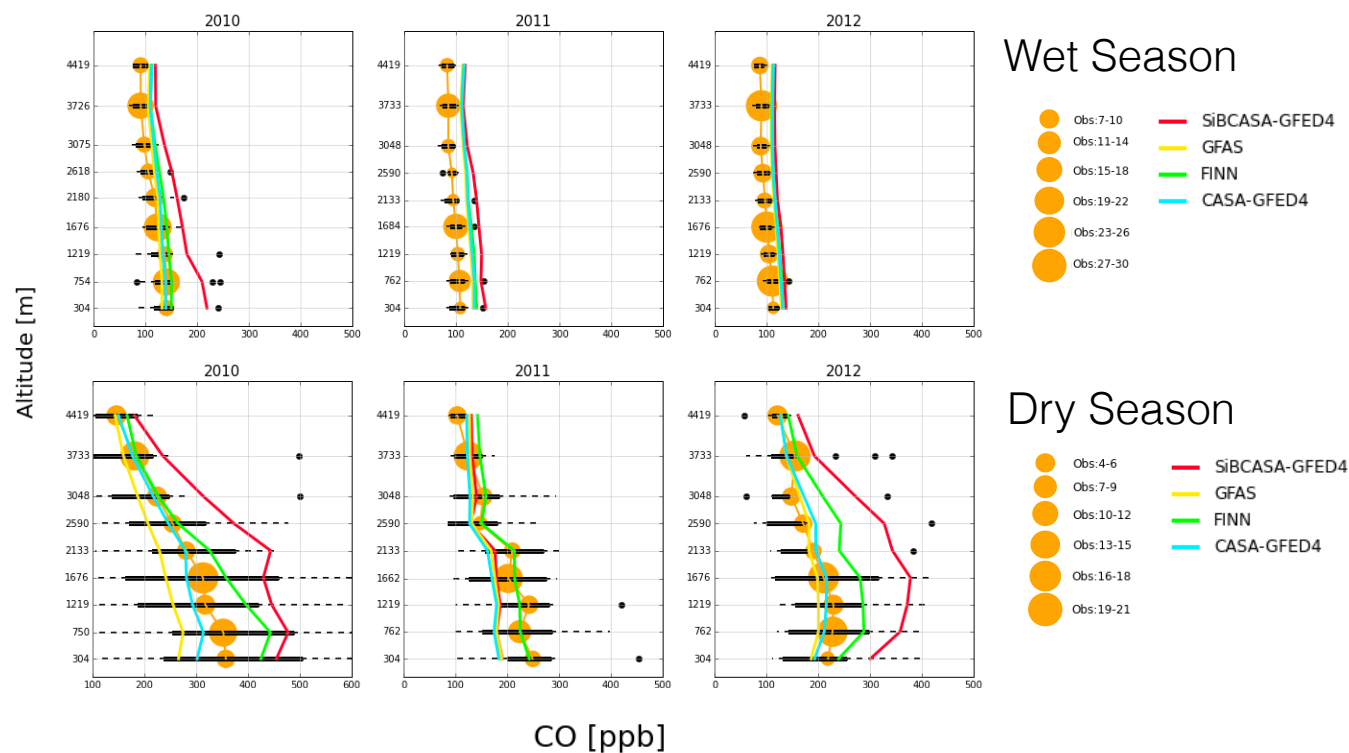Figure 30: Simulated and observed CO vertical profiles (ppb) for Rio Branco. The observations (orange) are plotted at the mean sampling height every 500m intervals. The size of the scatterpoint denotes the number of observations done at that 500m interval. The black bars indicate the 25% and 75% percentiles of the observations with dashed lines indicating the minimum and maximum values of the 25% and 75% percentiles.

4.2.1.4   Tabatinga

The CO (left panel) and CO_2 (right panel) vertical profiles for Tabatinga are shown in Figure 31. Due to lack of observations for the years after 2012, there are less vertical profiles available. Simulated CO_2 concentrations for the fire season tend to be underestimating observed values below 1000m, showing large spread between simulations, in particular for 2010. SiBCASA-GFED4 and CASA-GFED4-3hourly during this year have similar values, presenting a good match with observations above 1200m. Above this height CASA-GFED4-daily has higher values, whereas GFAS and FINN lower values relative observations. During 2011 the CASA inventories present an abrupt decrease between 2000m and 2500m, when at the same height observations are increasing. The latter might be explained by an uptake of CO_2 by the biosphere within the CASA model that is being propagated vertically. This can also be the case for the other fire inventories but to a much lesser extent as at this height interval the other simulated profiles (i.e. GFAS, FINN and SiBCASA-GFED4) fail to reproduce the seasonal observed mean values as well.

For the wet season there is a considerable improvement of the simulations with respect to the observations for 2010 and 2011. It is interesting to see that for 2011 at the 2000m - 2500m interval there is again a notable change, showing an increase in concentrations, but now for all inventories. This is the same height interval in which the abrupt change in the dry season was seen, supporting the idea that there might be a specific driver for that height and that year generating this behavior. This peak in the wet season of 2011 can be associated to a respiration signal within the SiBCASA and the CASA models. For 2012, there are no observations below 500m and the simulations deviate from the observed values until 2500m of altitude, where they all enter the 50% range of variability. Generally the simulated CO_2 profiles show high concentrations for the CASA inventories in both seasons, mainly at a daily resolution (light blue). However, the fire season of 2010 is an exception presenting lower concentrations for CASA daily and 3 hourly than the other three inventories, but inverting this above 2600m.

The observed CO profiles have a strong variability during the dry season of 2010, which suggest that the signal of intense fire seasons coming from the east and southeast is perceived in Tabatinga. During 2011 we observed the same tendency to high values as for CO_2 in 2011 dry and wet seasons. The high fire induced CO concentrations were much lower in 2012, almost 100 ppb less than in 2010. The wet season has a more steady vertical structure for all years, with observed concentrations lower than 150 ppb at lower heights and converging to 100 ppb aloft. This is matched mainly by GFAS, FINN and CASA-GFED4 but overestimated slightly by SiBCASA-GFED4. The CO signal from fires can reach Tabatinga but for years with low fire emissions at the Amazon scale, this might not be the case, as 2012.
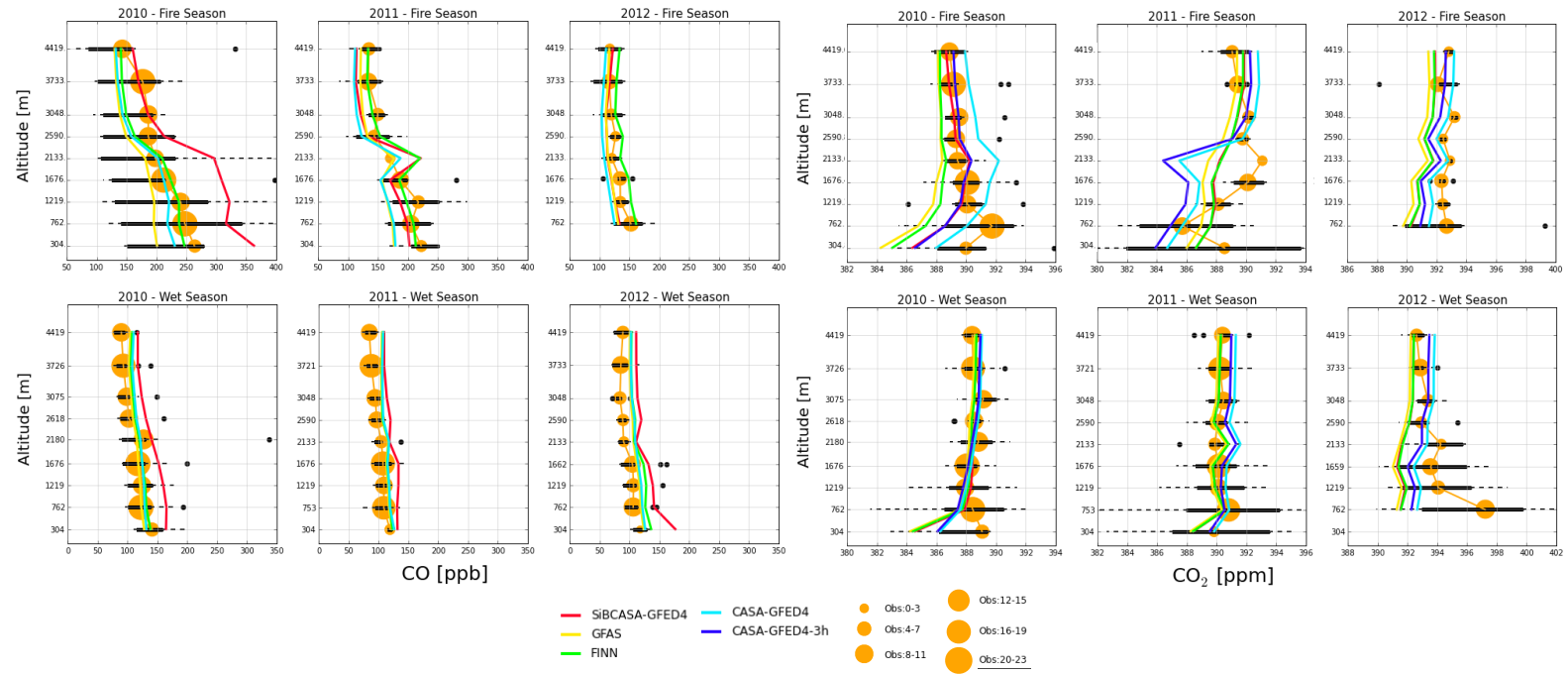
Figure 31: Simulated and observed CO (left, [ppb]) and CO_2 (right,[ppm]) vertical profiles for Tabatinga. The observations (orange) are plotted at the mean sampling height every 500m intervals. The size of the point denotes the number of observations within each 500m interval. The black bars indicate the 25% and 75% percentiles of the observations with dashed lines indicating the minimum and maximum values of the 25% and 75% percentiles. The black dots represent outliers. For the fire season of 2012 (CO and CO_2) there was only one measurement at the first height interval, so its was removed. The same applies for the 2012 wet season for CO_2. Note that For Tabatinga there are only measurements until 2012 and the CO vertical profiles were not done with the CASA-GFED4 3 hourly. For 2011 at 2100m (CO and CO_2 there was only one measurement, thus the absence of errorbar. It was not removed as it lies within the variability of the interval below.)

4.2.2 Root mean square differences (RMSD)

4.2.2.1 RMSD for each site and each fire inventory

In order to asses the skill of the TM5 simulations shown in the previous section, the RMSD between the observed and simulated mole fractions of CO_2 were calculated for each year, the dry and wet seasons. The results for all sites are shown in Figure 32. For Santarem SiBCASA-GFED4, GFAS and FINN had a better match during the wet season but for the fire season CASA-GFED4 daily and 3 hourly matched better the observed values. For the whole year analysis the CASA inventories show a similar pattern as for the wet season, but with slightly less variability, suggesting that the skill during the entire year is dominated by the wet season. In Alta Floresta CASA-GFED4 3 hourly was the best source of fire fluxes, indicating that in this site having a higher time resolution improves the simulations. At this site GFAS had the worst skill for the fire season of 2011, 2012, and 2013 and the dry season of 2010, 2012, and 2013. In Rio Branco during the dry season GFAS is again presenting the highest RMSD for 2011, 2012 and 2013, whereas during the wet season for the same years GFAS lies on the low side together with FINN and SiBCASA-GFED4. The CASA inventories for the wet season present the highest RMSD except in 2011. The entire year in Rio Branco the RMSD for the fire inventories changes from year to year. SiBCASA-GFED4 was the best inventory in 2010, CASA-GFED4 daily in 2011 and in 2012, in 2013 SiBCASA-GFED4 and FINN are the best inventories and finally in 2014 together with GFAS they are again presenting the lowest RMSD. In Tabatinga there were few observations during the dry months and the simulations are until 2012. During the fire season RMSD tend to decrease over time for all fire inventories, being 2012 the best year for all inventories. This is exactly the opposite for the wet and the all year plots, 2012 is the year in which all fire inventories present higher RMSD. Note that CASA-GFED4 daily in the fire season of 2010 has the highest RMSD but it ends up in 2012 with the lowest RMSD.

The RMSD between simulated and observed CO mole fractions are shown in Figure 33. The seasonal difference is again clear when comparing the RMSD for the dry and the wet seasons. The wet season for all sites was well represented by all fire inventories, however SiBCASA-GFED4 had the highest RMSD at all sites. The high RMSD for SiBCASA-GFED4 in Rio Branco in 2010 was probably due to an early onset of the fire season, there were already high fire emissions in July for this year (see Figure 13). The fire season was difficult to reproduce for all fire inventories in particular in Santarem for year 2012 and Alta Floresta in 2010, Rio Branco 2010 and 2012, and Tabatinga in 2010. FINN haves consistent low RMSD values at all sites, except in Rio Branco during the fire season. In Rio Branco the entire year RMSD is affected notably by the fire season, in particular in SiBCASA-GFED4 simulation, which shows lower peaks on the same years as the fire season. The RMSD for the CO simulations show a general tendency to high RMSD values of the SiBCASA-GFED4 inventory, being in line with the findings of chapter 2, where SiBCASA-GFED4 had on average the highest fire emissions for the years analyzed, except 2011.

Figure 32: Root Mean Square Differences (RMSD) between simulated and observed CO_2 mole fractions for all sites and the years simulated for that particular site. Note that the RMSD is shown for all the year (left column), the wet (center column) and the fire (right column) seasons. Note the difference x axis for Tabatinga and for all sites in the fire season.
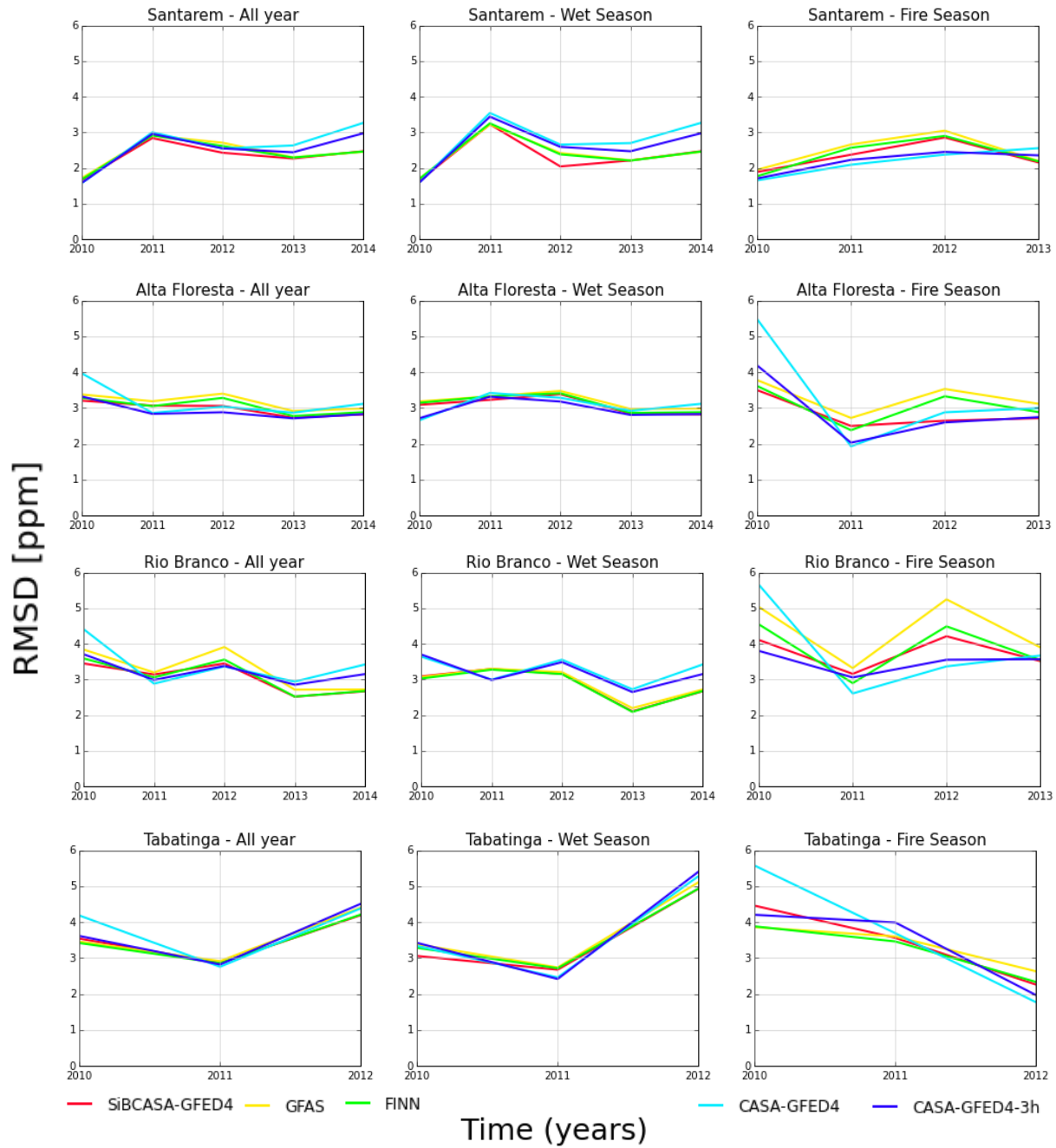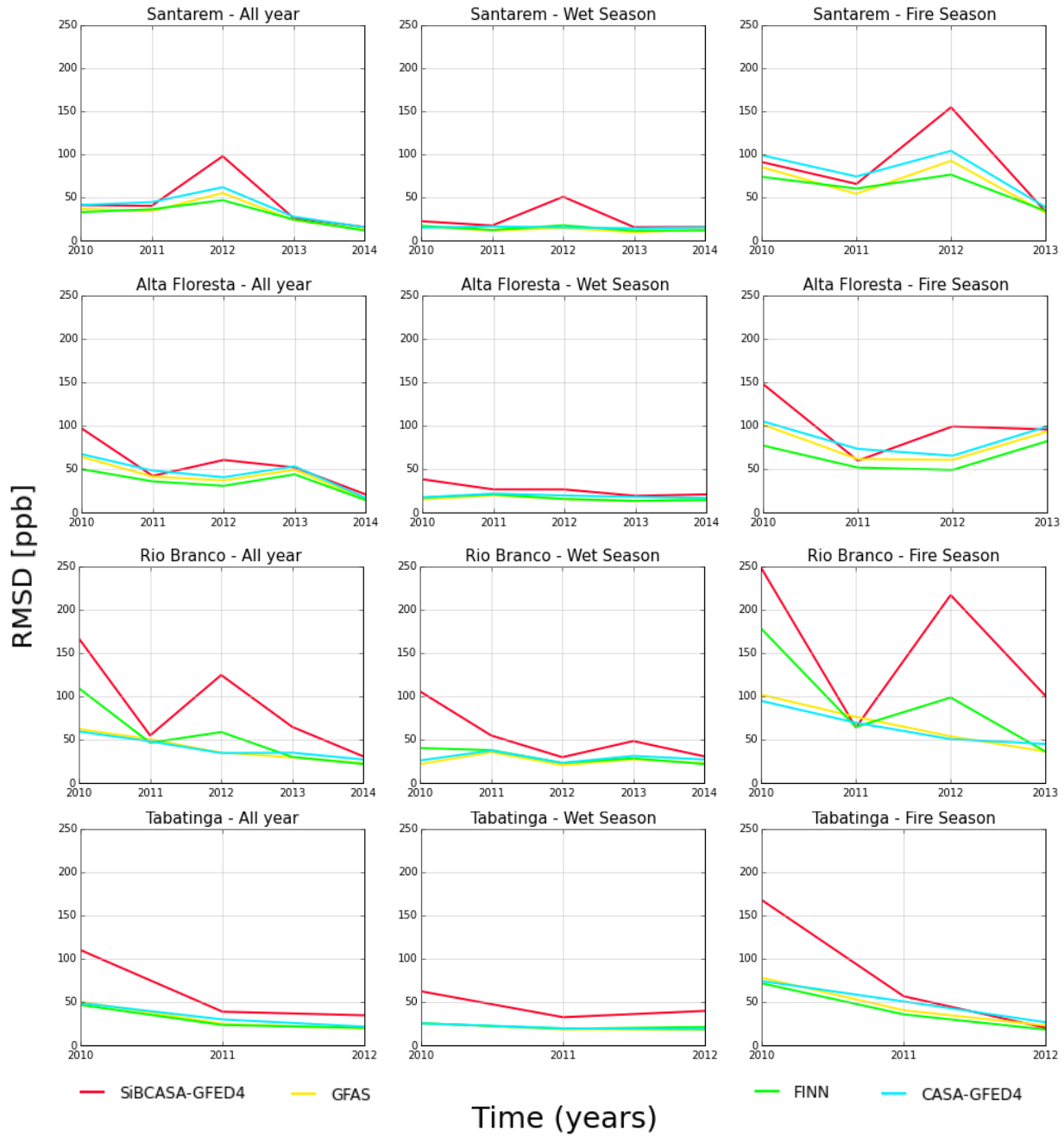
Figure 33: Root Mean Square Differences (RMSD) between simulated and observed CO mole fractions for all sites and the years simulated for that particular site. Note that the RMSD is shown for all the year (left column), the wet (center column) and the fire (right column) seasons. Note the difference x axis for Tabatinga and for all sites in the fire season.

4.2.2.2 RMSD for all the simulated period for all sites

Table 11 contains the RMSD between observed and simulated CO_2 mole fractions for all sites considering all the simulated years together. For this RMSD each simulated value was compared to the corresponding observation. The difference between fire inventories in the RMSD is small, in the order of 0.1-0.4 ppm. For the period 2010-2014 SiBCASA-GFED4 simulations were the more accurate reproducing the observed CO_2 vertical profiles in Santarem and Rio Branco. In Alta Floresta CASA-GFED4-3hourly had the lowest RMSD, suggesting that a high time resolution is better for this location. For Tabatinga FINN had the lowest RMSD which is similar to Van Der Laan-Luijkx et al. [2015] results for 2010 and 2011. For Tabatinga the performance was the worst for all simulations, but it was the site with less observations done and a shorter simulated time span (2010-2012). It is worth mentioning that in the CO_2 profiles the TM5 model aims to reproduce a mixed CO_2 signal, coming from fires and NBE, therefore this performance is affected by the biosphere flux calculated by SiBCASA (SiBCASA-GFED4, GFAS and FINN) and CASA (CASA-GFED4), which will hinder the performance if the model has a high respiration or a strong uptake of CO_2 .

The simulations performed with FINN to reproduce the observed CO profiles were the most accurate in Santarem, Alta Floresta and Tabatinga. Interestingly, FINN coincide with the best performance for CO and CO_2 in Tabatinga, indicating that this fire inventory might be more suitable to calculate fire emissions at the central part of the Amazon. However, in Tabatinga there were few observations done and it is constrained to 2010-2012. This might change if more observations are included and the time span extended. In Santarem and Alta Floresta, where more fire influence can be perceived the fire hot spots method in FINN seems to be more accurate to represent the observations. For Rio Branco the best perfomance was given by the CASA-GFED4-daily (43 ppb) inventory with GFAS (44 ppb) very close. In general terms CO profiles are difficult to reproduce in the fire season, which affects the overall performance of the simulations.

Table 11: Root Mean Square Differences (RMSD) between observed and simulated CO_2 mole fractions for the period 2010-2014 (2010-2012 for TAB) per site. All fire inventories used listed [ppm]. Lowest values indicated in bold.

	SAN	ALF	RBO	TAB
SiBCASA-GFED4	**2.36**	2.98	**3.19**	3.65
GFAS	2.47	3.21	3.47	3.68
FINN	2.44	3.09	3.24	**3.61**
CASA-GFED4-daily	2.58	3.20	3.54	4.06
CASA-GFED4-3hourly	2.51	**2.93**	3.31	3.84

Table 12: Root Mean Square Differences (RMSD) between observed and simulated CO mole fractions for the period 2010-2014 (2012-2012 for TAB) per site. All fire inventories used listed [ppb]. Lowest values indicated in bold.

	SAN	ALF	RBO	TAB
SiBCASA-GFED4	57	63	110	81
GFAS	38	46	44	38
FINN	**35**	**39**	66	**36**
CASA-GFED4-daily	44	50	**43**	39

4.3 Discussion

In the results a set of simulations are described using different biomass burning emissions inventories focusing on four sites of the Amazon. CO_2 and CO vertical profiles were plotted showing the averaged observed and simulated mole fractions at every 500m height interval. Vertical profiles are strongly influenced by the convection scheme and the vertical transport within the TM5 model [Van Der Laan-Luijkx et al., 2015]. In this study we used the same convection fields as Van Der Laan-Luijkx et al. [2015], an updated scheme from ECMWF which for them yielded a general better performance in TM5 in three out of four of the sites. The CO vertical profiles for the fire season could be improved by varying the injection height of the CO emissions within TM5. The injection height used here was at the surface, and despite of this for one dry season it was obtained a remarkable match with the observed variability (i.e. 2010 - Alta Floresta), thus this is something to be investigated in following work with TM5. In the supplementary information of Van Der Laan-Luijkx et al. [2015] several studies dealing with injection heights are mentioned, the reader is referred to that article for more information.

In Chapter 2 it was shown that SiBCASA-GFED4 had higher fire emissions for all years, except for 2011. The latter can be seen in the consistent overestimation of SiBCASA-GFED4 in the CO vertical profiles when compared to the observations, which was more clear during fire seasons. Note that this was not present in all years and sites, but was a general spatio-temporal pattern. The latter is also seen clearly for GFAS, which had low Amazon scale estimates and simulated CO vertical profiles underestimating the observed CO profiles. It is interesting to note that these high/low Amazon scale estimates presented in chapter 2 are difficult to evince in the CO_2 profiles, in which the CASA inventories had a general tendency to be on the high side of the observed mole fractions at all sites. This is explained by the fact that CO_2 concentrations have a mixed signal, strongly dominated by NBE fluxes. In the CO_2 simulations SiBCASA-GFED4, GFAS and FINN had the NBE flux simulated by SiBCASA whereas the CASA-GFED4-daily and CASA-GFED4-3hourly had the NBE simulated by CASA. Linking the CO_2 profiles with the NBE flux of these biosphere models indicate that there is indeed a strong NBE flux to the atmosphere in CASA and an uptake from the biosphere in SiBCASA. This happens mainly in 2010 and 2014 (see Table 4), and is also captured in the dry season CO_2 profiles for all sites. As is shown by Alden et al. [2016] NBE fluxes in the Amazon despite not having a clear seasonal pattern, they are sensible to heat, drought, with a positive correlation and to precipitation with a negative correlation. Heat and drought might decrease GPP and enhance respiration, although a direct link between NBE changes and GPP is not yet clear Alden et al. [2016], suggesting that high NBE fluxes might be driven by high respiration rates. Alden et al. [2016] found more conclusive correlations between precipitation and NBE, concluding that there is a strong relationship between both, having very likely a time lag effect. Simulated NBE fluxes in SiBCASA and CASA are either presenting a strong uptake or a release of carbon to the atmosphere, which indicates that this annual variability is not captured by the models. Therefore, the simulated CO_2 profiles are highly influenced by this misrepresentation in the models.

When the performance of the fire inventories was analyzed for CO_2 vertical profiles large differences were not seen between inventories in RMSD. The site in which the match with observed CO_2 mole fractions was the worst was Tabatinga, but this is also supported by the fact that at this location there were fewer observations available and for a shorter time period; for years 2010-2012 there were 462 observations. In contrast, for Santarem, Alta Floresta and Rio Branco the number of observations for the same time period were: 1101, 684, 676, respectively. These numbers are directly related to the performance shown in Table 11, where Santarem had the lowest RMSD for all inventories, followed by Alta Floresta and then Rio Branco.

When looking at particular wet and dry seasons the performance of the simulations has a strong seasonal dependence for both CO and CO_2 profiles. The latter affects the skill of the simulations considerably, but is stronger for CO. It is worth mentioning that the production of CO by non methane hydrocarbons is not chemically driven within the TM5, but a representation of this source is emitted in the vertical profile, which is not relevant for the Amazon during the fire season. A possible sink of CO, which is within the TM5 chemistry scheme, is the reaction with OH but it occurs at a relatively slow time scale, from weeks to months (Krol, 2017, personal communication). According to the latter, it is possible to conclude that the fire season is driving the high CO concentrations in the Amazon, inducing high variability in CO concentrations difficult to reproduce by the TM5 model mainly at low heights, where high mole fractions are observed (i.e. dry seasons of 2010 and 2012 in Santarem).

However, there were a few simulated CO mean seasonal profiles that matched very well the observations. In the dry season of 2010 in Alta Floresta, simulations followed very close the shape of the observations suggesting that the vertical transport within the model captured the observed increase of CO at 2100m. At this same height for Tabatinga in 2011, also in the fire season, this feature is again observed for the simulated CO and CO_2 vertical profiles. Despite the fact this is based in one single observed point, the simulated profiles can be explained by the following mechanisms. The reason for the simulated CO increase (for all inventories) at this height might be a propagation of fire emissions to the top of the boundary layer, but in this case this is not corroborated with the observed profile. In contrast, the reason of the CO_2 decrease at this height might point to a propagation of an enhanced CO_2 uptake to the top of the boundary layer by the TM5 model (Krol, 2017, personal communication). As this is seen only for the CASA inventories it is possible to conclude that is due to a CASA driven uptake, not observed in the CO_2 mole fractions profile. In the wet season of 2010 in Rio Branco SiBCASA-GFED4 had a notable difference with the observed CO mole fractions at low heights. This can be associated to an early onset of the fire season in SiBCASA-GFED4, but as this is not seen in CASA-GFED4, at a first sight this reason is likely to be rejected. However, Rio Branco is located in a region where SiBCASA-GFED4 mainly has tropical forest that is subjected to the GFED4 burned area causing these high CO concentrations. The latter is supported by our spatial distribution analysis of burned area and fire emissions in Chapter 2.

The fire season of 2010 resulted in higher observed CO concentrations at lower heights than other years. The latter was strongly seen in the average values at all sites; in Rio Branco, reaching 360 ppb below 500m, followed by Alta Floresta with 300 ppb, Tabatinga with 260 ppb and Santarem with 225 ppb. Gatti et al. [2014] reported a high release of carbon by burning in the fire season of 2010 mainly in Alta Floresta, followed by Santarem and Rio Branco with similar estimates and Tabatinga as the last one. Gatti et al. [2014] estimates suggest that the regions of intense fire sensitivity are captured, to a large extent, in both approaches. However, from our results is interesting to see higher CO concentration in Tabatinga than in Santarem, something that is unexpected due to the proximity of Santarem to the northeast of Brazil where the fire season is certainly having a strong effect. Tabatinga is located farther east with respect to Santarem, considered to be isolated from intense fire regions as it lies deep into the Amazon rainforest, but the CO observations confirmed that during intense fire season the signal is indeed reaching Tabatinga. High CO concentrations in Alta Floresta and Rio Branco are expected as they are in regions with high fire activity. Alta Floresta is located farther to the south with respect to Santarem and here it is expected to have a strong fire signal, as it lies within the arc of deforestation. Recalling Figure 8 in Chapter 2, is possible to associate Alta Floresta to the hot spots seen along the 10ºS parallel and between the 60ºW - 45ºW meridians. Rio Branco is located more to the west with respect to Alta Floresta, closer to the Andes mountain range but still within an intense deforestation region. The fire signal here is also expected to be high for both tracers.

Due to time constraints further analysis with $CO:CO_2$ were not possible and it is therefore recommended to investigate these ratios for the time period studied here. The latter will be comparable with the ratios obtained by Van Der Laan-Luijkx et al. [2015] and will give an idea about the stage of the combustion process in which the emissions are produced (flaming or smoldering stages). Furthermore, it is important to mention that the next step of this process in order to improve the fluxes and thus the performance of the simulations is to performed an entire cycle of data assimilation and optimized the differences seen between observed and simulated values [Van Der Laan-Luijkx et al., 2015]. The carbon balance presented in Chapter 2 can be estimated more precisely assimilating observations, to obtain more precise fire emissions.

4.4 Conclusions

CO_2 and CO forward simulations were performed in order to assess the skill of the TM5 model with different fire emission inventories when compared to observations done in 4 sites of the Amazon. The simulations for CO_2 showed a strong influence of the NBE flux simulated by SiBCASA and CASA. This influence seemed to be stronger in the fire season, where the CASA inventories showed higher mole fractions along the vertical profile. CO observed concentrations showed a strong seasonal variability, which was difficult to reproduce with the TM5 simulations generally.

The skill of the TM5 using different fire inventories showed considerable changes within the seasons of the same year. Therefore it is not possible to suggest a best fire inventory to simulate fire emissions in the Amazon from this annual perspective. This is heavily dependent on the particular season that is being simulated. Therefore, the RMSD for the profiles simulated with the TM5 model change when seen from and individual year perspective or a merged year perspective. However, a clear influence of the amount of observations on the RMSD for CO_2 simulations at each site was found. From this grouped year RMSD analysis, and acknowledging the fact that CO_2 comes from a mixed signal, it is possible to conclude that SiBCASA-GFED4 was the best fire emissions input for the TM5 at Santarem (with RMSD of 2.36 ppm) and Rio Branco (3.19 ppm), CASA-GFED4-3hourly had the best performance in Alta Floresta (2.93 ppm) and FINN in Tabatinga (3.61). Interestingly, for CO simulated profiles FINN was the best fire inventory in three of the sites, with RMSD below 40 ppb, except of Rio Branco in which CASA-GFED4-daily proved to be slightly better with 43 ppb.

Chapter 5

5   General conclusions and outlook

The impact of biomass burning on the carbon balance of the Amazon, together with the performance of the simulated vertical and horizontal transport of fire emissions was the core topic of the present thesis. Since this work was related to that of Van Der Laan-Luijkx et al. [2015], the same fire inventories were used, adding a new one and a new biosphere model. Chapter 2 presented the results of this first approach to investigate the main differences between these fire inventories. In this chapter we focused on the following research questions:

> **Research Question 1:** *What are the differences (in terms of yearly values, spatial distribution and biome attribution) between the fire inventories used to calculate fire emissions in the Amazon for years 2010-2015?*
>
> **Research Question 2:** *What is the carbon balance in the Amazon for years 2010-2015?*

To tackle the first question the differences in annual averages of biomass burning CO_2 emissions, their spatial distribution and their distribution within biomes in the Amazon were analyzed. For the second question I looked at the NBE fluxes simulated by two biosphere models for the Amazon. From this chapter the main conclusions are that the fire inventories are able to capture the fire season in the Amazon, however the magnitude of emissions reported differ considerably. Generally SiBCASA-GFED4 is higher than the other inventories and GFAS is the lowest. Spatially the fire emissions seems similarly distributed but again with varying magnitude, which resulted in large differences when attributing emissions to biomes in the SiBCASA land cover. The carbon balance was highly affected by the NBE simulated by each biosphere model, showing that for the majority of the years when using SiBCASA's NBE the Amazon was a sink whereas using CASA's NBE the Amazon was a source of carbon (Table 5). The differences between SiBCASA-GFED4 and CASA-GFED4, even though having the same burned area input, led to the next research question which was approached in Chapter 3:

> **Research Question 3:** *What are the main drivers causing different emission estimates between SiBCASA-GFED4 and CASA-GFED4, considering they have the same burned area input?*

To answer this question the analysis was based on the SiBCASA biosphere model, as the SiBCASA-GFED4 fire inventory was developed in the Meteorology and Air Quality Department of Wageningen University. The first guess was that the land cover was the main driver of differences, but when looking into the specifics within each fire scheme it was found that SiBCASA had prescribed fire parameters, whereas CASA dynamic parameters. Therefore, to investigate this from the SiBCASA perspective two experiments were set up to see to what extent were these prescribed fire parameters influencing the obtained fire emissions. In the experiments the CASA's land cover was represented with SiBCASA's simulated carbon stocks, changing the CASA's biome Savanna and Grasslands to 1. All Grasslands or 2. All Savannas in SiBCASA. From these experiments it was found that representing CASA's land

cover with SiBCASA's carbon stocks and the GFED4 burned area, yielded higher fire emissions when compared to the standard SiBCASA-GFED4 and more interestingly to CASA-GFED4. The latter together with estimates of SiBCASA's fuel load, fuel consumption and burned area in each biome led to conclude that fuel consumption in SiBCASA is one order of magnitude higher, when including and without including mortality, than values reported for Tall Evergreen Broadleaf trees [Van Leeuwen et al., 2014]. For Savanna and Grasslands SiBCASA has lower fuel consumption than reported values Van Leeuwen et al. [2014] when taking into account mortality. Therefore, the main source of differences between SiBCASA-GFED4 and CASA-GFED was not only the biome distribution within each model, but also the simulated carbon stocks in SiBCASA-GFED4 and high (low) mortality for tropical forests (Savanna and Grasslands). The distribution of burned area and CO_2 fertilization within SiBCASA proved to be important factors in this comparison. In Chapter 4 the fire inventories described in Chapter 2 were used to simulate the vertical and horizontal transport of CO and CO_2 concentrations emitted by fires in four sites of the Amazon. At these sites observations done at different heights were available from 2010-2014, thus in Chapter 4 the following research questions were approached:

> **Research Question 4:** *How well do transported atmospheric CO mole fractions match with CO observations made in four aircraft sites in the Amazon for the period of 2010-2014?*
>
> **Research Question 5:** *How well do transported atmospheric CO_2 mole fractions match with CO_2 observations made in four aircraft sites in the Amazon for the period of 2010-2014?*

To tackle these questions the TM5 global transport model was used with two nested regions with higher horizontal resolution focusing in South America and in the Amazon. The match between the simulations and observations was assessed for each site concentrating on the wet and the fire seasons of each year for both tracers. From the latter it was concluded that the TM5 model, when using the imposed fire fluxes corresponding to the fire inventories mentioned before, had difficulties representing the fire season at all sites for CO_2 and CO. For CO there was a strong seasonal influence well marked in the wet and fire seasons vertical profiles, which affected strongly the match between simulations and observations, and showing that CO is a good fire tracer whereas CO_2 represents a mixed signal coming from the biosphere and fires. The performance was assessed also looking at the entire simulation period. For CO, FINN seemed to be the better fire emission input for the TM5 whereas for CO_2 SiBCASA-GFED4 had the best performance in Santarem and Rio Branco, CASA-GFED4-3hourly in Alta Floresta and FINN in Tabatinga. Furthermore, NBE flux influenced to a large extent simulated CO_2 profiles, pointing to a high flux from the biosphere in CASA, which can be related to a high respiration rate within this model.

This research process is considered to be a fundamental step previous to a data assimilation cycle. The variability of the fire fluxes that could be potential prior fire fluxes in a data assimilation cycle is highlighted. For regional studies, like this one, is important to assess the variability of different sources to get correct estimates of fire emissions and NBE, which affect further the net biome exchange between the biosphere and the atmosphere. In particular for burned area fire inventories there can be large differences driven by the carbon stock source. As general recommendations and further work derived from this study the following is highlighted:

1. SiBCASA carbon stocks should be revised for all biomes, as well as the mortalities associated to them. Adjusting the vegetation recovery in SiBCASA is needed, as it is recovering very fast after each fire event. It is worth to include dynamic fire parameters within SiBCASA's fire scheme in order to represent more accurately the combustion completeness and mortality.

2. Further analyses with different simulated NBE is recommended to constrain the differences between SiBCASA and CASA.

3. Varying the injection heights in TM5 is worth analyzing to improve simulations, although a first step would be to optimized fire inventories with observed CO columns from satellite data.

4. Optimizing fire inventories and NBE fluxes is the next step to obtain better simulated profiles. The first step of this process is shown in Chapter 6 shown in the appendix.

5. Including more observations available for the Amazon, like those of the Amazon Tall Tower Observatory, might improve the flux estimates taking into account that the observed vertical profiles are taken every two weeks.

Chapter 6

6 Optimized fires inventories

As it was stated in the recommendations, one of the next steps that follow this thesis is to optimized the fire fluxes. This short chapter presents a preliminar analysis of optimized fires. It is worth mentioning that the optimizations were done by Narcisa Banda at Utrecht University, here her output is analyzed.

6.1 Methods

The fire products described in Chapter 2 were optimized using the Infrared Atmospheric Sounding Interferometer (IASI) on board the METOP-A satellite [Clerbaux et al., 2009]. The approach was divided in three main steps. First CO emissions were obtained by using emission factors from Andreae [2001] and the fire emissions given by SiBCASA-GFED4, GFAS, FINN and CASA-GFED4 inventories. Second, the optimization was done with CO from IASI using the TM5-4DVar method [Krol et al., 2013]. Finally the difference between the prior and the posterior (as CO) was applied as a percentage of change to the fire inventories per each 1°x1° grid cell and time step. To get more details on the methods of this optimization, the reader is referred to Van Der Laan-Luijkx et al. [2015]. It is important to note that the set up used in TM5-4Dvar permitted negative values for CO. Therefore adjustments were performed to these negative values in each time-step. First, negative emissions were quantified per time step and then they were set to zero. Second, a compensation was done by assigning, in the same time step, this negative quantity to the grid cells that presented the highest positive emissions (highest 90%). The compensation was postponed to the next time step if the amount of negative emissions was too high; the total emissions had to remain equal. We acknowledge the fact that this manipulation might hamper the optimization. However, it was performed to have a first approach to an optimized set of fire inventories that can be analyzed in this thesis. It is advisable to re-run the optimization without permitting negative concentrations in the TM5-4Dvar set up and compare those results with the ones presented here.

6.2 Results

The results from the optimization are shown separately for each fire inventory so they can be easily compared to the non-optimized version. Here the CASA-GFED4 3 hourly version was not used due to time constraints, but all the other 4 fire inventories presented in Chapter 2 are shown.

6.2.1 Optimized and non-optimized daily time series comparison

Figure 34 shows the non-optimized and the optimized comparison of SiBCASA-GFED4. The optimization of SiBCASA-GFED4 yielded lower maximum values compared to the non-optimized inventory and the timing of the fire season is delayed for all years compared to the non-optimized version. Note that for year 2015 there are two peaks of strong fires in the optimized SiBCASA-GFED4. This suggests a second onset of the fire season which is not observed in the non-optimized

SiBCASA-GFED4. The double peak in 2015 could be due to the adjustments performed to correct the negative values.

Figure 35 shows the comparison of the optimized and non-optimized of the GFAS inventory. Note that for the optimized GFAS there are no values for 2015. The latter was due to and mistake in the end date of the simulation, which was difficult to correct due to time constraints. The optimization of GFAS is interesting because it shows a higher optimized fire flux for 2010 and 2014, whereas for 2011, 2012 and 2013 the optimization might to follow the same pattern as the non-optimized curve. The timing of the fire season was not delayed in this case in the optimized curve.
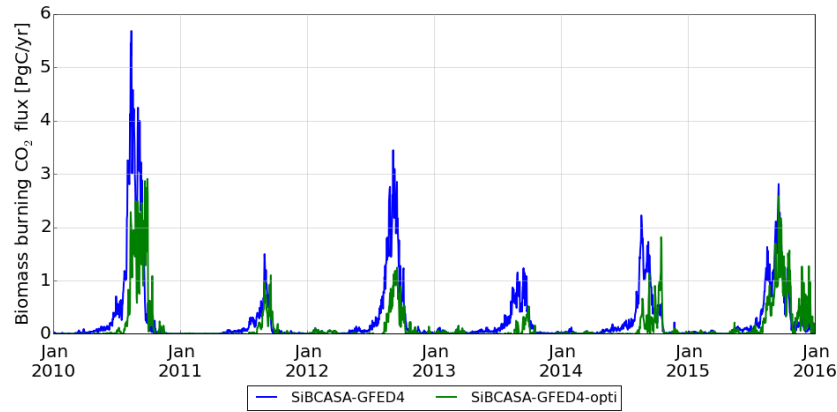

Figure 34: Daily time series of biomass burning carbon emissions in the Amazon for the optimized SiBCASA-GFED4 fire inventory.
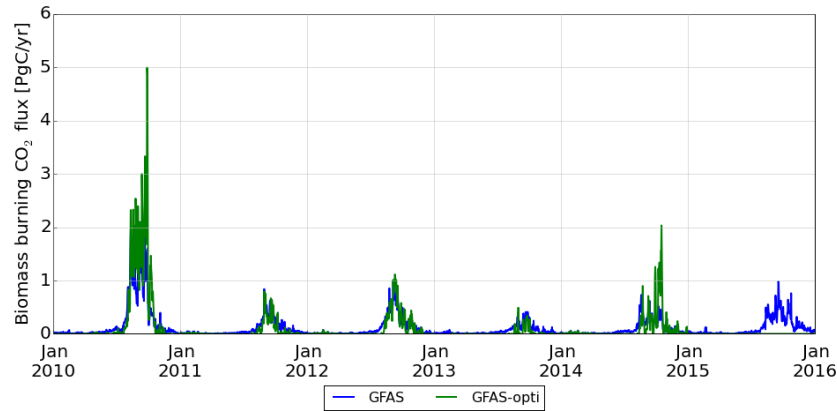

Figure 35: Daily time series of biomass burning carbon emissions in the Amazon for the optimized GFAS fire inventory.

Figure 36 shows the comparison of the both versions of the FINN fire inventory. The optimized inventory shows unexpected peaks in 2015 and 2014. In 2010 there is also a high peak during the fire season, but is more modest compared to 2015. The adjustments of the negative values might be responsible for these high fire emissions. In the years between 2011 and 2014 the optimized fire emissions are below the non-optimized FINN inventory, which suggests that in years with high fire emissions the optimization tends to yield high values and, for years with low fire emissions the optimization tends to yield low fire emissions. In Figure 37 the non-optimized and optimized CASA-GFED4 daily are shown. The optimization here had a similar effect as that with FINN. High values for 2010, 2014 and 2015 are presented. The other years both versions are very close to each other with similar variability. Note again the double peak in 2015 as in the SiBCASA-GFED4 optimization.
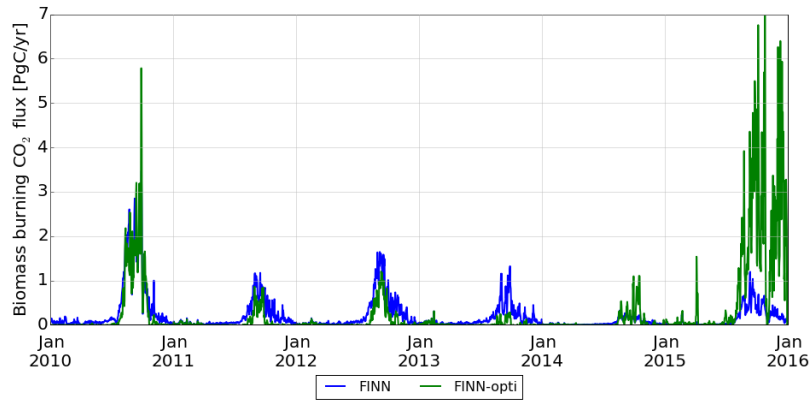
Figure 36: Daily time series of biomass burning carbon emissions in the Amazon for the optimized FINN fire inventory.
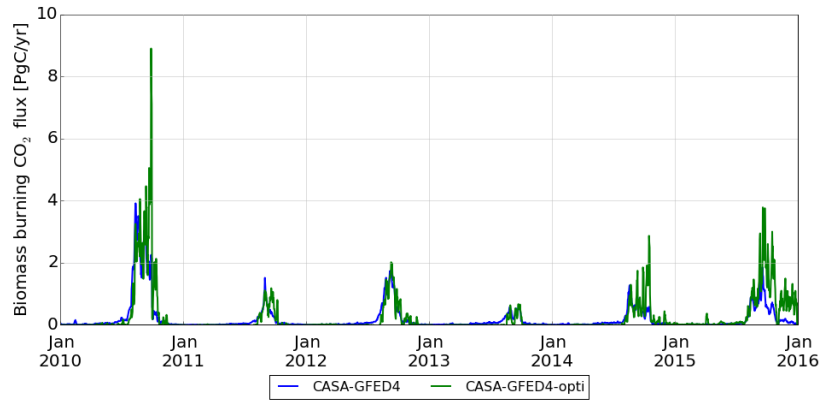
Figure 37: Daily time series of biomass burning carbon emissions in the Amazon for the CASA-GFED4 fire inventory.

6.2.2 CO$_2$ Vertical Profiles with optimized fire inventories and RMSD

In Table 13 the RMSD for the non-optimized and the optimized fire inventories are shown. Note that the values in brackets are indicating the Root Mean Squares Differences (RMSD) for the optimized inventories. It was expected that the optimizations will improve the RMSD relative to the RMSD calculated with the non-optimized inventories. However this was the case only for the CASA-GFED4 inventory. SiBCASA-GFED4, GFAS and FINN when optimized yielded higher RMSD at all sites. It is believed that the adjustments of the negative values influenced the RMSD as well as the NBE signal, which is the same for SiBCASA-GFED4, GFAS and FINN.

Table 13: General Root Mean Square Differences (RMSD) between observed and simulated CO$_2$ mole fractions for the entire simulated period. Values in brackets indicate the RMSD calculated with the optimized fire inventories. The optimized RMSD that are lower relative to the non-optimized are indicated in bold.

	SAN	ALF	RBO	TAB
SiBCASA-GFED4	2.36 (2.52)	2.98 (3.31)	3.19 (3.56)	3.65 (3.72)
GFAS	2.47 (2.52)	3.21 (3.28)	3.47 (3.53)	3.68 (3.69)
FINN	2.44 (2.50)	3.09 (3.22)	3.24 (3.51)	3.61 (3.67)
CASA-GFED4-daily	2.58 (**2.57**)	3.20 (**3.09**)	3.54 (**3.39**)	4.06 (**3.98)**

The simulated vertical profiles for the optimized fire inventories are not shown here as the vertical distribution did not show considerable changes with respect to the non-optimized inventories. The forward simulations were done as in Chapter 4, for all sites: Santarem, Alta Floresta, Rio Branco and Tabatinga. For all sites the optimized profiles for SiBCASA-GFED4, GFAS, and FINN are closer to each other, whereas the optimized CASA-GFED4 is, in most of the cases, considerably higher. SiBCASA-GFED4, GFAS and FINN are similar because the NBE signal used for these inventories is that of SiBCASA. The simulated profiles presented here, show almost no considerable changes in the vertical distribution when compared to the non-optimized profiles. This is related to the fact that the IASI observations are more sensitive between 4km and 6km of altitude [Van Der Laan-Luijkx et al., 2015].

6.3 Follow up work

From these preliminar results it is recommended to continue with the following points:

1. Perform optimizations without allowing negative values and compared to the results given here.

2. Assess the feasibility of including other observation sources in the optimization, such as data from the Amazonian Tall Tower Observatory (ATTO).
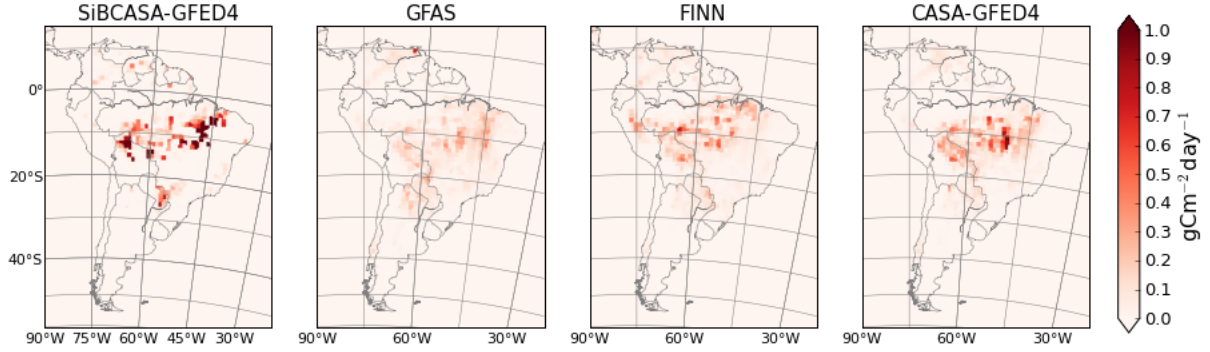
7 Appendix

Chapter 2

Figure 38: Averaged fire emissions for each fire inventory for the period 2010-2015

Chapter 3

Table 14: Area distribution for the biomes of the Amazon in SiBCASA's land cover

	$*10^6$ km^2	%
Evergreen Broadleaf trees	4.71	66.88
Broadleaf and needleleaf trees	0.34	4.82
Savanna	0.97	13.89
Grasslands	0.84	12.06
Shrubs	0.07	0.99
Tundra	0.03	0.51
Agriculture	0.06	0.85

Table 15: Area distribution for the biomes of the Amazon in CASA land cover

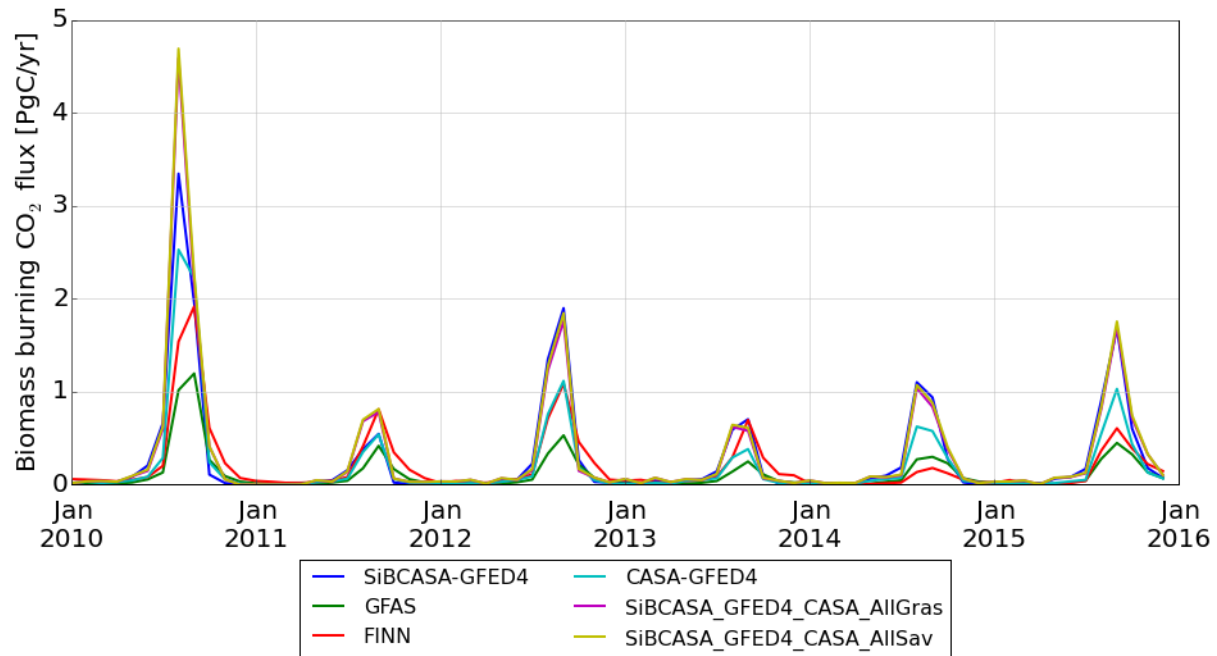|	$*10^6$ km^2	%
Evergreen Broadleaf forest	5.72	81.20
Deciduos broadleaf forest	0.07	0.99
Shrublands	0.09	1.4
Savanna and Grasslands	1.12	15.91
Croplands	0.03	0.50

Figure 39: Monthly time series for all fire inventories and the two experiments described in chapter 3: All Grasslands and All Savanna.
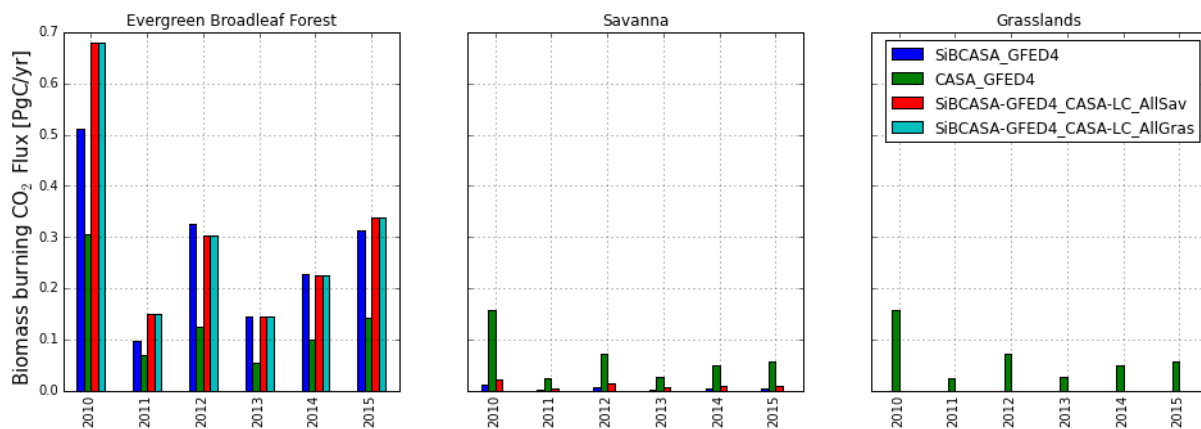

Figure 40: CO_2 flux in petagrams per year for each biome within the two experiments described in Chapter 3 and for the SiBCASA-GFED4 and CASA-GFED4 fire inventories.
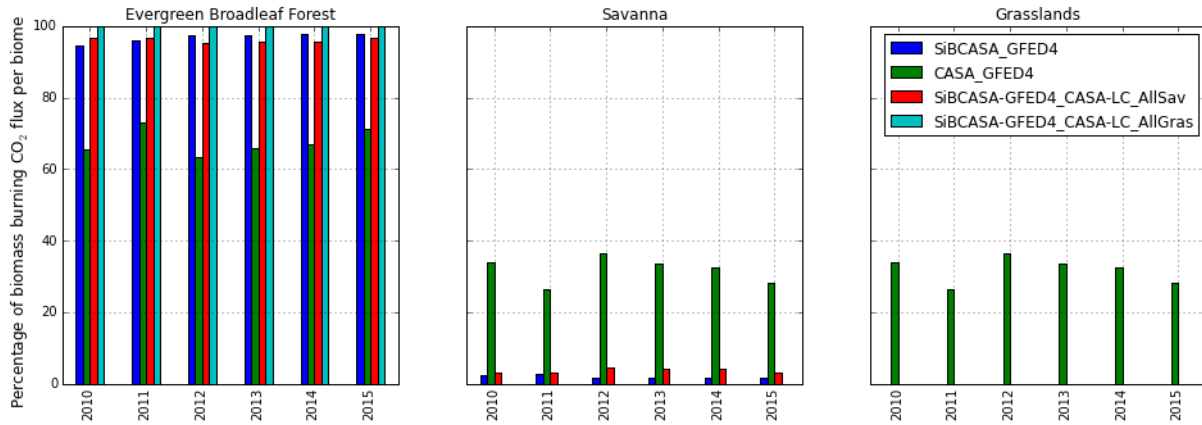
Figure 41: CO_2 flux percentage for each biome within the two experiments described in Chapter 3 and for the SiBCASA-GFED4 and CASA-GFED4 fire inventories.
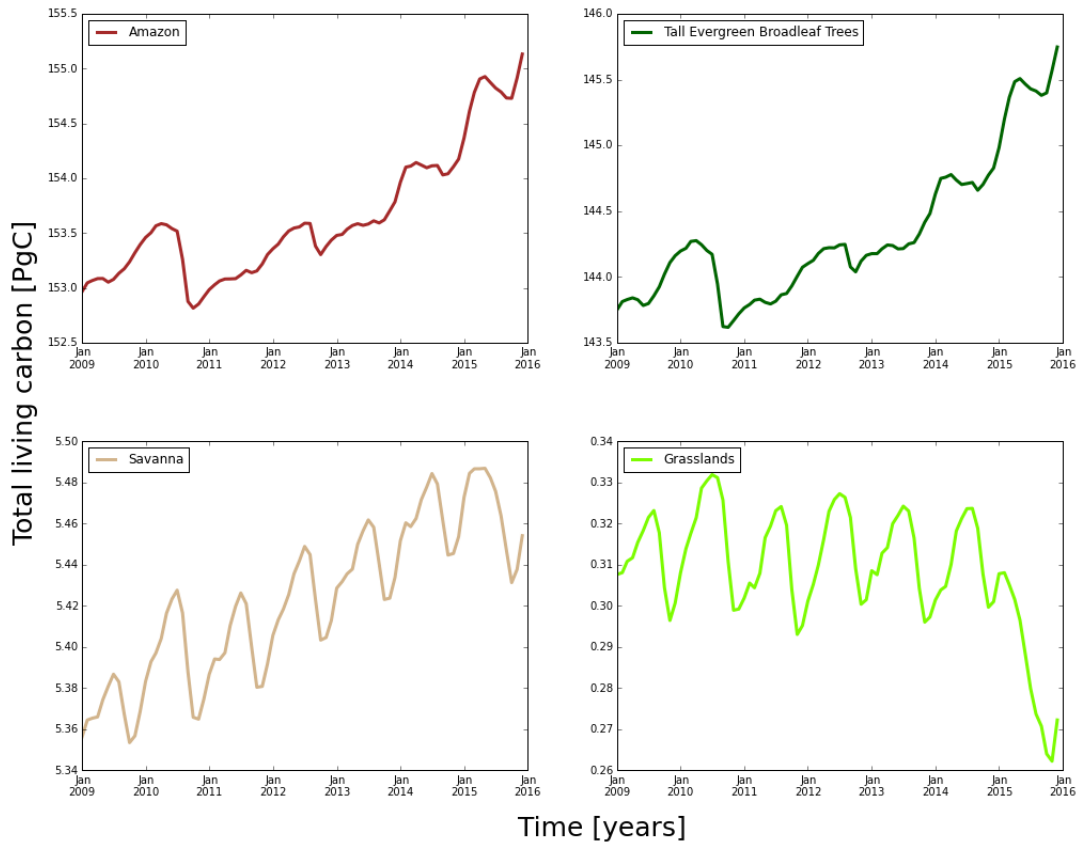

Figure 42: Total living carbon evolution (2009-2015) for all the Amazon and the main biomes within the Amazon area: the Tall Evergreen Broadleaf trees, Savanna and Grasslands biomes. Note the different y axis.
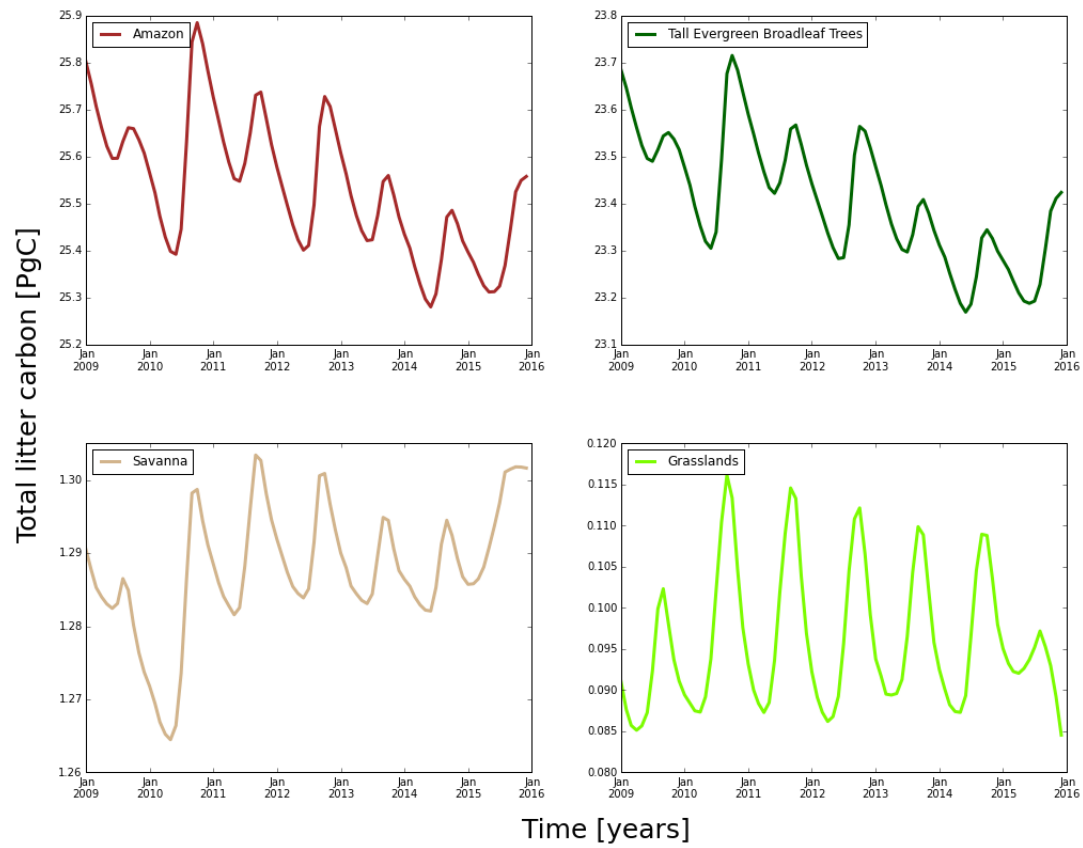
Figure 43: Total litter carbon evolution (2009-2015) for all the Amazon and the main biomes within the Amazon area: the Tall Evergreen Broadleaf trees, Savanna and Grasslands biomes. Note the different y axis.

References

S. K. Akagi, R. J. Yokelson, C. Wiedinmyer, M. J. Alvarado, J. S. Reid, T. Karl, J. D. Crounse, and P. O. Wennberg. Emission factors for open and domestic biomass burning for use in atmospheric models. *Atmospheric Chemistry and Physics*, 11(9):4039–4072, 2011. doi: 10.5194/acp-11-4039-2011.

Caroline B. Alden, John B. Miller, Luciana V. Gatti, Manuel M. Gloor, Kaiyu Guan, Anna M. Michalak, Ingrid T. van der Laan-Luijkx, Danielle Touma, Arlyn Andrews, Luana S. Basso, Caio S C Correia, Lucas G. Domingues, Joanna Joiner, Maarten C. Krol, Alexei I. Lyapustin, Wouter Peters, Yoichi P. Shiga, Kirk Thoning, Ivar R. van der Velde, Thijs T. van Leeuwen, Vineet Yadav, and Noah S. Diffenbaugh. Regional atmospheric CO2 inversion reveals seasonal and geographic differences in Amazon net biome exchange. *Global Change Biology*, 22(10):3427–3443, 2016. doi: 10.1111/gcb.13305.

N. Andela, J.W. Kaiser, A. Heil, T.T. van Leeuwen, G.R. van der Werf, M.J. Wooster, S. Remy, and M.G. Schultz. Assessment of the Global Fire Assimilation System GFAS v1.0. pages 1–75, 2013. URL http://www.gmes-atmosphere.eu/about/project_structure/input_data/d_fire/.

Niels Andela, Guido R. Van Der Werf, Johannes W. Kaiser, Thijs T. Van Leeuwen, Martin J. Wooster, and Caroline E R Lehmann. Biomass burning fuel consumption dynamics in the tropics and subtropics assessed from satellite. *Biogeosciences*, 13(12):3717–3734, 2016. doi: 10.5194/bg-13-3717-2016.

M O Andreae. Emission of trace gases and aerosols from biomass burning. *Biogeochemistry*, 15(4): 955–966, 2001.

M. O. Andreae, O. C. Acevedo, A. Araùjo, P. Artaxo, C. G G Barbosa, H. M J Barbosa, J. Brito, S. Carbone, X. Chi, B. B L Cintra, N. F. Da Silva, N. L. Dias, C. Q. Dias-Júnior, F. Ditas, R. Ditz, A. F L Godoi, R. H M Godoi, M. Heimann, T. Hoffmann, J. Kesselmeier, T. Könemann, M. L. Krüger, J. V. Lavric, A. O. Manzi, A. P. Lopes, D. L. Martins, E. F. Mikhailov, D. Moran-Zuloaga, B. W. Nelson, A. C. Nölscher, D. Santos Nogueira, M. T F Piedade, C. Pöhlker, U. Pöschl, C. A. Quesada, L. V. Rizzo, C. U. Ro, N. Ruckteschler, L. D A Sá, M. De Oliveira Sá, C. B. Sales, R. M N Dos Santos, J. Saturno, J. Schöngart, M. Sörgel, C. M. De Souza, R. A F De Souza, H. Su, N. Targhetta, J. Tóta, I. Trebs, S. Trumbore, A. Van Eijck, D. Walter, Z. Wang, B. Weber, J. Williams, J. Winderlich, F. Wittmann, S. Wolff, and A. M. Yáñez-Serrano. The Amazon Tall Tower Observatory (ATTO): Overview of pilot measurements on ecosystem ecology, meteorology, trace gases, and aerosols. *Atmospheric Chemistry and Physics*, 15(18):10723–10776, 2015. doi: 10.5194/acp-15-10723-2015.

Dennis D Baldocchi. 'Breathing'of the terrestrial biosphere: lessons learned from a global network of carbon dioxide flux measurement systems. *Australian Journal of Botany*, 56(15):1–26, 2008. doi: doi:10.1071/BT07151.

D.M.J.S. Bowman, Jennifer K Balch, Paulo Artaxo, William J Bond, Jean M Carlson, Mark A Cochrane, C M A D'Antonio, Ruth S DeFries, John C Doyle, Sandy P Harrison, Fay H Johnston, Jon E Keeley, Meg A Krawchuk, Christian a Kull, J Brad Marston, Max a Moritz, I Colin Prentice, Christopher I Roos, Andrew C Scott, Thomas W Swetnam, Guido R van der Werf, David M J S Bowman, Pyne S.J., Carla M D'Antonio, and Stephen J Pyne. Fire in the Earth System. *Science*, 324(5926):481–484, 2009. doi: 10.1126/science.1163886.

R. J. W. Brienen, O. L. Phillips, T. R. Feldpausch, E. Gloor, T. R. Baker, J. Lloyd, G. Lopez-Gonzalez, A. Monteagudo-Mendoza, Y. Malhi, S. L. Lewis, R Martinez Vasquez, M. Alexiades,

E Dávila Álvarez, P. Alvarez-Loayza, A. Andrade, L.E. O. Araga, C. Aragao, A. Araujo-Murakami, E. J. M. M. Arets, L. Arroyo, G. A. Aymard C, O. S. Banki, C. Baraloto, J. Barroso, D. Bonal, R. G. A. Boot, J. L.C. Camargo, C. V. Castilho, V. Chama, K. J. Chao, J. Chave, J. A. Comiskey, F. Cornejo Valverde, L. da Costa, E. A. de Oliveira, A. Di Fiore, T. L. Erwin, S. Fauset, M. Forsthofer, D. R. Galbraith, E. S. Grahame, N. Groot, B. Herault, N. Higuchi, E. N. Honorio Coronado, H. Keeling, T. J. Killeen, W. F. Laurance, S. Laurance, J. Licona, W. E. Magnussen, B. S. Marimon, B.H. Marimon-Junior, C. Mendoza, D. A. Neill, E. M. Nogueira, P. Nunez, N.C. Pallqui Camacho, A. Parada, G. Pardo-Molina, J. Peacock, M. Peña-Claros, G. C. Pickavance, N. C. A. Pitman, L. Poorter, A. Prieto, C. A. Quesada, F. Ramírez, H. Ramírez-Angulo, Z. Restrepo, A. Roopsind, A. Rudas, R.P. Salomao, M. Schwarz, N. Silva, J. E. Silva-Espejo, M. Silveira, J. Stropp, J. Talbot, H. ter Steege, J. Teran-Aguilar, J. Terborgh, R. Thomas-Caesar, M. Toledo, M. Torello-Raventos, R. K. Umetsu, G. M. F. van der Heijden, P. van der Hout, I. C. Guimaraes Vieira, S. A. Vieira, E. Vilanova, and V. A. Vos. Long-term decline of the Amazon carbon sink. *Nature*, 519:344–348, 2015. doi: 10.1038/nature14283.

Philippe Ciais, Christopher Sabine, G Bala, Laurent Bopp, Victor Brovkin, J. Canadell, A Chhabra, R DeFries, J. Galloway, Martin Heimann, C Jones, C. Le Quéré, R.B. Myneni, S Piao, and P Thornton. The physical science basis. Contribution of working group I to the fifth assessment report of the intergovernmental panel on climate change. *Change, IPCC Climate*, pages 465–570, 2013. doi: 10.1017/CBO9781107415324.015.

C. Clerbaux, A. Boynard, L. Clarisse, M. George, J. Hadji-Lazaro, H. Herbin, D. Hurtmans, M. Pommier, A. Razavi, S. Turquety, C. Wespes, and P.-F. Coheur. Monitoring of atmospheric composition using the thermal infrared IASI/MetOp sounder. *Atmospheric Chemistry and Physics*, 9(16):6041–6054, 2009. doi: 10.5194/acp-9-6041-2009.

Jhan Carlo Espinoza, Josyane Ronchail, Jean Loup Guyot, Clementine Junquas, Philippe Vauchel, Waldo Lavado, Guillaume Drapeau, and Rodrigo Pombosa. Climate variability and extreme drought in the upper Solimões River (western Amazon Basin): Understanding the exceptional 2010 drought. *Geophysical Research Letters*, 38(13):1–6, 2011. doi: 10.1029/2011GL047862.

T R Feldpausch, O L Phillips, R J W Brienen, E Gloor, J Lloyd, Y Malhi, A Alarcón, E Álvarez Dávila, A Andrade, L E O C Aragao, L Arroyo, G A C Aymard, T R Baker, C Baraloto, J Barroso, D Bonal, W Castro, V Chama, J Chave, T F Domingues, S Fauset, N Groot, E Honorio Coronado, S Laurance, W F Laurance, S L Lewis, J C Licona, B S Marimon, C Mendoza Bautista, D A Neill, E A Oliveira, C Oliveira Santos, N C Pallqui Camacho, A Prieto, C A Quesada, F Ramírez, A Rudas, G Saiz, R P Salomão, M Silveira, H Steege, J Stropp, J Terborgh, G M F Heijden, R Vásquez Martinez, E Vilanova, and V A Vos. Global Biogeochemical Cycles. pages 1–19, 2016. doi: 10.1002/2015GB005133.Received.

L V Gatti, M Gloor, J B Miller, C E Doughty, Y Malhi, L G Domingues, L S Basso, A Martinewski, C S C Correia, V F Borges, S Freitas, R Braz, L O Anderson, H Rocha, J Grace, O L Phillips, and J Lloyd. Drought sensitivity of Amazonian carbon balance revealed by atmospheric measurements. *Nature*, 506(7486):76–80, 2014. doi: 10.1038/nature12957.

Louis Giglio, James T. Randerson, and Guido R. Van Der Werf. Analysis of daily, monthly, and annual burned area using the fourth-generation global fire emissions database (GFED4). *Journal of Geophysical Research: Biogeosciences*, 118(1):317–328, 2013. doi: 10.1002/jgrg.20042.

M. Gloor, L. Gatti, R. Brienen, T. R. Feldpausch, O. L. Phillips, J. Miller, J. P. Ometto, H. Rocha, T. Baker, B. De Jong, R. A. Houghton, Y. Malhi, L. E O C. Arag??o, J. L. Guyot, K. Zhao, R. Jackson, P. Peylin, S. Sitch, B. Poulter, M. Lomas, S. Zaehle, C. Huntingford, P. Levy, and

J. Lloyd. The carbon balance of South America: A review of the status, decadal trends and main determinants, 2012.

M. Gloor, J. Barichivich, G. Ziv, R. Brienen, J. Schöngart, P. Peylin, B. Barcante Ladvocat Cintra, T. Feldpausch, O. Phillips, and J. Baker. Recent Amazon climate as background for possible ongoing and future changes of Amazon humid forests. *Global Biogeochemical Cycles*, 29(9):1384–1399, 2015. doi: 10.1002/2014GB005080.

Stijn Hantson, Almut Arneth, Sandy P. Harrison, Douglas I. Kelley, I. Colin Prentice, Sam S. Rabin, Sally Archibald, Florent Mouillot, Steve R. Arnold, Paulo Artaxo, Dominique Bachelet, Philippe Ciais, Matthew Forrest, Pierre Friedlingstein, Thomas Hickler, Jed O. Kaplan, Silvia Kloster, Wolfgang Knorr, Gitta Lasslop, Fang Li, Stephane Mangeon, Joe R. Melton, Andrea Meyn, Stephen Sitch, Allan Spessa, Guido R. Van Der Werf, Apostolos Voulgarakis, and Chao Yue. The status and challenge of global fire modelling. *Biogeosciences*, 13(11):3359–3375, 2016. doi: 10.5194/bg-13-3359-2016.

Andrew R. Jacobson, Sara E Mikaloff Fletcher, Nicolas Gruber, Jorge L. Sarmiento, and Manuel Gloor. A joint atmosphere-ocean inversion for surface fluxes of carbon dioxide: 1. Methods and global-scale fluxes. *Global Biogeochemical Cycles*, 21(1), 2007. doi: 10.1029/2005GB002556.

Juan C Jiménez-Muñoz, Cristian Mattar, Jonathan Barichivich, Andrés Santamaría-Artigas, Ken Takahashi, Yadvinder Malhi, José A Sobrino, and Gerard van der Schrier. Record-breaking warming and extreme drought in the Amazon rainforest during the course of El Niño 2015–2016. *Scientific Reports*, 6:33130, 2016. doi: 10.1038/srep33130.

J. W. Kaiser, A. Heil, M. O. Andreae, A. Benedetti, N. Chubarova, L. Jones, J. J. Morcrette, M. Razinger, M. G. Schultz, M. Suttie, and G. R. Van Der Werf. Biomass burning emissions estimated with a global fire assimilation system based on observed fire radiative power, 2012.

Jaya Khanna, David Medvigy, Stephan Fueglistaler, and Robert Walko. Regional dry-season climate changes due to three decades of Amazonian deforestation. *Nature Climate Change*, (February), 2017. doi: 10.1038/NCLIMATE3226.

Markus Kottek, Jürgen Grieser, Christoph Beck, Bruno Rudolf, and Franz Rubel. World map of the Köppen-Geiger climate classification updated. *Meteorologische Zeitschrift*, 15(3):259–263, 2006. doi: 10.1127/0941-2948/2006/0130.

M Krol, S Houweling, B Bregman, M van den Broek, A Segers, P van Velthoven, W Peters, F Dentener, and P Bergamaschi. The two-way nested global chemistry-transport zoom model TM5: algorithm and applications. *Atmospheric Chemistry and Physics*, 5:417–432, 2005. doi: 10.5194/acpd-4-3975-2004.

M. Krol, W. Peters, P. Hooghiemstra, M. George, C. Clerbaux, D. Hurtmans, D. McInerney, F. Sedano, P. Bergamaschi, M. El Hajj, J. W. Kaiser, D. Fisher, V. Yershov, and J. P. Muller. How much CO was emitted by the 2010 fires around Moscow? *Atmospheric Chemistry and Physics*, 13 (9):4737–4747, 2013. doi: 10.5194/acp-13-4737-2013.

Corinne Le Queré, Robbie M. Andrew, Josep G. Canadell, Stephen Sitch, Jan Ivar Korsbakken, Glen P. Peters, Andrew C. Manning, Thomas A. Boden, Pieter P. Tans, Richard A. Houghton, Ralph F. Keeling, Simone Alin, Oliver D. Andrews, Peter Anthoni, Leticia Barbero, Laurent Bopp, Fr??d??ric Chevallier, Louise P. Chini, Philippe Ciais, Kim Currie, Christine Delire, Scott C. Doney, Pierre Friedlingstein, Thanos Gkritzalis, Ian Harris, Judith Hauck, Vanessa Haverd, Mario Hoppema, Kees Klein Goldewijk, Atul K. Jain, Etsushi Kato, Arne Kortzinger, Peter Landschutzer, Nathalie

Lefevre, Andrew Lenton, Sebastian Lienert, Danica Lombardozzi, Joe R. Melton, Nicolas Metzl, Frank Millero, Pedro M S Monteiro, David R. Munro, Julia E M S Nabel, Shin Ichiro Nakaoka, Kevin O'Brien, Are Olsen, Abdirahman M. Omar, Tsuneo Ono, Denis Pierrot, Benjamin Poulter, Christian Rodenbeck, Joe Salisbury, Ute Schuster, Jorg Schwinger, Roland Séférian, Ingunn Skjelvan, Benjamin D. Stocker, Adrienne J. Sutton, Taro Takahashi, Hanqin Tian, Bronte Tilbrook, Ingrid T. Van Der Laan-Luijkx, Guido R. Van Der Werf, Nicolas Viovy, Anthony P. Walker, Andrew J. Wiltshire, and Sonke Zaehle. Global Carbon Budget 2016. *Earth System Science Data*, 8 (2):605–649, 2016. doi: 10.5194/essd-8-605-2016.

Simon L Lewis, Paulo M Brando, Oliver L Phillips, Geertje M F Van Der Heijden, and Daniel Nepstad. The 2010 Amazon Drought. *Science*, 331, 2011. doi: 10.1126/science.1200807.

Yongqiang Liu, Scott Goodrick, and Warren Heilman. Wildland fire emissions, carbon, and climate: Wildfire-climate interactions. *Forest Ecology and Management*, 317:80–96, 2014. doi: 10.1016/j.foreco.2013.02.020.

Rachel A. Loehman, Elizabeth Reinhardt, and Karin L. Riley. Wildland fire emissions, carbon, and climate: Seeing the forest and the trees - A cross-scale assessment of wildfire and carbon dynamics in fire-prone, forested ecosystems. *Forest Ecology and Management*, 317:9–19, 2014. doi: 10.1016/j.foreco.2013.04.014.

Yiqi Luo and Ensheng Weng. Dynamic disequilibrium of the terrestrial carbon cycle under global change. *Trends in Ecology and Evolution*, 26(2):96–104, 2011. doi: 10.1016/j.tree.2010.11.003.

Yadvinder Malhi, Daniel Wood, Timothy R. Baker, James Wright, Oliver L. Phillips, Thomas Cochrane, Patrick Meir, Jerome Chave, Samuel Almeida, Luzmilla Arroyo, Niro Higuchi, Timothy J. Killeen, Susan G. Laurance, William F. Laurance, Simon L. Lewis, Abel Monteagudo, David A. Neill, Percy Núñez Vargas, Nigel C A Pitman, Carlos Alberto Quesada, Rafael Salomão, José Natalino M Silva, Armando Torres Lezama, John Terborgh, Rodolfo Vásquez Martínez, and Barbara Vinceti. The regional variation of aboveground live biomass in old-growth Amazonian forests. *Global Change Biology*, 12(7):1107–1138, 2006. doi: 10.1111/j.1365-2486.2006.01120.x.

J. A. Marengo and J. C. Espinoza. Extreme seasonal droughts and floods in Amazonia: Causes, trends and impacts. *International Journal of Climatology*, 36(3):1033–1050, 2016. doi: 10.1002/joc.4420.

Robert S. Nowak. CO2 fertilization: Average is best. *Nature Climate Change*, 7(2):101–102, 2017. doi: 10.1038/nclimate3212.

Yude Pan, Richard A. Birdsey, Jingyun Fang, Richard Houghton, Pekka E. Kauppi, Werner A. Kurz, Oliver L. Phillips, Anatoly Shvidenko, Simon L. Lewis, Josep G. Canadell, Philippe Ciais, Robert B. Jackson, Stephen W. Pacala, David McGuire, Shilong Piao, Aapo Rautiainen, Stephen Sitch, and Daniel Hayes. A Large and Persistent Carbon Sink in the World's Forest. *Science*, 333(August): 988–993, 2011.

Wouter Peters, J. B. Miller, J. Whitaker, a. S. Denning, A. Hirsch, M. C. Krol, D. Zupanski, L. Bruhwiler, and P. P. Tans. An ensemble data assimilation system to estimate CO2 surface fluxes from atmospheric trace gas observations. *Journal of Geophysical Research: Atmospheres*, 110(D24):1–18, 2005. doi: 10.1029/2005JD006157.

Wouter Peters, Andrew R Jacobson, Colm Sweeney, Arlyn E Andrews, Thomas J Conway, Kenneth Masarie, John B Miller, Lori M P Bruhwiler, Gabrielle Pétron, Adam I Hirsch, Douglas E J Worthy, Guido R van der Werf, James T Randerson, Paul O Wennberg, Maarten C Krol, and Pieter P Tans. An atmospheric perspective on North American carbon dioxide exchange: CarbonTracker.

Proceedings of the National Academy of Sciences of the United States of America, 104(48):18925–18930, 2007. doi: 10.1073/pnas.0708986104.

C S. Potter, James T. Randerson, C. Field, P. Matson, P. Vitousek, H. Mooney, and S. Klooster. Terrestrial ecosystem production: a process model based on global satellite and surface data. *Global Biogeochemical Cycles*, 7(4):811–841, 1993. doi: 10.1029/93GB02725.

J. T. Randerson, Y. Chen, G. R. Van Der Werf, B. M. Rogers, and D. C. Morton. Global burned area and biomass burning emissions from small fires. *Journal of Geophysical Research: Biogeosciences*, 117(4), 2012. doi: 10.1029/2012JG002128.

A. Rap, D. V. Spracklen, L. Mercado, C. L. Reddington, J. M. Haywood, R. J. Ellis, O. L. Phillips, P. Artaxo, D. Bonal, N. Restrepo Coupe, and N. Butt. Fires increase Amazon forest productivity through increases in diffuse radiation. *Geophysical Research Letters*, 42(11):4654–4662, 2015. ISSN 19448007. doi: 10.1002/2015GL063719.

Sassan Saatchi, R. A. Houghton, R. C. Dos Santos Alvalá, J. V. Soares, and Y. Yu. Distribution of aboveground live biomass in the Amazon basin. *Global Change Biology*, 13(4):816–837, 2007. doi: 10.1111/j.1365-2486.2007.01323.x.

Kevin Schaefer, G. James Collatz, Pieter Tans, A. Scott Denning, Ian Baker, Joe Berry, Lara Prihodko, Neil Suits, and Andrew Philpott. Combined simple biosphere/carnegie-ames-stanford approach terrestrial carbon cycle model. *Journal of Geophysical Research: Biogeosciences*, 113(3), 2008. doi: 10.1029/2007JG000603.

David Schimel, Britton B. Stephens, and Joshua B. Fisher. Effect of increasing CO_2 on the terrestrial carbon cycle. *Proceedings of the National Academy of Sciences*, 112(2):201407302, 2014. doi: 10.1073/pnas.1407302112.

Wolfgang Seiler and Paul J. Crutzen. Estimates of gross and net fluxes of carbon between the biosphere and the atmosphere from biomass burning. *Climatic Change*, 2(3):207–247, 1980. doi: 10.1007/BF00137988.

Carlos A Sierra. Modelling processes at the ecosystem level. Technical report, Max Planck Institute for Biogeochemistry, 2015. URL `https://github.com/crlsierra/lectNotes_TB`.

Thomas F Stocker, Qin Dahe, Gian-Kasper Plattner, Lisa V Alexander, Simon K Allen, Nathaniel L Bindoff, Francois-Marie Bréon, John A Church, Ulrich Cubash, Seita Emori, Piers Forster, Pierre Friedlingstein, Lynne D Talley, David G Vaughan, and Shang-Ping Xie. Technical Summary. *Climate Change 2013: The Physical Science Basis. Contribution of Working Group I to the Fifth Assessment Report of the Intergovernmental Panel on Climate Change*, pages 33–115, 2013. doi: 10.1017/CBO9781107415324.005.

I. T. Van Der Laan-Luijkx, I. R. Van Der Velde, M. C. Krol, L. V. Gatti, L. G. Domingues, C. S C Correia, J. B. Miller, M. Gloor, T. T. Van Leeuwen, J. W. Kaiser, C. Wiedinmyer, S. Basu, C. Clerbaux, and W. Peters. Response of the Amazon carbon balance to the 2010 drought derived with CarbonTracker South America. *Global Biogeochemical Cycles*, 29(7):1092–1108, 2015. doi: 10.1002/2014GB005082.

I R Van Der Velde, J B Miller, K Schaefer, G R Van Der Werf, M C Krol, and W Peters. Terrestrial cycling of 13 CO_2 by photosynthesis, respiration, and biomass burning in SiBCASA. *Biogeosciences*, 11:6553–6571, 2014. doi: 10.5194/bg-11-6553-2014.

G. R. Van Der Werf, J. T. Randerson, L. Giglio, G. J. Collatz, M. Mu, P. S. Kasibhatla, D. C. Morton, R. S. Defries, Y. Jin, and T. T. Van Leeuwen. Global fire emissions and the contribution of deforestation, savanna, forest, agricultural, and peat fires (1997-2009). *Atmospheric Chemistry and Physics*, 10(23):11707–11735, 2010. doi: 10.5194/acp-10-11707-2010.

T. T. Van Leeuwen and G. R. Van Der Werf. Spatial and temporal variability in the ratio of trace gases emitted from biomass burning. *Atmospheric Chemistry and Physics*, 11(8):3611–3629, 2011. doi: 10.5194/acp-11-3611-2011.

T. T. Van Leeuwen, G. R. Van Der Werf, A. A. Hoffmann, R. G. Detmers, G. Rücker, N. H F French, S. Archibald, J. A. Carvalho, G. D. Cook, W. J. De Groot, C. Hély, E. S. Kasischke, S. Kloster, J. L. McCarty, M. L. Pettinari, P. Savadogo, E. C. Alvarado, L. Boschetti, S. Manuri, C. P. Meyer, F. Siegert, L. A. Trollope, and W. S W Trollope. Biomass burning fuel consumption rates: A field measurement database. *Biogeosciences*, 11(24):7305–7329, 2014. doi: 10.5194/bg-11-7305-2014.

Thijs T. Van Leeuwen. *Modeling Spatio-Temporal Variability in Biomass Burning Emission Factors*. PhD thesis, VU University Amsterdam, 2014.

C Wiedinmyer, S K Akagi, R J Yokelson, L K Emmons, J A Al-Saadi, J J Orlando, and A J Soja. The Fire INventory from NCAR (FINN) – a high resolution global model to estimate the emissions from open burning. *Geoscientific Model Development Discussions*, 3(4):2439–2476, 2010. doi: 10. 5194/gmdd-3-2439-2010.